CHARACTERIZATION OF THE INNATE HOST RESPONSE TO VENEZUELAN EQUINE ENCEPHALITIS VIRUS, FROM THE FIRST INFECTED CELLS TO SYSTEM-WIDE MODULATION IN VIVO

Jennifer Lynn Konopka

A dissertation submitted to the faculty of the University of North Carolina at Chapel Hill in partial fulfillment of the requirements for the degree of Doctor of Philosophy in the Department of Microbiology and Immunology.

Chapel Hill
2007

Approved by:

Advisor: Robert E. Johnston, Ph.D.

Reader: Steven L. Bachenheimer, Ph.D.

Reader: Ralph S. Baric, Ph.D.

Reader: Jack D. Keene, Ph.D.

Reader: Jenny P-Y. Ting, Ph.D.

ABSTRACT

JENNIFER LYNN KONOPKA: Characterization of the Innate Host Response to Venezuelan Equine Encephalitis Virus, from the First Infected Cells to System-Wide Modulation In Vivo.
(Under the direction of Dr. Robert E. Johnston)

The specific host changes induced following viral infection are reflective of the complex interaction occurring between pathogen and host. These changes are often evident in a cascade of altered transcription patterns. However, the elucidation of such cascades *in vivo* has been limited by a general inability to distinguish changes occurring within the minority of infected cells from that in surrounding uninfected cells. Therefore, an innovative mRNP-tagging system was employed to isolate host mRNA specifically from infected cells following Venezuelan equine encephalitis virus (VEE) infection. To dissect the contributions of autocrine and paracrine signaling events, simultaneous total RNA analysis was utilized in conjunction with this novel approach to directly analyze the infected cell response. The result was a multifaceted profile of the early response to VEE in primary dendritic cells, as well as within the initially targeted tissue *in vivo*, the draining lymph node. A two-phase innate response to infection was revealed, in which the activation of host genes within infected cells led to the activation of surrounding bystander cells. To further determine the impact of this robust innate immune response on the entire animal, we utilized VEE replicon particles (VRP) to limit infection *in vivo* to the initially infected cells, and examined the host antiviral

response within tissues distal to the site of replication. Although these remote tissues had not encountered VRP, they nevertheless were exposed to high levels of soluble immune modulators, including serum interferon. In the liver and brain, the rapid activation of a panel of interferon-stimulated genes was detected by 3h following VRP footpad inoculation, reaching peak expression levels of greater than 100-fold over mock. Moreover, mice receiving a footpad VRP inoculation 6, 12, or 24h prior to an otherwise lethal VEE challenge were completely protected from death. The results presented here document the rapid modulation of the host innate response within hours of pathogen invasion, a response that is capable of transforming the entire infected animal, and largely determining the outcome of infection.

For my parents,

Marcia, Ed and Lori,
whose love, support and unwavering belief in me
has made all the difference in my life…

And for my brothers,

Eric and Phil
who help keep laughter in my heart
by reminding me of the kid that lives inside us all.

ACKNOWLEDGEMENTS

So many folks have made this process possible for me, and beyond that, have made this experience an incredible chapter in my life. I would like to extend my utmost appreciation to my dissertation advisor and mentor, Bob Johnston, as well as to Nancy Davis, for granting me the opportunity to be a part of this incredible group, and for their guidance, support, and patience throughout my graduate training. I truly feel honored to share a part of their scientific pedigrees. I would like to thank the members of my thesis committee—Steve Bachenheimer, Ralph Baric, Jack Keene, and Jenny Ting—for their scientific input and intellectual guidance. I am particularly indebted to Jack Keene, whose committed support was absolutely indispensable to the ribonomics project, both in terms of reagents and intellectual contribution.

I am thankful to all members of the Carolina Vaccine Institute, past and present, for their support, fantastic technical help, open sharing of ideas, and friendship—all of which formed the foundation for me to grow into the scientist I am today. In particular, I'd like to thank Laura White and Clayton Beard for their encouragement, support, and kindness, which has meant the world to me. I would also like to thank Mark Heise for his openness and honesty when it came to advice about everything from choosing projects to choosing labs for postdoctoral training. I can not imagine what it would have been like without my fellow Johnston Lab

graduate students, Stephanie, Tim, and Jody, there alongside me experiencing this dissertation process. Their support and friendship sincerely made all the difference to me.

Finally, I would like to thank my family for their endless support, encouragement and love, without which I could not have accomplished even a fraction of what I have today. They truly are my rocks, and have kept me ever mindful of what the “bigger picture” is all about. In thanking my family, I include friends here in Chapel Hill who have become some of the closest friends I have, and in particular, I especially thank Jody and Mindy for friendship that I am forever grateful for having in my life.

TABLE OF CONTENTS

LIST OF TABLES

LIST OF FIGURES

LIST OF ABBREVIATIONS

ATF-2	c-Jun/activated transcription factor-2
AMD	Actinomycin D
AST	Average survival time
BMDC	Bone marrow dendritic cell
CARD	Caspase recruitment domain
cDNA	Complimentary DNA
CNS	Central nervous system
CRE	c-AMP-responsive element
C_T	Cycle threshold
Cxcl	Chemokine (C-X-C motif) ligand
DC	Dendritic cell
DLN	Draining lymph node
DNA	Deoxyribonucleic acid
DSG	dsRNA-stimulated gene
dsRNA	Double stranded ribonucleic acid
FACS	Fluorescence-activated cell sorting
GAPDH	Glyceraldehyde-3-phosphate dehydrogenase
GBP	Guanylate nucleotide binding protein
GFP	Green fluorescent protein
hpi	Hours post infection
IFIT	Interferon-induced protein with tetratricopeptide repeats
IFN	Interferon

IFNαβR	Interferon alpha/beta receptor
IL	Interleukin
iNOS	Inducible nitric oxide synthase
IP-10	Interferon-gamma-inducible protein-10
IRF	Interferon regulatory factor
ISG	Interferon stimulated gene
ISRE	Interferon stimulated response element
IU	Infectious units
Jak	Janus tyrosine kinase
LOD	Limit of detection
LPS	Lipopolysaccharide
LRFP	Left rear footpad
MDA-5	Melanoma differentiation associated protein-5
MOI	Multiplicity of infection
mRNA	Messenger ribonucleic acid
mRNP	mRNA binding protein; mRNA ribonucleoprotein
MTT	3-[4,5-dimethylthylthiazol-2yl]-2,5-diphenyltetrazolium bromide
Mx	Myxovirus resistance protein
MyD88	Myeloid differentiation primary response gene 88
NK	Natural killer
nsP	Nonstructural protein
nt	Nucleotide
OAS	2-5-oligoadenylate synthetase

PABP	Poly(A) binding protein
PAMP	Pathogen-associated molecular pattern
PARP	Poly (ADP-ribose) polymerase
PBS	Phosphate buffered saline
PCR	Polymerase chain reaction
PFU	Plaque forming units
PKR	Protein kinase, interferon-inducible dsRNA dependent
PRD	Positive regulatory domain
PRR	Pattern recognition receptor
RIG-I	Retinoic acid-inducible gene-I
RNA	Ribonucleic acid
RNP	RNA binding protein; ribonucleoprotein
RPA	RNase protection assay
RRFP	Right rear footpad
RRV	Ross River virus
SEM	Standard error of the mean
SFV	Semliki Forest virus
SIN	Sindbis virus
STAT	Signal transducer and activator of transcription
TD	Triply deficient
TIR	Toll-interleukin 1 receptor
TLR	Toll-like receptor
TNFα	Tumor necrosis factor-alpha

TRIF	TIR domain-containing adaptor-inducing IFN-β
UTR	Untranslated region
VEE	Venezuelan equine encephalitis virus
VRP	VEE replicon particle
VSV	Vesicular stomatitis virus

CHAPTER ONE

INTRODUCTION

THE INNATE RESPONSE TO VIRAL INFECTION

The first-line host defense

The innate immune system is an evolutionarily ancient, universal form of host defense against infection, with some form of innate immunity likely existing in all multicellular organisms (1, 2). The innate host response provides the critical first line of defense against invading pathogens, inducing an antiviral state designed to impede the spread of infection in the body. It is within this immediate response that pathogen invasion is initially sensed, and the rapid, non-specific host response is evoked. It is termed “nonspecific” in the sense that it lacks immunological memory, and relies on inborn defense mechanisms encoded within the germline to defend the host from pathogen infection. This also means that the innate immune system can recognize and respond to pathogens in an immediate manner, but unlike the adaptive immune response, cannot confer long-lasting protection. However, the process of innate pathogen recognition triggers signaling cascades that induce the early expression of antiviral mediators, such as the type I interferon response, that are critical to the earliest stages of pathogen control. Not only do these innate responses allow time and proper context for the antigen-specific response of the adaptive arm of immunity to be formed, increasing evidence suggests that the innate response is essential to shaping an effective adaptive response (3-6).

Once the invading pathogen has been recognized (see below), the innate immune system encompasses a variety of cell-mediated defense mechanisms, as well as the antiviral activities of soluble defense molecules. Cell-mediated

components of the innate immune response include the actions of phagocytic cells (e.g., dendritic cells, macrophages, and neutrophils), proinflammatory cells (e.g., mast cells, basophils), the non-T/non-B lymphocytes, and natural killer cells. The process of pathogen recongition as well as the activation of innate immune cells induces the expression and release of soluble defense molecules, including components of the complement system, as well as the emmense repretoire of cytokines and chemokines. An in-depth discussion of all arms of the innate response is beyond the scope of this review, and as such, the primary focus will be on the process of innate virus recognition, and a key modulator of the innate antiviral response, the type I interferon (IFN) system.

Innate recognition of pathogens

The innate immune system may lack the specificity of the adaptive response, and it may not recognize every existing antigen, but it can nonetheless effectively detect the invasion of the "nonself." It does so by utilizing receptors that recognize highly conserved molecular structures, termed pathogen-associated molecular patterns (PAMPs), that are shared by a broad gamut of pathogens. These receptors of the innate immune system, termed pattern-recognition receptors (PRRs), have evolved to recognize PAMPs such as lipopolysaccharide (LPS), peptidoglycan, mannans, and double-stranded RNA (dsRNA). Additionally, these PAMPs are usually essential to the survival and spread of pathogens, and in this manner, the innate immune system has developed an effective way of alerting the host to the presence of infectious "nonself" (2).

Extracellular and endosomal sensors. Thus far, there have been two major pathways elucidated for innate pathogen recognition and subsequent activation of the innate immune response. The first utilizes extracellular or endosomal receptors, comprised predominately of members from the Toll-like receptor (TLR) family. In recent years, the TLRs have become the prototype in modeling how the host senses pathogen stimuli and subsequently activates the innate immune response. TLRs are primarily expressed on the surface of macrophages and dendritic cells; however, a subset of TLRs are found intracellularly, signaling from within endosomes. It is estimated that most mammalian species have 10 to 15 different TLRs, each recognizing a unique set of PAMPs from viruses as well as other microorganisms (7). TLRs 1, 2, 4, 5 and 6 seem to specialize mainly in the recognition of bacterial PAMPs, products that are unique to these pathogens and are not made by the host. TLRs 3, 7, 8 and 9 are primarily responsible for viral detection and recognize nucleic acids. TLR7 and TLR8 recognize single-stranded RNA, and are activated in response to RNA viruses, while TLR9 recognizes DNA and is activated by DNA viruses. TLR3, on the other hand, is activated upon recognition of dsRNA, and as such, can detect the dsRNA by-products of both RNA and DNA viruses (8). As nucleic acids are obviously not unique to viruses, this subset of TLRs are localized to the intracellular compartment of late endosomes or lysosomes in order to prevent interaction with host nucleic acids (7).

TLRs are defined by two domains: the extracellular leucine-rich repeat domain responsible for ligand recognition, and the intracellular TIR (Toll-interleukin-1 receptor) domain responsible for inducing downstream signaling events, including

the induction of type I interferon, through adapter molecules. These adaptor molecules include myeloid differentiation primary response protein 88 (MyD88) in the case of TLR7/8/9, and TIR domain-containing adaptor-inducing IFN-β (TRIF) for TLR3-mediated signaling (8, 9). By signaling through these adaptor molecules, TLRs activate the transcriptional pathways responsible for modulating the type I interferon response following innate pathogen recognition (reviewed in (10)).

Cytoplasmic sensors. A second class of recognition receptors exists that is ubiquitously expressed, and exclusively localized intracellularly. These cytoplasmic sensors specialize in recognition of dsRNA, and are responsible for TLR-independent mechanisms of virus recognition. Until recently, the PKR (dsRNA-dependent protein kinase) and the 2'-5'-oligoadenylate synthase (OAS)/RNaseL pathways were the predominant members of this class of sensors (1). PKR, activated by dsRNA, phosphorylates and inactivates the translation initiation factor eIF2α, thereby blocking protein synthesis in infected cells. Upon binding and processing of dsRNA by OAS, RNaseL is activated and degrades all RNAs within infected cells.

The most recently emerging class of cytoplasmic PRRs with the ability to recognize dsRNA are the caspase recruitment domain (CARD)-containing RNA-helicases, specifically retinoic acid-inducible gene-I (RIG-I) and melanoma differentiation antigen 5 (MDA-5) (11). To activate the interferon-induced antiviral response, both of these helicases utilize the MAVS/IPS-1/CARDIF/VISA adapter molecule, which interestingly is associated with host mitochondria, (10, 12-15). In

addition, recent evidence suggests that RIG-I and MDA5 can further distinguish viral pathogens based on recognition of different RNA structures induced during infection, and as such, can distinguish between different RNA viruses. This included the finding that RIG-I was essential for the production of interferons in response to RNA viruses (e.g., influenza virus, paramyxoviruses, and flaviviruses), while MDA5 was critical for picornavirus recognition (16, 17). Therefore, although some redundancy exists in the type of PAMP(s) recognized by the various PRRs, clearly multiple levels of regulation exist within these recognition processes. Furthermore, a key element in the innate recognition of such a broad range of pathogens is the reliance on the multiplicity of PRRs available, presumably to increase the odds of innate pathogen recognition and activation of this critical first-line of defense.

The interferon response to viral infection

During viral infection, interferons are among the most prominent and potent cytokines induced. Interferons were first discovered based on their ability to "interfere" with viral replication in cell culture (18, 19), and since then have been implicated as critical mediators of the global antiviral state, as well as important regulators of both the innate and adaptive immune response. The interferon system affects many aspects of cell physiology (19); however, the focus here will be on the host defense response.

Interferon classification and regulation. Interferons are classified into two major categories, either type I (IFNα/β) or type II (IFNγ). The type I superfamily is further

divided into 14 to 20 distinct IFNα members, a single IFNβ, and the lesser defined IFNω, κ, ε, δ (pig), τ (cattle and sheep) subtypes (20). The type I interferons are secreted proteins made by both hematopoietic (IFNα and ω) and nonhematopoietic cells (mainly IFNβ), and their expression can be directly induced by PRR recognition of invading pathogens. The IFN-mediated host antiviral response is initiated through the binding of type I IFNs to a common receptor, the type I IFNαβ receptor (IFNαβR or IFNAR), and the induction of antiviral genes can happen within minutes of this interaction (21). The type I receptor is present in low abundance on all major cell types, at an estimated 2 - 5 x 10^3 binding sites per cell (19, 22).

The type II interferon family consists of one member, IFNγ, a secreted glycoprotein made only by cells of the immune system, with natural killer cells being the main producers of IFNγ during the innate immune response. IFNγ is primarily associated with the secondary wave of responses to infection, and not generally induced directly by invading pathogens. An additional class of interferon-like cytokines has also been revealed, proposed by some as a type III interferon family consisting of IFNλs and ζ, which may function somewhat like type I IFNs. However, this new class is still being characterized (20, 23, 24). Being that the focus of this overview is on the earliest host response to viral infection, the emphasis will fall on the type I interferon response.

The most immediate response to many viral infections is the induction of high levels of type I interferon (22). Events such as the direct binding of viruses to the cell surface, as well as the recognition of any number of viral products by PRRs (discussed above), result in the triggering of complex signaling cascades that

ultimately lead to the production of type I interferon. The transcriptional activation of the IFN$\alpha\beta$ genes is complex and is often dependent on the specific mechanism of pathogen recognition. However, these cascades converge onto the same regulatory elements within the type I genes.

The IFNβ promoter has been extensively characterized in this regard. At least three families of transcription factors are responsible for activating the IFNβ promoter through binding to positive regulatory domains (PRDs): 1) IFN regulatory factors (IRFs; mainly IRF-3 and 7) bind to the IFN-stimulated response element (ISRE) sites (PRD-I and III); 2) nuclear factor (NF)-κB binds to the κB site (PRD-II); and 3) c-Jun/activated transcription factor-2 (ATF-2) heterodimer binds to the c-AMP-responsive element (CRE)(PRD-IV) (25). Upon viral infection, these transcription factors rely on phosphorylation for activation and/or translocation into the nucleus; activities that are controlled by the signaling cascades initiated by PAMP-PRR interactions. While cJun/ATF-2 and NF- κB become activated by multiple stimuli, IRF-3 is more tightly regulated. IRF-3 is expressed constitutively in all cells, existing in a latent state until viral infection and PAMP recognition leads to its phosphorylation (by TANK-binding kinase-1 or inducible IκB kinase), dimerization, and nuclear translocation (9). The coordinated interaction of these activated transcription factors into an enhanceosome complex drives the transcription and early expression of IFNβ and IFNα_4 in infected cells.

Interferon-induced antiviral signaling. Once induced and secreted into the extracellular environment, type I interferons bind to the IFN$\alpha\beta$R on bystander

uninfected cells, and in a paracrine fashion, elicit an antiviral state in nearby cells to block the spread of infection. Once interferon binds to the IFNαβR, dimerization of the receptor and tyrosine phosphorylation by members of the Janus kinase (Jaks) family ensues (Jak1 and Tyk2). The receptor units, as well as specifically recruited members of the signal transducers and activators of transcription (STAT) family, are phosphorylated (19, 25). The phosphorylated STATs (STAT1 and 2) form dimers (homo- or heterodimers), and translocate to the nucleus where they activate transcription of specific interferon-stimulated genes (ISGs, see below) by forming a transcription factor complex (ISGF3) with the DNA-binding protein IRF9 (also known as p48 or ISGF3γ). An important ISG transcribed following engagement of the IFNαβR by early type I interferons is IRF-7, a component whose importance lies within the autocrine positive feedback loop (26).

IFN secreted by infected cells may also bind to the type I receptor on the surface of other surrounding infected cells, or the very cell it was secreted from, and directly amplify the ensuing antiviral state (27, 28). Interferon receptor signaling would again lead to newly synthesized IRF-7. However, in cells where viral infection is still ongoing, IRF-7 becomes phosphorylated and thus active, leading to the induction of the remaining non-α4 members of the IFNα gene family. Although some of the details of this positive feedback loop may still be controversial (25), it is likely responsible for the robust induction of type I interferon in infected cells, and explains why pretreatment with interferon in cell culture can prime its own expression (26, 29, 30).

A simplified overview of the regulation of interferon production would be as follows. The initial sensing of viral infection by innate recognition mechanisms is required to induce the rapid production of IFNβ and IFNα_4. If these initial levels of IFN produced during infection can successfully block viral replication, then IFN production would decline due to latent IRF-7 (26). However, if infection continues, then accumulating newly synthesized IRF-7 would be phosphorylated and lead to the robust induction of the full repertoire of type I interferons.

Perhaps the most striking evidence of the critical nature of the interferon signaling pathways comes from studies in which either IFNα/β itself was blocked (e.g., through administration of blocking antibodies) or the activity of the receptor itself was inhibited (e.g., genetic deletion of the genes encoding the receptor). For example, in mice naturally susceptible to infection, administration of anti-IFNαβ antibodies greatly aggravated infection with Semliki Forest virus (SFV) and herpes simplex virus-1 (31). This administration also exacerbated the course of infection in naturally resistant mice following infection with viruses such as Sindbis virus, mouse hepatitis virus-3, and influenza virus (31). In other examples, the targeted deletion of the IFNαβR greatly increased the susceptibility of mice to vesicular stomatitis virus, SFV, and vaccinia virus (32). Numerous studies, including these few examples, clearly indicate the importance of early interferon production in determining the outcome of viral infection.

ISGs and the induction of the "antiviral state"

By signaling through the type I receptor in both a paracrine and autocrine fashion, interferons induce the expression of hundreds of proteins that together establish what is termed the "antiviral state." These interferon-stimulated genes (ISGs) encode proteins that have antiviral, antiproliferative, and immunomodulatory activities, all aimed at preventing or limiting viral spread (19). These activities can directly interfere with virus-specific processes, leading to the inhibition of any number of stages during the viral replication cycle. This interference may also be directed at general cellular processes that are critical for the virus as well as the host, including inhibition of translation, cell cycle arrest, and the induction of apoptosis.

*Functional genomics and the antiviral state***.** Advances in microarray technology, bioinformatics, and functional genomics over the past decade have led to an enormous burst of information regarding genes that are regulated by viral infection and/or stimulation by interferon. Prior to these technologies, it was thought that only 30-40 antiviral and interferon stimulated genes existed (33). However, it has become increasingly apparent that there are hundreds of genes that are regulated by interferon and/or viral infection.

The number of microarray studies designed to assess the modulation of host gene expression following infection with specific viruses is steadily increasing (e.g., influenza virus (34, 35), herpes simplex virus (36, 37), Sindbis virus (38, 39), and hepatitis C (40, 41)). While these studies are undoubtedly invaluable to each

particular viral field, a handful of array studies have aimed more generally at characterizing the effects of interferon or particular PAMPs on host cells, greatly contributing to our understanding of the overall host response to infection (34, 42, 43). In two such studies, human and murine cell lines were treated with IFNα, β, and γ, either individually or in combination, and the effect on host gene expression was assessed (42, 43). The result was the identification of over 300 ISGs, and a pivotal breakthrough not only in the sense that they provided target genes for further study, but also in the manner in which virologists viewed the host response to infection. An additional study focused on the PAMP-mediated activation of the antiviral host response, using cell lines that lacked all type I IFN genes such that the effects of the autocrine actions of interferon were eliminated (34). This study specifically examined the modulation of host antiviral gene expression by dsRNA-mediated signaling pathways. Nearly 300 dsRNA-stimulated genes (DSGs) were identified, being either induced or repressed by dsRNA treatment in the rapid, robust, and transient manner characteristic of the innate response to viral infection.

The ISGs and DSGs identified in these studies have a broad range of cellular functions, belonging to a wide range of biological pathways (e.g., cytokine, chemokine, and growth factors; apoptosis; cell cycle regulation; metabolism; cell adhesion). A few of what seem to be emerging as key antiviral genes from the expansive list are discussed below in more detail. Additionally, as gene expression studies are translated into investigations of protein function, the specific contributions of these individual genes are being elucidated within the context of viral

infection. As such, reference to specific studies in which a particular ISG/DSG was found to have an impact during viral infection will be mentioned.

PKR. In addition to mediating transcriptional signaling in response to viral infection and interferon, PKR (serine-threonine protein kinase) is itself an interferon-stimulated gene, activated by dsRNA. The most well-known antiviral activity of PKR is the inhibition of mRNA translation following PKR-mediated phosphorylation of the translation initiation factor, eIF2α. PKR may also be activated in response to cellular stress (44), and can induce apoptosis through a Fas-dependent pathway (45). It appears however, that like many ISGs, the role of PKR in the infected host can be virus-specific. For instance, mice with targeted deletion of the PKR gene are more susceptible to vesicular stomatitis virus infection, but are still able to successfully clear influenza virus infection (46, 47). A large number of viruses have evolved various strategies to block the activation and/or activities of PKR, demonstrating its critical role in the host response to infection, and rendering it one of the most extensively studies ISGs (19).

OAS and RNaseL. The coordinated activity of these two ISGs results in the global degradation of RNA in the infected cell. Induced by interferon, the OAS gene family encodes a class of enzymes that are activated by dsRNA. Even small or partial dsRNA structures, which are present during a wide variety of viral infections, activate the OAS enzymes to polymerize ATP into 2'-5' linked oligoadenylates (48). These molecules then go on to activate the RNase L ribonuclease, which in turn degrades

both host and viral RNA within infected cells. The expression of the OAS and RNaseL genes is induced following infection with numerous viruses, with the antiviral actions of their products documented to play pivotal role in the host response to viral infections, including West Nile virus (49, 50).

Mx and GBP. A growing class of antiviral genes exists having GTPase and/or guanylate binding activity. The most well known may be the Mx proteins, which were originally identified as host antiviral molecules that could limit influenza virus infection (19). The principal activity of Mx is the sequestering of viral nucleocapsids into specific intracellular compartments, including that of several bunyaviruses (e.g., Crimean-Congo hemorrhagic fever virus and La Crosse virus (51, 52)) (53).

An additional class of GTPases, the guanylate-binding proteins (GBPs), is also induced following viral infection. Their antiviral activity is speculated to be at the level of RNA synthesis, although the specific mechanism is unknown. They are induced by a wide variety of viruses, and in particular, GBP-1 plays a role in the antiviral response to vesicular stomatitis virus and encephalomyocarditis virus (51).

Antiviral chemokines. There are increasing numbers of reports documenting the induction of interferon-stimulated proinflammatory molecules during the early immune response to viral infection (4). The chemokine IP-10/Cxcl10 falls into this category, possessing interferon-stimulated response elements within its promoter. The best-described function of chemokines is leukocyte recruitment, an activity pivotal to the innate inflammatory response as well as the adaptive immune

response. The key antiviral activity of chemokines, like IP-10, that are induced during the innate response to viral infection is likely mediated by their roles in recruitment of activated natural killer cells to the site of infection (e.g., during infection with Dengue virus (54)).

IFIT family. A growing class of proteins containing tetratricopeptide repeat domains (IFITs) is emerging as interferon-induced antiviral mediators. These genes are induced strongly but transiently following infection with a variety of viruses, or stimulation with interferon or double-stranded RNA (55, 56). IFIT1, also known as ISG56 or p56, belongs to this family, and has been regarded as the most strongly induced ISG (19, 43). The antiviral activity of IFIT1/p56 appears to involve the inhibition of mRNA translation by binding to subunits of the translation initiation factor eIF3, with human and murine p56 targeting different subunits (57-59). A recent study characterizing the closely related IFIT4/p54 protein found that while the kinetics of ISG54 and ISG56 induction in response to dsRNA, IFN, and Sendai virus were quite distinct, they both targeted eIF3 to inhibit translation (56). These results document the subtle differences in antiviral mediators, which may seem to overlap mechanistically, but potentially serve to ensure protection from a multitude of pathogens.

A dynamic system

The information generated from the studies mentioned here, as well as countless others, consistently demonstrate that the host response to infection, including the

interferon-induced antiviral state, is differentially regulated from system to system, dependent upon the viral and host systems examined. It is intriguing to think about the particular manner in which these pathways converge, as well as diverge, in forming the host antiviral state that is appropriate for each virus, at a specific time during infection, within a particular host. The level of fine-tuning of the innate host response, seeming to occur specifically to each invading pathogen, is particularly impressive considering the responsible genes are fixed within the germline.

However, viruses have likewise evolved equally elegant ways of subverting the interferon-induced antiviral state. In fact, viral evasion of the interferon system has been documented on several levels, and includes virus-mediated activities such as the blocking of IFN synthesis, interfering with interferon signaling, and disrupting the functions of interferon-induced proteins [reviewed in (19, 33, 60). Fortunately, the interferon response often targets more than one critical component or step in each viral life cycle, such that even if a key antiviral protein is disabled or blocked by infection, other antiviral proteins can usually compensate to ensure that infection is limited. Indeed there are a growing number of examples documenting this phenomenon, as systems become available in which individual or combinations of ISGs or recognition receptors have been abrogated. For example, mice triply deficient for Mx, PKR, and RNaseL can still mount an effective antiviral state (61). In fact, while IFN$\alpha\beta$R-/- mice rapidly succumb to fatal Sindbis infection, mice triply deficient for Mx, PKR, and RNaseL develop only mild disease and survive (62). As more of these model systems become available, and as novel ways to profile the host response evolve from the field of functional genomics, certainly new

breakthroughs can be expected that will transcend the gaps remaining in our understanding of the host-pathogen interface.

VENEZUELAN EQUINE ENCEPHALITIS VIRUS

Overview

Venezuelan equine encephalitis virus (VEE) is an arbovirus belonging to the *Togaviridae* family of viruses, specifically within the alphavirus genus. Alphaviruses are generally divided into two categories, the Old World and New World viruses, based on their geographic distribution and disease outcome (63). New World alphaviruses have the potential to cause febrile illness and encephalitis, and include VEE as well as Eastern and Western equine encephalitis viruses. Old World alphaviruses, causing disease characterized by rash and arthritis, include Sindbis (SIN), Semliki Forest virus (SFV), Ross River virus (RRV), Chikungunya, and O'nyong-nyong virus. All alphaviruses are transmitted by arthropod vectors, cycling primarily between mosquitoes and small mammals or birds. Larger mammals, such as horses and humans, tend to develop more severe disease and are often dead-end hosts (63). Venezuelan equine encephalitis was first recognized in the 1930s as a disease of horses, donkeys and mules in South America, with VEE identified as the causative viral agent in 1938, isolated from the brain of a horse that had succumbed to lethal encephalitis (64).

VEE is maintained in an enzootic cycle within subtropical North and South America, involving the *Culex* (*Melanoconion*) subgenus of mosquitoes and small rodents (64). The enzootic serotypes of VEE (1D-1F and II-IV) are antigenically distinct from epizootic VEE serotypes (1AB and 1C), and cause little to no viremia in experimentally infected horses (64). The first widely recognized outbreak of

epizootic VEE occurred in 1935, spreading across Columbia and Venezuela through the mid-1940s, causing a high incidence of disease and mortality among donkeys and horses. Epizootic viruses isolated during the outbreak were primarily from *Psorophora confinnis* and *Aedes sollicitans* mosquitoes, suggesting that the epizootic and enzootic transmission cycles differed (63, 65). Although it is likely that VEE-induced human disease occurred during this early epidemic, it wasn't until the 1950s that the connection between equine and human disease was established (66). VEE was isolated from human cases during this epidemic outbreak; however, the ability of VEE to infect humans had been documented previously in laboratory personnel (67). While infection with epizootic VEE results in a high mortality rate in horses (ranging from 19%-83%), mortality in humans is quite rare (less than 1%), with neurological disease appearing in 4%-14% of cases (66).

A widespread and long-lasting VEE epidemic began in 1969, which spread over the next few years through Central America, Mexico, and into Texas in 1971, causing human disease and high mortality among horses. During this time, the extensive use of the TC-83 vaccine strain of VEE was instituted (66). This live-attenuated vaccine was developed by passaging the virulent 1AB subtype strain, Trinidad donkey, 83 times in cultured guinea pig heart cells (68). The high equine mortality observed in the 1969-1973 outbreak, the presence of high levels of neutralizing antibody titers in the survivors, and the wide use of the TC-83 vaccine likely contributed to a nearly 20 year hiatus in epidemic VEE outbreaks until the 1990s (64). Small outbreaks of VEE were followed in Venezuela and Mexico in the

early 1990s, however one of the largest VEE epidemics occurred in 1995, involving an estimated 75,000-100,000 human cases (69, 70).

Seeming to disappear at times for years between outbreaks, the viral source of the epizootic VEE has not been fully revealed. Outbreaks of epizootic VEE tend to correlate with periods of heavy rainfall, during which increased populations of the epizootic mosquito vectors results. While enzootic strains of VEE usually cause asymptomatic or mild infection in equines, the availability of susceptible equines is a key factor to epidemic VEE potential (65). The high titer serum viremia that ensues following infection with epizootic VEE strains renders equines as the principal amplifying species for transmission, especially to nearby humans. Evidence suggests that naturally maintained, enzootic pools of VEE may be the source, with amplification-competent epizootic variants emerging by mutation (64, 66, 71). As the mechanism(s) of host-range change remains poorly understood for several emerging/reemerging viruses, future studies addressing the emergence of epizootic VEE serotypes will likely contribute to our overall understanding of this phenomenon.

VEE structure, genome and replication

VEE is a spherical, enveloped virus, 70nm in diameter with a single-stranded, positive-sense RNA genome of approximately 11,400 nucleotides in length that is 5' capped and 3' polyadenylated (63). The genome has extensive secondary structure, including within the 5' and 3' untranslated regions (UTRs) where important regulatory signals for RNA replication exist (72-74). The 5' two-thirds of the VEE genome encodes the four nonstructural proteins (nsP1-4) which participate in viral

replication and protein processing (72). nsP1 possesses methyl- and guanyltransferase activities. nsP2 has at least two functions, serving as a helicase/NTPase and as the protease that cleaves the nonstructural proteins during replication. The role of the nsP3 phosphoprotein is not fully understood, but it is essential to viral replication. nsP4 serves as the viral RNA-dependent RNA polymerase. The final 3' one-third encodes the viral structural proteins (capsid, and the E1 and E2 glycoproteins) under an internal subgenomic 26S promoter (72). The RNA genome is encased by a T=4 icosahedral nucleocapsid, consisting of 240 copies of the capsid protein, which in turn is enveloped by a lipid bilayer derived from the plasma membrane, imbedded with the viral glycoproteins also in a T=4 symmetry (75-77). Evidence from structural analysis of other alphaviruses has demonstrated that the E2 glycoprotein forms the spikes protruding from the surface of the virion, while the E1 glycoprotein lies tangential to the lipid envelope, creating the icosahedral scaffold (78, 79).

A single, definitive receptor for VEE binding and entry has not been identified. Though candidates have been identified or proposed, including the laminin-binding protein, c-type lectins DC-SIGN and L-SIGN, and heparin sulfate. Considering the wide cell tropism of VEE, it may be more likely that VEE uses multiple receptors or a highly conserved receptor (80-82). E2 is regarded as the glycoprotein responsible for interaction with the host cell receptor(s), while the E1 glycoprotein is involved in fusion events during entry (63). The concept of alphavirus entry has also been a topic of some debate, with one camp supporting endocytosis for entry and low pH-mediated membrane fusion for release into the cytoplasm (72, 83), while the other

supports a novel mechanism featuring a “pore-like” structure that would mediate entry at the plasma membrane independent of membrane fusion and endocytic internalization (84).

Following binding and entry into the host cell, the nucleocapsid disassembles, and the RNA genome is released into the cytoplasm. The message-sense genomic RNA is immediately translated by host translation machinery into the polyprotein precursor P123, or if read-through of an opal stop codon occurs, a P1234 precursor is synthesized. VEE RNA replication is regulated through specific polyprotein cleavage events, mediated by the protease domain of nsP2, resulting in the processing of the precursor into the four mature nonstructural proteins (72). The P123 intermediate, together with the nsP4 RNA-dependent RNA polymerase, mediates negative-sense viral RNA synthesis early in infection. The subsequent cleavage of P123, releasing nsP1 plus the P23 intermediate, mediates the switch from minus-strand to plus-strand synthesis. Upon further processing, the four individual nonstructural proteins comprise the plus-strand replicase complex, which drives the synthesis of positive-sense, full-length genomic and subgenomic RNAs from minus-strand templates.

Subgenomic RNA from the internal 26S promoter is synthesized in a 5- to 10-fold excess to genomic RNA, leading to a large pool of glycoproteins and capsid available for packaging new virions (72). Full-length genomic RNA is specifically encapsidated by the interaction of the capsid protein with a packaging signal within the 5’ nonstructural region of the genome. Assembly and budding of infectious progeny virions occurs at the plasma membrane. Preformed nucleocapsids interact

with the plasma membrane, specifically at sites where the viral glycoproteins are present. The interaction of the nucleocapsid with the glycoproteins nucleates the budding process, resulting in the acquisition of a tightly-fitted lipid bilayer envelope, and release of progeny virions from the host cell (63). The cytopathic effects of infection are readily apparent in cultured vertebrate cells (e.g., cell rounding, detachment from the monolayer, membrane blebbing), as infection eventually leads to host cell transcription and translation shutoff, culminating in apoptosis of infected cells (63, 85, 86).

VEE pathogenesis

Clinical disease. In equines, infection with VEE induces a wide spectrum of disease ranging from asymptomatic to lethal encephalitis. While enzootic strains cause little (e.g., low viremia, short duration fever) to no clinical illness, disease induced by epizootic strains can be quite severe, including high mortality (87, 88). Clinical signs usually appear within 2-5 days after infection with epizootic VEE, characterized by fever, depression, and anorexia. Progression to encephalitis and death correlates with the magnitude of the viremia, with clinical signs of encephalitis (e.g., circling, ataxia, hyperexcitability) developing within 5-10 days after infection (66). Pathology in fatal cases shows a profound peripheral leukopenia that coincides with viremia, as well as pancreatic necrosis. In the brains of animals presenting with signs of neurologic involvement, swollen cerebrovascular endothelial cells, edema, and leukocytic infiltration into the perivenular spaces has been documented (89, 90).

Approximately 7 days after infection, antibody appears in equines that have survived (89).

A similar incubation period of 2-5 days occurs during human VEE infection, presenting with clinical symptoms including fever, malaise, and severe headache frequently associated with intense retro-orbital pain. Interestingly, the same lymphopenia observed in horses is also observed in infected humans. Clinical disease manifestations seem to vary with age, as children younger than 15 years of age are most likely to develop fulminant disease, while young adults and individuals older than 50 mostly develop flu-like symptoms (63, 91, 92). As a result, the incidence of encephalitis as well as mortality in humans is relatively rare (less than 5% and 1%, respectively) (91).

Several animal models have been utilized over the years to investigate VEE-induced pathogenesis, including macaques (93-95), rabbits (96), chickens (97, 98), hamsters (99-102), and guinea pigs (96, 103). However, pathogenesis studies in the mouse model, combined with the development of the infectious clone of VEE, have yielded a great wealth of information. Derived from the virulent, epizootic Trinidad donkey strain of VEE, the infectious cDNA clone (V3000) provided the means to study the progression of pathogenesis in the mouse model from an inoculum that was far more homogeneous than stocks of natural isolates (104). Additionally, it provided a system in which specific mutations could be inserted into the genome of the virus and the resulting effects on the progression of pathogenesis evaluated, greatly increasing our knowledge of the genetic determinants of VEE-induced disease.

VEE pathogenesis in the murine model. An early, comparative study of VEE pathogenesis in several animal models identified the mouse as an experimental host sharing many of the same elements of pathogenesis naturally observed in the equine host (90). Following subcutaneous inoculation of VEE, two distinct disease phases occur: An initial peripheral phase within 1 to 2 days post-inoculation, in which the virus mainly replicates in lymphoid and myeloid tissues (thus termed the "lymphotropic" phase), and is characterized by the development of a high titer serum viremia. This is followed by clearance of the virus from the serum and periphery. CNS invasion occurs 2 to 3 days post-inoculation when the neurotropic phase of the disease is initiated, leading to the death of the animal by 6 to 7 days post-inoculation.

The progression of pathogenesis was further defined, years later, using the infectious cDNA clone (105). Following subcutaneous footpad inoculation with 10^3 plaque forming units (PFU) of V3000, a route chosen to mimic delivery by the bite of an infected mosquito, replication in the draining popliteal lymph node was detected by 4 h post-inoculation (pi). By 12 hpi, virus was detected in the serum, spleen, heart, lung, kidney, and adrenal gland, and by 18 hpi had also reached the thymus, pancreas, salivary gland, and the contralateral popliteal lymph node. At 24 hpi, a high titer serum viremia (2×10^7 PFU/ml) was underway, and the characteristic VEE-induced lymphopenia was observed. Replication in the indicated tissues continued until clearance from the periphery occurred at 72 to 96 hpi. By 5 to 6 days pi, peripheral tissues were completely clear of detectable infectious virus, and characterized by a return to nearly normal histological appearance, including signs

of cell repopulation within lymphoid tissues. However, by this time, virus had already invaded the central nervous system (CNS). By 48 to 72 hpi, virus could be detected in the brain, and reached a peak of 1 x 10^7 PFU/gram by 96 hpi. At the earliest times that VEE antigen could be detected in the brain, it was present within areas involving olfaction. VEE invasion of the CNS occurs primarily through the olfactory neuroepithelium, with the trigeminal nerve seeming to serve as a secondary entry point if the neuroepithelium is disrupted (106-108). VEE can be found in all areas of the brain by 4 to 5 days pi, with evidence of neuronal apoptosis (109). Mice infected by footpad inoculation succumb to lethal encephalitis by 5 to 6 days pi, with a 100% rate of mortality.

A series of studies using site-directed mutagenesis of the infectious clone further defined critical elements in the progression of VEE-induced pathogenesis. The basis for these mutations had come from a panel of attenuated mutants of VEE that had been isolated during selection for rapid penetration of cultured cells (110). Several E2 glycoprotein mutants were characterized, with individual mutations affecting different aspects of the progression of VEE pathogenesis, and all leading to attenuation (82, 105, 111-114). For instance, one mutant (V3010) was delayed in its movement from the site of inoculation to the draining lymph node, resulting in a lowered serum viremia, while another mutant (V3014) rarely progressed beyond the draining lymph node at all (105). Additional mutants with intriguing phenotypes included one virus (V3032) that could spread from the site of inoculation and seed the periphery, but did so with little to no viremia. The V3034 mutant (V3034) spread to the periphery with similar kinetics to wildtype VEE; however, it could only

sporadically invade the CNS and was attenuated even after direct intracranial inoculation (105). Studies involving this panel of viruses also demonstrated that revertants, with compensating mutations, could arise during infection with an avirulent mutant, and were capable of overcoming the block in viral spread to at least partially restore virulence (113). This body of work defined parameters critical to successful viral spread, further delineated the process of VEE pathogenesis, and demonstrated the central role of viral genetics in the outcome of infection.

VEE replicon particles. A tool essential to the study of early events in VEE pathogenesis are VEE replicon particles (VRP). VRP are propagation-defective particles which contain a VEE-derived genome, based on the infectious cDNA clone. However, the genome is modified such that the structural genes are deleted and replaced by a heterologous gene of interest (115). To facilitate assembly of VRP, two helper RNAs encoding the capsid and glycoprotein genes, but lacking a packaging signal, are supplied *in trans*. When VRP infect cells, they undergo only one round of infection, in which the VRP genome is expressed at high levels. However, no new progeny are packaged or released, as the VRP genome does not encode the VEE structural proteins.

VRP provide at least two advantages in their application to the study of VEE pathogenesis. First, as replication is limited to the first round of infected cells, VRP provide a system in which the earliest events of VEE pathogenesis can be modeled and characterized accurately within the host, without the confounding effects of viral spread. Although infection in the murine model has been well studied for some time,

surprisingly little is known concerning the earliest features of VEE-induced disease. The body of work presented in the following chapters demonstrates the utility of VRP to facilitate the characterization of early virus-host interactions *in vitro* as well as *in vivo*. A second advantage that VRP offer is the ability to express a marker gene, such as green fluorescent protein (GFP), specifically within infected host cells. The expression of GFP from the VRP genome yields a fluorescent marker designating which cells have been infected.

In fact, the utilization of GFP-VRP facilitated the identification of the cell population initially targeted by VEE *in vivo*. Although the draining lymph node had been identified as a critical site of early viral amplification (105), and spread from the skin to the DLN was shown to be a key initial step in pathogenesis (105, 113), the identity of the specific cell type infected at the site of inoculation was unknown. Inoculation of VRP expressing GFP into the footpad of mice, facilitated the identification of Dendritic cells, specifically the resident Langerhans cells within the epidermis, as the initial viral target *in vivo* (116). GFP-positive Langerhans cells were tracked, by fluorescence microscopy and serial tissue sectioning, from the site of inoculation in the skin, to the paracortex of the DLN. By just 30 minutes following GFP-VRP footpad inoculation, GFP-positive cells were already present in the DLN, while the number of GFP-positive cells present in the footpad declined. The data from this study suggested a model in which VEE delivered subcutaneously (e.g., by the bite of an infected mosquito), initially infects Langerhans cells resident within the skin at the site of inoculation. The infected Langerhans cells then rapidly migrate from the site of inoculation to the peripheral draining lymph node, where replication

ensues. Studies are currently underway in the Johnston laboratory in which the E2 glycoprotein mutations, which conferred blocks at various stages of infection, are introduced into the replicon system and the effects on cell targeting and migration examined.

Aside from their use in VEE pathogenesis studies, VRP have also been extensively utilized as vaccine vectors for the expression of a number of heterologous antigens. Expression of these heterologous proteins from VRP often induces strong, protective antibody and T-cell responses, including the induction of mucosal IgA (115, 117-123). The high level of antigen expression from the 26S subgenomic promoter, combined with the ability of VRP to target DCs and lymphoid tissue, are at least two factors that contribute to the efficacy of VRP as vaccine vectors.

Protection from disease

Both the innate and adaptive arms of the immune system are essential to the control of VEE infection and protection from VEE-induced disease. Protection against VEE infection has typically been associated with neutralizing antibody (91, 124-127). However, nonspecific protection against VEE has also been suggested, including the involvement of the innate immune response (128-133). The known contributions of the adaptive response will be briefly touched upon here, while the innate host response to VEE will be covered in more detail within a separate section (see below).

It has been well documented that protection in equines is often mediated by a protective neutralizing antibody response, established either through previous exposure to an avirulent enzootic strain of VEE or through vaccination with the TC-83 vaccine strain of VEE (64). The production of VEE-specific IgM appears to be critical for clearance of virus from the serum and peripheral organs, with production being independent of T-cell help (131). While neutralizing antibodies are most often directed against the E2 glycoprotein, non-neutralizing antibodies against both E1 and E2 also appear to be important mediators of protection (72). However, while antibody responses are effective in preventing infection (e.g., after vaccination) and/or limiting viral spread in the periphery, they are not sufficient to prevent neuroinvasion and death in a primary exposure to virulent VEE (63).

Instead of protecting animals from disease, the immune response to alphaviruses can also exacerbate disease by mediating direct CNS immunopathology (72). While this has been demonstrated for Sindbis and Semliki Forest virus infections, the role of host-induced immunopathology seems to play a lesser role in VEE pathogenesis. This was demonstrated by the continued destruction of the CNS in VEE-infected SCID mice—a pathology that was induced in a lymphocyte-independent manner (131). However, the disease induced in these mice was more along the lines of a spongiform encephalopathy rather than the characteristic VEE-induced encephalitis. Therefore, unlike other neurovirulent alphaviruses, VEE has a direct cytopathic effect in the CNS, even in the absence of the host immune response.

THE INNATE HOST RESPONSE TO VEE

In vivo models

Over thirty years ago, the sensitivity of VEE to the host interferon response was first proposed as a critical virulence determinant, with naturally virulent and avirulent strains displaying differences in their relative sensitivity to IFN$\alpha\beta$ (99, 134). Therefore, in addition to the adaptive host response, nonspecific protection against VEE also has been documented. Although the full mechanism of this nonspecific protection against VEE is not well understood, it is likely that the interferon response as well as other soluble mediators play a crucial role. In fact, particular regimens of interferon administered therapeutically in small animal models have proven effective in limiting disease (135, 136). Additionally, following infection of mice, high levels of serum IFN$\alpha\beta$ rapidly appear (up to nearly 400,000 IU/ml by 6 h post-inoculation), limiting virus replication early, and allowing time for the specific immune response to be induced (63, 133)[J.L.K., Fig. 3.2]. This is further evident following VEE infection of IFN$\alpha\beta$R-/- mice, in which the average survival time is greatly reduced in comparison to wildtype animals (24 to 48 h versus 6 to 7 days, respectively) (132, 133).

Experimental infection of equines has typically revealed that enzootic strains of VEE produce little or no viremia and disease, while epizootic IC strains generate high-titer viremia and encephalitis. Observations such as these gave rise to a commonly shared hypothesis that the relative sensitivity of these strains to the innate equine immune response mediated their different phenotypes. Specifically,

epizootic strains were generally thought of as inherently resistant to the host IFNαβ response, leading to more efficient replication and higher viremia. However, a recent report investigating the 1992 emergence of epizootic strains of VEE cautions against using murine IFNαβ sensitivity as a marker for epizootic potential in equines (87) .

Nevertheless, exploring the interferon sensitivity of VEE in the murine model has facilitated the identification of VEE virulence determinants. Specifically, the 5' UTR of the VEE genome segregated with the relative IFNαβ resistance of the virulent Trinidad donkey strain versus the TC-83 vaccine strain (137, 138). Upon further characterization, a single noncoding nucleotide change in the 5' UTR was identified as a major attenuating mutation (133). The substitution of G-to-A in the third nucleotide of the 5' UTR resulted in the complete attenuation of VEE, from the observed 100% mortality in mice infected with wildtype VEE to 0% mortality with the nt3A mutant. A major role for the innate immune response in this loss of virulence was indicated by its heightened sensitivity to IFNαβ (133). Furthermore, this sensitivity appeared to be driven by a pathway independent of Mx, PKR, and RNaseL, as infection of mice triply deficient (TD) for these three factors were still protected upon infection with the nt3A mutant (L.J. White and R.E. Johnston, unpublished data). This suggested that an alternative innate pathway may be capable of mediating protection from VEE infection.

A similar investigation of Sindbis virus pathogenesis yielded a comparable phenotype, with TD and wildtype mice equally protected from Sindbis virus infection (62). A group of over 40 candidate effectors at play within this potential alternative

antiviral pathway were identified by microarray, including the interferon-stimulated genes IFIT1 (p56), IFIT2 (p54), GBP-2, and the ubiquitin homolog ISG15, among others (38). A recent study supported the notion of ISG15 being a central innate mediator following alphavirus infection, as ISG15-/- mice were more susceptible to Sindbis virus infection (139). Furthermore, the increased susceptibility of ISG15-/- mice to Sindbis virus infection could be rescued by expressing wild-type ISG15. Together, these results lend further evidence to the notion that several host innate antiviral factors play a role in protection from alphavirus infection.

In addition to the interferon-mediated innate response, a rapid proinflammatory response to VEE has been described. Highly elevated levels of proinflammatory cytokine gene expression have been documented in the DLN of mice infected with virulent VEE, including proinflammatory IL-6, IL-10, IL-12, and tumor necrosis factor alpha (TNFα) (130). Interestingly a similar level of expression was observed following avirulent VEE infection; however, the kinetics of expression were delayed by 24 h in comparison to virulent VEE. These results suggested that the kinetics of proinflammatory cytokine expression, in addition to relative sensitivity to IFN$\alpha\beta$, may influence the outcome of VEE infection.

However, there is evidence that this proinflammatory response as well as the interferon response, may also contribute to alphavirus-induced disease. For example, the production of large amounts of interferon and proinflammatory cytokines (e.g., TNFα, IL-1, and IL-6) during the acute-phase of alphavirus infection has been correlated with the rapid induction of fatal disease resembling toxic shock in newborn mice (140). iNOS and TNF receptor knockout mice exhibit extended

average survival times following infection with VEE, suggesting that the inflammatory response in the brain of infected animals mediated by these pathways may actually contribute to VEE-induced neurodegeneration (141, 142), consistent with the studies in SCID mice mentioned above (131). Therefore, regulation of the host response following alphavirus infection is critical, such that a balance can be found somewhere between an insufficient innate response and the induction of immunopathology.

In vitro models

In vitro studies also have yielded information regarding the specific components of innate immunity that are critical in the response to alphavirus infection. Treatment of cultured cells with IFN$\alpha\beta$ establishes an antiviral state that inhibits alphavirus replication, although the specific mechanism(s) of this inhibition are still not fully understood (63). However, it has been well established that the formation of dsRNA replication intermediates is a necessary step for interferon induction following alphavirus infection (143, 144). A recent study, investigating the role of interferon signaling in alphavirus-induced host translation shutoff, specifically examined the contribution of the dsRNA-mediated PKR pathway in host translation inhibition (145). Their findings revealed that PKR-dependent pathways were not the only means of inhibiting host translation during alphavirus infection, and suggested that a PKR-independent mechanism was more likely to be the major pathway mediating host translational shutoff. Furthermore, while this PKR-independent mechanism strongly affected the translation of cellular templates, translation of

Sindbis subgenomic RNA was resistant to inhibition, suggesting that 1) interferon signaling may inhibit alphavirus replication downstream of translation, and 2) alphaviruses may co-opt the interferon system to some extent in promoting their own replication (145).

In fact, recent data suggests that efficiency in the processing of the alphavirus nonstructural polyprotein precursor by the nsP2 protease may be a key determinant of virulence. Mutants with an accelerated rate of nonstructural protein processing are attenuated *in vivo*, while viruses with slower nonstructural protein processing demonstrate increased virulence potential (146). Furthermore, a recent correlation has been made between this accelerated processing phenotype and a subsequent increase in the amount of interferon induced during infection, which likely contributes to the attenuated phenotype of these mutants [M. Suthar and M. Heise, submitted manuscript]. The nonstructural polyprotein, as well as processing intermediates, may potentially play a role in the alphavirus resistance to the type I interferon response, possibly through interaction with and/or cleavage of the RIG-I pattern recognition receptor. Future studies along these lines will certainly yield valuable information regarding the innate recognition of, and innate immune response to, alphavirus infection.

REFERENCES

1. Janeway, C. A., and R. Medzhitov. 2002. Innate Immune Recognition. *Annual Review of Immunology* 20:197-216.

2. Medzhitov, R., and C. Janeway. 2000. Innate Immunity. *N Engl J Med* 343:338-344.

3. Akira, S., K. Takeda, and T. Kaisho. 2001. Toll-like receptors: critical proteins linking innate and acquired immunity. *Nat Immunol* 2:675-680.

4. Luster, A. D. 2002. The role of chemokines in linking innate and adaptive immunity. *Current Opinion in Immunology* 14:129-135.

5. Hoebe, K., E. Janssen, and B. Beutler. 2004. The interface between innate and adaptive immunity. *Nat Immunol* 5:971-974.

6. Steinman, R. M., and H. Hemmi. 2006. Dendritic cells: translating innate to adaptive immunity. *Curr Top Microbiol Immunol* 311:17-58.

7. Iwasaki, A., and R. Medzhitov. 2004. Toll-like receptor control of the adaptive immune responses. *Nat Immunol* 5:987-995.

8. Garcia-Sastre, A., and C. A. Biron. 2006. Type 1 Interferons and the Virus-Host Relationship: A Lesson in Detente. *Science* 312:879-882.

9. Perry, A. K., G. Chen, D. Zheng, H. Tang, and G. Cheng. 2005. The host type I interferon response to viral and bacterial infections. *Cell Res* 15:407-422.

10. Kawai, T., and S. Akira. 2006. Innate immune recognition of viral infection. *Nat Immunol* 7:131-137.

11. Yoneyama, M., M. Kikuchi, T. Natsukawa, N. Shinobu, T. Imaizumi, M. Miyagishi, K. Taira, S. Akira, and T. Fujita. 2004. The RNA helicase RIG-I has an essential function in double-stranded RNA-induced innate antiviral responses. *Nat Immunol* 5:730-737.

12. Seth, R. B., L. Sun, C. K. Ea, and Z. J. Chen. 2005. Identification and characterization of MAVS, a mitochondrial antiviral signaling protein that activates NF-kappaB and IRF 3. *Cell* 122:669-682.

13. Kawai, T., K. Takahashi, S. Sato, C. Coban, H. Kumar, H. Kato, K. J. Ishii, O. Takeuchi, and S. Akira. 2005. IPS-1, an adaptor triggering RIG-I- and Mda5-mediated type I interferon induction. *Nat Immunol* 6:981-988.

14. Meylan, E., J. Curran, K. Hofmann, D. Moradpour, M. Binder, R. Bartenschlager, and J. Tschopp. 2005. Cardif is an adaptor protein in the RIG-I antiviral pathway and is targeted by hepatitis C virus. *Nature* 437:1167-1172.

15. Xu, L. G., Y. Y. Wang, K. J. Han, L. Y. Li, Z. Zhai, and H. B. Shu. 2005. VISA is an adapter protein required for virus-triggered IFN-beta signaling. *Mol Cell* 19:727-740.

16. Stetson, D. B., and R. Medzhitov. 2006. Type I interferons in host defense. *Immunity* 25:373-381.

17. Kato, H., O. Takeuchi, S. Sato, M. Yoneyama, M. Yamamoto, K. Matsui, S. Uematsu, A. Jung, T. Kawai, K. J. Ishii, O. Yamaguchi, K. Otsu, T. Tsujimura, C. S. Koh, C. Reis e Sousa, Y. Matsuura, T. Fujita, and S. Akira. 2006. Differential roles of MDA5 and RIG-I helicases in the recognition of RNA viruses. *Nature* 441:101-105.

18. Isaacs, A., and J. Lindenmann. 1957. Virus interference. I. The interferon. *Proc R Soc Lond B Biol Sci* 147:258-267.

19. Sen, G. C. 2001. Viruses and interferons. *Annual Review of Microbiology* 55:255-281.

20. Pestka, S., C. D. Krause, and M. R. Walter. 2004. Interferons, interferon-like cytokines, and their receptors. *Immunological Reviews* 202:8-32.

21. Williams, B. R. 1991. Transcriptional regulation of interferon-stimulated genes. *Eur J Biochem* 200:1-11.

22. Biron, C. A., and G. C. Sen. 2001. Interferons and other cytokines. In *Fields virology, 4th ed.* D. M. Knipe, B. N. Fields, and P. M. Howley, eds. Lippincott Williams & Wilkins, Philadelphia, Pa.

23. Sheppard, P., W. Kindsvogel, W. Xu, K. Henderson, S. Schlutsmeyer, T. E. Whitmore, R. Kuestner, U. Garrigues, C. Birks, J. Roraback, C. Ostrander, D. Dong, J. Shin, S. Presnell, B. Fox, B. Haldeman, E. Cooper, D. Taft, T. Gilbert, F. J. Grant, M. Tackett, W. Krivan, G. McKnight, C. Clegg, D. Foster, and K. M. Klucher. 2003. IL-28, IL-29 and their class II cytokine receptor IL-28R. *Nat Immunol* 4:63-68.

24. Kotenko, S. V., G. Gallagher, V. V. Baurin, A. Lewis-Antes, M. Shen, N. K. Shah, J. A. Langer, F. Sheikh, H. Dickensheets, and R. P. Donnelly. 2003. IFN-[lambda]s mediate antiviral protection through a distinct class II cytokine receptor complex. *Nat Immunol* 4:69-77.

25. Malmgaard, L. 2004. Induction and Regulation of IFNs During Viral Infections. *Journal of Interferon & Cytokine Research* 24:439-454.

26. Levy, D. E., I. Marie, E. Smith, and A. Prakash. 2002. Enhancement and diversification of IFN induction by IRF-7-mediated positive feedback. *J Interferon Cytokine Res* 22:87-93.

27. Marie, I., J. E. Durbin, and D. E. Levy. 1998. Differential viral induction of distinct interferon-alpha genes by positive feedback through interferon regulatory factor-7. *Embo J* 17:6660-6669.

28. Sato, M., N. Hata, M. Asagiri, T. Nakaya, T. Taniguchi, and N. Tanaka. 1998. Positive feedback regulation of type I IFN genes by the IFN-inducible transcription factor IRF-7. *FEBS Letters* 441:106-110.

29. Prakash, A., E. Smith, C.-k. Lee, and D. E. Levy. 2005. Tissue-specific Positive Feedback Requirements for Production of Type I Interferon following Virus Infection. *J. Biol. Chem.* 280:18651-18657.

30. Yoneyama, M., W. Suhara, Y. Fukuhara, M. Sato, K. Ozato, and T. Fujita. 1996. Autocrine Amplification of Type I Interferon Gene Expression Mediated by Interferon Stimulated Gene Factor 3 (ISGF3). *J Biochem (Tokyo)* 120:160-169.

31. Gresser, I. 1984. Role of interferon in resistance to viral infection in vivo. In *Interferon: Vol 2: Interferons and the immne system*. J. Vilcek, De Maeyer E., ed. Elsevier Science, Amsterdam. 221-247.

32. Muller, U., U. Steinhoff, L. F. Reis, S. Hemmi, J. Pavlovic, R. M. Zinkernagel, and M. Aguet. 1994. Functional role of type I and type II interferons in antiviral defense. *Science* 264:1918-1921.

33. Katze, M. G., Y. He, and M. Gale, Jr. 2002. Viruses and interferon: a fight for supremacy. *Nat Rev Immunol* 2:675-687.

34. Geiss, G., G. Jin, J. Guo, R. Bumgarner, M. G. Katze, and G. C. Sen. 2001. A Comprehensive View of Regulation of Gene Expression by Double-stranded RNA-mediated Cell Signaling. *Journal of Biological Chemistry* 276:30178-30182.

35. Kash, J. C., C. F. Basler, A. Garcia-Sastre, V. Carter, R. Billharz, D. E. Swayne, R. M. Przygodzki, J. K. Taubenberger, M. G. Katze, and T. M. Tumpey. 2004. Global Host Immune Response: Pathogenesis and Transcriptional Profiling of Type A Influenza Viruses Expressing the Hemagglutinin and Neuraminidase Genes from the 1918 Pandemic Virus. *J. Virol.* 78:9499-9511.

36. Kent, J. R., and N. W. Fraser. 2005. The cellular response to herpes simplex virus type 1 (HSV-1) during latency and reactivation. *J Neurovirol* 11:376-383.

37. Mossman, K. L., P. F. Macgregor, J. J. Rozmus, A. B. Goryachev, A. M. Edwards, and J. R. Smiley. 2001. Herpes Simplex Virus Triggers and Then Disarms a Host Antiviral Response. *J. Virol.* 75:750-758.

38. Ryman, K. D., K. C. Meier, E. M. Nangle, S. L. Ragsdale, N. L. Korneeva, R. E. Rhoads, M. R. MacDonald, and W. B. Klimstra. 2005. Sindbis Virus Translation Is Inhibited by a PKR/RNase L-Independent Effector Induced by Alpha/Beta Interferon Priming of Dendritic Cells. *The Journal of Virology* 79:1487-1499.

39. Labrada, L., X. H. Liang, W. Zheng, C. Johnston, and B. Levine. 2002. Age-Dependent Resistance to Lethal Alphavirus Encephalitis in Mice: Analysis of Gene Expression in the Central Nervous System and Identification of a Novel Interferon-Inducible Protective Gene, Mouse ISG12. *The Journal of Virology* 76:11688-11703.

40. Fang, X., M. B. Zeisel, J. Wilpert, B. Gissler, R. Thimme, C. Kreutz, T. Maiwald, J. Timmer, W. V. Kern, J. Donauer, M. Geyer, G. Walz, E. Depla, F. von Weizsacker, H. E. Blum, and T. F. Baumert. 2006. Host cell responses induced by hepatitis C virus binding. *Hepatology* 43:1326-1336.

41. Geiss, G. K., V. S. Carter, Y. He, B. K. Kwieciszewski, T. Holzman, M. J. Korth, C. A. Lazaro, N. Fausto, R. E. Bumgarner, and M. G. Katze. 2003. Gene Expression Profiling of the Cellular Transcriptional Network Regulated by Alpha/Beta Interferon and Its Partial Attenuation by the Hepatitis C Virus Nonstructural 5A Protein. *J. Virol.* 77:6367-6375.

42. de Veer, M. J., M. Holko, M. Frevel, E. Walker, S. Der, J. M. Paranjape, R. H. Silverman, and B. R. G. Williams. 2001. Functional classification of interferon-stimulated genes identified using microarrays. *J Leukoc Biol* 69:912-920.

43. Der, S. D., A. Zhou, B. R. G. Williams, and R. H. Silverman. 1998. Identification of genes differentially regulated by interferon alpha , beta , or gamma using oligonucleotide arrays. *PNAS* 95:15623-15628.

44. Ito, T., M. Yang, and W. S. May. 1999. RAX, a Cellular Activator for Double-stranded RNA-dependent Protein Kinase during Stress Signaling. *J. Biol. Chem.* 274:15427-15432.

45. Tan, S. L., and M. G. Katze. 1999. The emerging role of the interferon-induced PKR protein kinase as an apoptotic effector: a new face of death? *J Interferon Cytokine Res* 19:543-554.

46. Stojdl, D. F., N. Abraham, S. Knowles, R. Marius, A. Brasey, B. D. Lichty, E. G. Brown, N. Sonenberg, and J. C. Bell. 2000. The Murine Double-Stranded RNA-Dependent Protein Kinase PKR Is Required for Resistance to Vesicular Stomatitis Virus. *J. Virol.* 74:9580-9585.

47. Abraham, N., D. F. Stojdl, P. I. Duncan, N. Methot, T. Ishii, M. Dube, B. C. Vanderhyden, H. L. Atkins, D. A. Gray, M. W. McBurney, A. E. Koromilas, E. G. Brown, N. Sonenberg, and J. C. Bell. 1999. Characterization of Transgenic Mice with Targeted Disruption of the Catalytic Domain of the Double-stranded RNA-dependent Protein Kinase, PKR. *J. Biol. Chem.* 274:5953-5962.

48. Sarkar, S. N., S. Bandyopadhyay, A. Ghosh, and G. C. Sen. 1999. Enzymatic Characteristics of Recombinant Medium Isozyme of 2'-5' Oligoadenylate Synthetase. *J. Biol. Chem.* 274:1848-1855.

49. Scherbik, S. V., J. M. Paranjape, B. M. Stockman, R. H. Silverman, and M. A. Brinton. 2006. RNase L Plays a Role in the Antiviral Response to West Nile Virus. *J. Virol.* 80:2987-2999.

50. Samuel, M. A., K. Whitby, B. C. Keller, A. Marri, W. Barchet, B. R. G. Williams, R. H. Silverman, M. Gale, Jr., and M. S. Diamond. 2006. PKR and RNase L Contribute to Protection against Lethal West Nile Virus Infection by Controlling Early Viral Spread in the Periphery and Replication in Neurons. *J. Virol.* 80:7009-7019.

51. Anderson, S. L., J. M. Carton, J. Lou, L. Xing, and B. Y. Rubin. 1999. Interferon-induced guanylate binding protein-1 (GBP-1) mediates an antiviral effect against vesicular stomatitis virus and encephalomyocarditis virus. *Virology* 256:8-14.

52. Kochs, G., C. Janzen, H. Hohenberg, and O. Haller. 2002. Antivirally active MxA protein sequesters La Crosse virus nucleocapsid protein into perinuclear complexes. *PNAS* 99:3153-3158.

53. Frese, M., G. Kochs, H. Feldmann, C. Hertkorn, and O. Haller. 1996. Inhibition of bunyaviruses, phleboviruses, and hantaviruses by human MxA protein. *J. Virol.* 70:915-923.

54. Chen, J.-P., H.-L. Lu, S.-L. Lai, G. S. Campanella, J.-M. Sung, M.-Y. Lu, B. A. Wu-Hsieh, Y.-L. Lin, T. E. Lane, A. D. Luster, and F. Liao. 2006. Dengue Virus Induces Expression of CXC Chemokine Ligand 10/IFN-{gamma}-Inducible Protein 10, Which Competitively Inhibits Viral Binding to Cell Surface Heparan Sulfate. *J Immunol* 177:3185-3192.

55. Guo, J., K. L. Peters, and G. C. Sen. 2000. Induction of the human protein P56 by interferon, double-stranded RNA, or virus infection. *Virology* 267:209-219.

56. Terenzi, F., D. J. Hui, W. C. Merrick, and G. C. Sen. 2006. Distinct Induction Patterns and Functions of Two Closely Related Interferon-inducible Human Genes, ISG54 and ISG56. *J. Biol. Chem.* 281:34064-34071.

57. Terenzi, F., S. Pal, and G. C. Sen. 2005. Induction and mode of action of the viral stress-inducible murine proteins, P56 and P54. *Virology* 340:116-124.

58. Hui, D. J., C. R. Bhasker, W. C. Merrick, and G. C. Sen. 2003. Viral Stress-inducible Protein p56 Inhibits Translation by Blocking the Interaction of eIF3 with the Ternary Complex eIF2{middle dot}GTP{middle dot}Met-tRNAi. *J. Biol. Chem.* 278:39477-39482.

59. Hui, D. J., F. Terenzi, W. C. Merrick, and G. C. Sen. 2005. Mouse p56 Blocks a Distinct Function of Eukaryotic Initiation Factor 3 in Translation Initiation. *J. Biol. Chem.* 280:3433-3440.

60. Garcia-Sastre, A. 2002. Mechanisms of inhibition of the host interferon [alpha]/[beta]-mediated antiviral responses by viruses. *Microbes and Infection* 4:647-655.

61. Zhou, A., J. M. Paranjape, S. D. Der, B. R. G. Williams, and R. H. Silverman. 1999. Interferon Action in Triply Deficient Mice Reveals the Existence of Alternative Antiviral Pathways. *Virology* 258:435-440.

62. Ryman, K. D., L. J. White, R. E. Johnston, and W. B. Klimstra. 2002. Effects of PKR/RNase L-Dependent and Alternative Antiviral Pathways on Alphavirus Replication and Pathogenesis. *Viral Immunology* 15:53-76.

63. Griffin, D. E. 2001. Alphaviruses. In *Fields virology, 4th ed.* D. M. Knipe, B. N. Fields, and P. M. Howley, eds. Lippincott Williams & Wilkins, Philadelphia, Pa. 917-962.

64. Weaver, S. C., and A. D. T. Barrett. 2004. Transmission cycles, host range, evolution and emergence of arboviral disease. *Nature Reviews Microbiology* 2:789-801.

65. Sudia, W. D., and V. F. Newhouse. 1975. Epidemic Venezuelan equine encephalitis in North America: A summary of virus-vector-host relationships. *Am. J. Epidemiol.* 101:1-13.

66. Weaver, S. C., C. Ferro, R. Barrera, J. Boshell, and J.-C. Navarro. 2004. Venezuelan equine encephalitis. *Annual Review of Entomology* 49:141-174.

67. Casals, J., E. C. Curnen, and L. Thomas. 1943. Venezuelan equine encephalomyelitis in man *J. Exp. Med.* 77:521-530.

68. Berge, T. O., I. S. Banks, and W. D. Tigertt. 1961. Attenuation of Venezuelan equine encephalomyelitis virus by in vitro cultivation in guinea-pig heart cells. *Am. J. Epidemiol.* 73:209-218.

69. Weaver, S. C., R. Salas, R. Rico-Hesse, G. V. Ludwig, M. S. Oberste, J. Boshell, and R. B. Tesh. 1996. Re-emergence of epidemic Venezuelan equine encephalomyelitis in South America. *The Lancet* 348:436-440.

70. Rico-Hesse, R., S. C. Weaver, J. de Siger, G. Medina, and R. A. Salas. 1995. Emergence of a New Epidemic/Epizootic Venezuelan Equine Encephalitis Virus in South America. *PNAS* 92:5278-5281.

71. Anishchenko, M., R. A. Bowen, S. Paessler, L. Austgen, I. P. Greene, and S. C. Weaver. 2006. Venezuelan encephalitis emergence mediated by a phylogenetically predicted viral mutation. *PNAS* 103:4994-4999.

72. Strauss, J. H., and E. G. Strauss. 1994. The alphaviruses: gene expression, replication, and evolution. *Microbiol Rev* 58:491-562.

73. Niesters, H. G., and J. H. Strauss. 1990. Defined mutations in the 5' nontranslated sequence of Sindbis virus RNA. *J Virol* 64:4162-4168.

74. Kuhn, R. J., Z. Hong, and J. H. Strauss. 1990. Mutagenesis of the 3' nontranslated region of Sindbis virus RNA. *J Virol* 64:1465-1476.

75. Paredes, A. M., D. T. Brown, R. Rothnagel, W. Chiu, R. J. Schoepp, R. E. Johnston, and B. V. V. Prasad. 1993. Three-Dimensional Structure of a Membrane-Containing Virus. *PNAS* 90:9095-9099.

76. Paredes, A. M., M. N. Simon, and D. T. Brown. 1992. The mass of the Sindbis virus nucleocapsid suggests it has T = 4 icosahedral symmetry. *Virology* 187:329-332.

77. Cheng, R. H., R. J. Kuhn, N. H. Olson, M. G. Rossmann, H. K. Choi, T. J. Smith, and T. S. Baker. 1995. Nucleocapsid and glycoprotein organization in an enveloped virus. *Cell* 80:621-630.

78. Zhang, W., S. Mukhopadhyay, S. V. Pletnev, T. S. Baker, R. J. Kuhn, and M. G. Rossmann. 2002. Placement of the Structural Proteins in Sindbis Virus. *J. Virol.* 76:11645-11658.

79. Pletnev, S. V., W. Zhang, S. Mukhopadhyay, B. R. Fisher, R. Hernandez, D. T. Brown, T. S. Baker, M. G. Rossmann, and R. J. Kuhn. 2001. Locations of

carbohydrate sites on alphavirus glycoproteins show that E1 forms an icosahedral scaffold. *Cell* 105:127-136.

80. Ludwig, G. V., J. P. Kondig, and J. F. Smith. 1996. A putative receptor for Venezuelan equine encephalitis virus from mosquito cells. *J. Virol.* 70:5592-5599.

81. Klimstra, W. B., E. M. Nangle, M. S. Smith, A. D. Yurochko, and K. D. Ryman. 2003. DC-SIGN and L-SIGN Can Act as Attachment Receptors for Alphaviruses and Distinguish between Mosquito Cell- and Mammalian Cell-Derived Viruses. *J. Virol.* 77:12022-12032.

82. Bernard, K. A., W. B. Klimstra, and R. E. Johnston. 2000. Mutations in the E2 Glycoprotein of Venezuelan Equine Encephalitis Virus Confer Heparan Sulfate Interaction, Low Morbidity, and Rapid Clearance from Blood of Mice. *Virology* 276:93-103.

83. Kolokoltsov, A. A., E. H. Fleming, and R. A. Davey. 2006. Venezuelan equine encephalitis virus entry mechanism requires late endosome formation and resists cell membrane cholesterol depletion. *Virology* 347:333-342.

84. Paredes, A. M., D. Ferreira, M. Horton, A. Saad, H. Tsuruta, R. Johnston, W. Klimstra, K. Ryman, R. Hernandez, W. Chiu, and D. T. Brown. 2004. Conformational changes in Sindbis virions resulting from exposure to low pH and interactions with cells suggest that cell penetration may occur at the cell surface in the absence of membrane fusion. *Virology* 324:373-386.

85. Garmashova, N., R. Gorchakov, E. Volkova, S. Paessler, E. Frolova, and I. Frolov. 2007. The Old World and New World Alphaviruses Use Different Virus-Specific Proteins for Induction of Transcriptional Shutoff. *J. Virol.* 81:2472-2484.

86. Gorchakov, R., E. Frolova, and I. Frolov. 2005. Inhibition of Transcription and Translation in Sindbis Virus-Infected Cells. *J. Virol.* 79:9397-9409.

87. Wang, E., R. A. Bowen, G. Medina, A. M. Powers, W. Kang, L. M. Chandler, R. E. Shope, and S. C. Weaver. 2001. Virulence and viremia characteristics of 1992 epizootic subtype IC Venezuelan equine encephalitis viruses and closely related enzootic subtype ID strains. *Am J Trop Med Hyg* 65:64-69.

88. Johnson, K. M., and D. H. Martin. 1974. Venezuelan equine encephalitis. *Adv Vet Sci Comp Med* 18:79-116.

89. Kissling, R. E., R. W. Chamberlain, D. B. Nelson, and D. D. Stamm. 1956. Venezuelan equine encephalomyelitis in horses. *Am J Hyg* 63:274-287.

90. Gleiser, C. A., W. S. Gochenour, Jr., T. O. Berge, and W. D. Tigertt. 1962. The comparative pathology of experimental Venezuelan equine encephalomyelitis infection in different animal hosts. *J Infect Dis* 110:80-97.

91. Rivas, F., L. A. Diaz, V. M. Cardenas, E. Daza, L. Bruzon, A. Alcala, O. De la Hoz, F. M. Caceres, G. Aristizabal, J. W. Martinez, D. Revelo, F. De la Hoz, J. Boshell, T. Camacho, L. Calderon, V. A. Olano, L. I. Villarreal, D. Roselli, G. Alvarez, G. Ludwig, and T. Tsai. 1997. Epidemic Venezuelan equine encephalitis in La Guajira, Colombia, 1995. *J Infect Dis* 175:828-832.

92. Ehrenkranz, N. J., and A. K. Ventura. 1974. Venezuelan equine encephalitis virus infection in man. *Annu Rev Med* 25:9-14.

93. Muehlenbein, M., F. Cogswell, M. James, J. Koterski, and G. Ludwig. 2006. Testosterone correlates with Venezuelan equine encephalitis virus infection in macaques. *Virology Journal* 3:19.

94. Reed, D. S., C. M. Lind, L. J. Sullivan, W. D. Pratt, and M. D. Parker. 2004. Aerosol infection of cynomolgus macaques with enzootic strains of venezuelan equine encephalitis viruses. *J Infect Dis* 189:1013-1017.

95. Monath, T. P., C. H. Calisher, M. Davis, G. S. Bowen, and J. White. 1974. Experimental studies of rhesus monkeys infected with epizootic and enzootic subtypes of Venezuelan equine encephalitis virus. *J Infect Dis* 129:194-200.

96. Danes, L., V. Rychterova, V. Kliment, and J. Hruskova. 1973. Penetration of Venezuelan equine encephalomyelitis virus into the brain of guinea pigs and rabbits after intranasal infection. *Acta Virol* 17:138-146.

97. Koprowski, H., and E. H. Lennette. 1944. Pathogenesis of Venezuelan Equine Encephalomyelitis Virus Infections in the Developing Chick Embryo. *J Bacteriol* 48:463-472.

98. Koprowski, H., and E. H. Lennette. 1946. Comparative Sensitivity of Venezuelan Equine Encephalomyelitis Virus Neutralization Tests in Chick Embryos and in Mice. *J Bacteriol* 51:257-261.

99. Jahrling, P. B., E. Navarro, and W. F. Scherer. 1976. Interferon induction and sensitivity as correlates to virulence of Venezuelan encephalitis viruses for hamsters. *Arch Virol* 51:23-35.

100. Jahrling, P. B., and F. Scherer. 1973. Histopathology and distribution of viral antigens in hamsters infected with virulent and benign Venezuelan encephalitis viruses. *Am J Pathol* 72:25-38.

101. Jahrling, P. B., and W. F. Scherer. 1973. Growth curves and clearance rates of virulent and benign Venezuelan encephalitis viruses in hamsters. *Infect Immun* 8:456-462.

102. Jackson, A. C., S. K. SenGupta, and J. F. Smith. 1991. Pathogenesis of Venezuelan equine encephalitis virus infection in mice and hamsters. *Vet Pathol* 28:410-418.

103. Jahrling, P. B., G. B. Heisey, and R. A. Hesse. 1977. Evaluation of vascular clearance as a marker for virulence of alphaviruses: disassociation of rapid clearance with low virulence of venezuelan encephalitis virus strains in guinea pigs. *Infect Immun* 17:356-360.

104. Davis, N. L., L. V. Willis, J. F. Smith, and R. E. Johnston. 1989. In vitro synthesis of infectious venezuelan equine encephalitis virus RNA from a cDNA clone: analysis of a viable deletion mutant. *Virology* 171:189-204.

105. Grieder, F. B., N. L. Davis, J. F. Aronson, P. C. Charles, D. C. Sellon, K. Suzuki, and R. E. Johnston. 1995. Specific Restrictions in the Progression of Venezuelan Equine Encephalitis Virus-Induced Disease Resulting from Single Amino Acid Changes in the Glycoproteins. *Virology* 206:994-1006.

106. Charles, P. C., E. Walters, F. Margolis, and R. E. Johnston. 1995. Mechanism of Neuroinvasion of Venezuelan Equine Encephalitis Virus in the Mouse. *Virology* 208:662-671.

107. Vogel, P., D. Abplanalp, W. Kell, M. S. Ibrahim, M. B. Downs, W. D. Pratt, and K. J. Davis. 1996. Venezuelan equine encephalitis in BALB/c mice: kinetic analysis of central nervous system infection following aerosol or subcutaneous inoculation. *Arch Pathol Lab Med* 120:164-172.

108. Ryzhikov, A. B., E. I. Ryabchikova, A. N. Sergeev, and N. V. Tkacheva. 1995. Spread of Venezuelan equine encephalitis virus in mice olfactory tract. *Arch Virol* 140:2243-2254.

109. Jackson, A. C., and P. R. John. 1997. Apoptotic cell death is an important cause of neuronal injury in experimental Venezuelan equine encephalitis virus infection of mice. *Acta Neuropathologica* V93:349-353.

110. Johnston, R. E., and J. F. Smith. 1988. Selection for accelerated penetration in cell culture coselects for attenuated mutants of Venezuelan equine encephalitis virus. *Virology* 162:437-443.

111. Davis, N. L., F. B. Grieder, J. F. Smith, G. F. Greenwald, M. L. Valenski, D. C. Sellon, P. C. Charles, and R. E. Johnston. 1994. A molecular genetic

approach to the study of Venezuelan equine encephalitis virus pathogenesis. *Arch Virol Suppl* 9:99-109.

112. Davis, N. L., N. Powell, G. F. Greenwald, L. V. Willis, B. J. Johnson, J. F. Smith, and R. E. Johnston. 1991. Attenuating mutations in the E2 glycoprotein gene of Venezuelan equine encephalitis virus: construction of single and multiple mutants in a full-length cDNA clone. *Virology* 183:20-31.

113. Aronson, J. F., F. B. Grieder, N. L. Davis, P. C. Charles, T. Knott, K. Brown, and R. E. Johnston. 2000. A Single-Site Mutant and Revertants Arising in Vivo Define Early Steps in the Pathogenesis of Venezuelan Equine Encephalitis Virus. *Virology* 270:111-123.

114. Davis, N. L., K. W. Brown, G. F. Greenwald, A. J. Zajac, V. L. Zacny, J. F. Smith, and R. E. Johnston. 1995. Attenuated Mutants of Venezuelan Equine Encephalitis Virus Containing Lethal Mutations in the PE2 Cleavage Signal Combined with a Second-Site Suppressor Mutation in E1. *Virology* 212:102-110.

115. Pushko, P., M. Parker, G. V. Ludwig, N. L. Davis, R. E. Johnston, and J. F. Smith. 1997. Replicon-Helper Systems from Attenuated Venezuelan Equine Encephalitis Virus: Expression of Heterologous Genes in Vitro and Immunization against Heterologous Pathogens in Vivo. *Virology* 239:389-401.

116. MacDonald, G. H., and R. E. Johnston. 2000. Role of Dendritic Cell Targeting in Venezuelan Equine Encephalitis Virus Pathogenesis. *The Journal of Virology* 74:914-922.

117. Polo, J. M., J. P. Gardner, Y. Ji, B. A. Belli, D. A. Driver, S. Sherrill, S. Perri, M. A. Liu, and T. W. Dubensky, Jr. 2000. Alphavirus DNA and particle replicons for vaccines and gene therapy. *Dev Biol (Basel)* 104:181-185.

118. Davis, N. L., A. West, E. Reap, G. MacDonald, M. Collier, S. Dryga, M. Maughan, M. Connell, C. Walker, K. McGrath, C. Cecil, L. H. Ping, J. Frelinger, R. Olmsted, P. Keith, R. Swanstrom, C. Williamson, P. Johnson, D. Montefiori, and R. E. Johnston. 2002. Alphavirus replicon particles as candidate HIV vaccines. *IUBMB Life* 53:209-211.

119. Thornburg, N. J., C. A. Ray, M. L. Collier, H. X. Liao, D. J. Pickup, and R. E. Johnston. 2007. Vaccination with Venezuelan equine encephalitis replicons encoding cowpox virus structural proteins protects mice from intranasal cowpox virus challenge. *Virology*.

120. Lee, J. S., J. L. Groebner, A. G. Hadjipanayis, D. L. Negley, A. L. Schmaljohn, S. L. Welkos, L. A. Smith, and J. F. Smith. 2006. Multiagent vaccines vectored by Venezuelan equine encephalitis virus replicon elicits immune

responses to Marburg virus and protection against anthrax and botulinum neurotoxin in mice. *Vaccine* 24:6886-6892.

121. Balasuriya, U. B., H. W. Heidner, N. L. Davis, H. M. Wagner, P. J. Hullinger, J. F. Hedges, J. C. Williams, R. E. Johnston, W. David Wilson, I. K. Liu, and N. James MacLachlan. 2002. Alphavirus replicon particles expressing the two major envelope proteins of equine arteritis virus induce high level protection against challenge with virulent virus in vaccinated horses. *Vaccine* 20:1609-1617.

122. Schultz-Cherry, S., J. K. Dybing, N. L. Davis, C. Williamson, D. L. Suarez, R. Johnston, and M. L. Perdue. 2000. Influenza virus (A/HK/156/97) hemagglutinin expressed by an alphavirus replicon system protects chickens against lethal infection with Hong Kong-origin H5N1 viruses. *Virology* 278:55-59.

123. Thompson, J. M., A. C. Whitmore, J. L. Konopka, M. L. Collier, E. M. B. Richmond, N. L. Davis, H. F. Staats, and R. E. Johnston. 2006. Mucosal and systemic adjuvant activity of alphavirus replicon particles. *PNAS* 103:3722-3727.

124. Greenway, T. E., J. H. Eldridge, G. Ludwig, J. K. Staas, J. F. Smith, R. M. Gilley, and S. M. Michalek. 1998. Induction of protective immune responses against Venezuelan equine encephalitis (VEE) virus aerosol challenge with microencapsulated VEE virus vaccine. *Vaccine* 16:1314-1323.

125. Pittman, P. R., R. S. Makuch, J. A. Mangiafico, T. L. Cannon, P. H. Gibbs, and C. J. Peters. 1996. Long-term duration of detectable neutralizing antibodies after administration of live-attenuated VEE vaccine and following booster vaccination with inactivated VEE vaccine. *Vaccine* 14:337-343.

126. Charles, P. C., K. W. Brown, N. L. Davis, M. K. Hart, and R. E. Johnston. 1997. Mucosal immunity induced by parenteral immunization with a live attenuated Venezuelan equine encephalitis virus vaccine candidate. *Virology* 228:153-160.

127. Hart, M. K., W. Pratt, F. Panelo, R. Tammariello, and M. Dertzbaugh. 1997. Venezuelan equine encephalitis virus vaccines induce mucosal IgA responses and protection from airborne infection in BALB/c, but not C3H/HeN mice. *Vaccine* 15:363-369.

128. Casals, J., S. M. Buckley, and D. W. Barry. 1973. Resistance to arbovirus challenge in mice immediately after vaccination. *Appl Microbiol* 25:755-762.

129. Huprikar, J., M. C. Dal Canto, and S. G. Rabinowitz. 1990. Protection against lethal Venezuelan equine encephalitis (VEE) virus infection by cell-free

supernatant obtained from immune spleen cells. *Journal of the Neurological Sciences* 97:143-153.

130. Grieder, F. B., B. K. Davis, X. D. Zhou, S. J. Chen, F. D. Finkelman, and W. C. Gause. 1997. Kinetics of Cytokine Expression and Regulation of Host Protection Following Infection with Molecularly Cloned Venezuelan Equine Encephalitis Virus. *Virology* 233:302-312.

131. Charles, P. C., J. Trgovcich, N. L. Davis, and R. E. Johnston. 2001. Immunopathogenesis and Immune Modulation of Venezuelan Equine Encephalitis Virus-Induced Disease in the Mouse. *Virology* 284:190-202.

132. Grieder, F. B., and S. N. Vogel. 1999. Role of Interferon and Interferon Regulatory Factors in Early Protection against Venezuelan Equine Encephalitis Virus Infection. *Virology* 257:106-118.

133. White, L. J., J. g. Wang, N. L. Davis, and R. E. Johnston. 2001. Role of Alpha/Beta Interferon in Venezuelan Equine Encephalitis Virus Pathogenesis: Effect of an Attenuating Mutation in the 5' Untranslated Region. *The Journal of Virology* 75:3706.

134. Jordan, G. W. 1973. Interferon sensitivity of Venezuelan equine encephalomyelitis virus. *Infect Immun* 7:911-917.

135. Pinto, A. J., P. S. Morahan, and M. A. Brinton. 1988. Comparative study of various immunomodulators for macrophage and natural killer cell activation and antiviral efficacy against exotic RNA viruses. *International Journal of Immunopharmacology* 10:197-209.

136. Lukaszewski, R. A., and T. J. G. Brooks. 2000. Pegylated Alpha Interferon Is an Effective Treatment for Virulent Venezuelan Equine Encephalitis Virus and Has Profound Effects on the Host Immune Response to Infection. *J. Virol.* 74:5006-5015.

137. Spotts, D. R., R. M. Reich, M. A. Kalkhan, R. M. Kinney, and J. T. Roehrig. 1998. Resistance to Alpha/Beta Interferons Correlates with the Epizootic and Virulence Potential of Venezuelan Equine Encephalitis Viruses and Is Determined by the 5' Noncoding Region and Glycoproteins. *The Journal of Virology* 72:10286-10291.

138. Kinney, R. M., G. J. Chang, K. R. Tsuchiya, J. M. Sneider, J. T. Roehrig, T. M. Woodward, and D. W. Trent. 1993. Attenuation of Venezuelan equine encephalitis virus strain TC-83 is encoded by the 5'-noncoding region and the E2 envelope glycoprotein. *The Journal of Virology* 67:1269-1277.

139. Lenschow, D. J., N. V. Giannakopoulos, L. J. Gunn, C. Johnston, A. K. O'Guin, R. E. Schmidt, B. Levine, and H. W. I. V. Virgin. 2005. Identification of Interferon-Stimulated Gene 15 as an Antiviral Molecule during Sindbis Virus Infection In Vivo. *J. Virol.* 79:13974-13983.

140. Klimstra, W. B., K. D. Ryman, K. A. Bernard, K. B. Nguyen, C. A. Biron, and R. E. Johnston. 1999. Infection of Neonatal Mice with Sindbis Virus Results in a Systemic Inflammatory Response Syndrome. *J. Virol.* 73:10387-10398.

141. Schoneboom, B. A., K. M. K. Catlin, A. M. Marty, and F. B. Grieder. 2000. Inflammation is a component of neurodegeneration in response to Venezuelan equine encephalitis virus infection in mice. *Journal of Neuroimmunology* 109:132-146.

142. Schoneboom, B. A., J. S. Lee, and F. B. Grieder. 2000. Early Expression of IFN-alpha/beta and iNOS in the Brains of Venezuelan Equine Encephalitis Virus-Infected Mice. *Journal of Interferon & Cytokine Research* 20:205-216.

143. Hahn, Y. S., E. G. Strauss, and J. H. Strauss. 1989. Mapping of RNA-temperature-sensitive mutants of Sindbis virus: assignment of complementation groups A, B, and G to nonstructural proteins. *J Virol* 63:3142-3150.

144. Marcus, P. I., and F. J. Fuller. 1979. Interferon induction by viruses. II. Sindbis virus: interferon induction requires one-quarter of the genome--genes G and A. *J Gen Virol* 44:169-177.

145. Gorchakov, R., E. Frolova, B. R. G. Williams, C. M. Rice, and I. Frolov. 2004. PKR-Dependent and -Independent Mechanisms Are Involved in Translational Shutoff during Sindbis Virus Infection. *J. Virol.* 78:8455-8467.

146. Heise, M. T., L. J. White, D. A. Simpson, C. Leonard, K. A. Bernard, R. B. Meeker, and R. E. Johnston. 2003. An Attenuating Mutation in nsP1 of the Sindbis-Group Virus S.A.AR86 Accelerates Nonstructural Protein Processing and Up-Regulates Viral 26S RNA Synthesis. *J. Virol.* 77:1149-1156.

CHAPTER TWO

A NOVEL TWO-PHASE INNATE HOST RESPONSE TO ALPHAVIRUS INFECTION IDENTIFIED BY mRNP-TAGGING IN VIVO

Jennifer L. Konopka, Luiz O. Penalva, Joseph M. Thompson, Laura J. White, Jack D. Keene, and Robert E. Johnston

ABSTRACT

A concept fundamental to viral pathogenesis is that infection induces specific changes within the host cell, within specific tissues, or within the entire animal. These changes are reflected in a cascade of altered transcription patterns evident following infection. However, elucidation of this cascade *in vivo* has been limited by a general inability to distinguish changes occurring in the minority of infected cells from those in surrounding uninfected cells. To circumvent this inherent limitation of traditional gene expression profiling methods, an innovative mRNP-tagging technique was implemented to isolate host mRNA specifically from infected cells *in vitro* as well as *in vivo* following Venezuelan equine encephalitis virus (VEE) infection. This technique facilitated a direct characterization of the host defense response specifically within the first cells infected with VEE, while simultaneous total RNA analysis assessed the collective response of both the infected and uninfected cells. The result was a unique, multifaceted profile of the early response to VEE infection in primary dendritic cells, as well as in the draining lymph node, the initially targeted tissue in the mouse model. A dynamic environment of complex interactions was revealed, and suggested a two step innate response in which activation of a subset of host genes in infected cells subsequently leads to activation of the surrounding uninfected cells. In addition to wildtype infection, the host response to infection with a mutant containing a single noncoding change in the 5'UTR was explored. Although this mutation confers a heightened sensitivity to the interferon-induced antiviral state, the mRNP-tagging system demonstrated that the resulting attenuation was not a function of an increased induction of antiviral effectors at early

times within infected cells. Our findings suggest that the application of viral mRNP-tagging systems, as introduced here, will facilitate a much more detailed understanding of the highly coordinated host response to infectious agents.

INTRODUCTION

At the interface of pathogen infection and host response lies a complex network of regulated interactions. As the host seeks to eradicate the pathogen and maintain survival, the pathogen itself seeks to continue its own proliferation at whatever cost is necessary to the host cell. Therefore, the insult associated with viral infection often involves numerous changes in host gene expression. Fundamental to many viral pathogenesis studies is the investigation of these specific changes within the host cell, or on a more global scale, within a specific tissue, organ, or the entire animal. Although it has been possible in several systems to singularly identify cellular genes that are altered in expression due to infection, these genes most likely represent a very small fraction of all the genes induced or repressed. The advent of high-throughput genomic profiling technologies has greatly expanded the ability to monitor the cellular response to pathogen stimuli in a global manner. In an attempt to more fully understand the interactions between pathogen and host, virologists have turned to cDNA array analysis within the past decade to evaluate the status of host gene expression post-infection. Although widely informative, there remains an inherent limitation in applying microarray analysis to viral pathogenesis studies. In the absence of an acutely susceptible system in which all cells can be uniformly infected, a heterogeneous environment of infected and uninfected cells naturally exists during viral infection. This is

particularly true *in vivo*, where only a minority of cells in a given tissue or organ are infected, even when that tissue is a major target of infection. In traditional microarray analysis utilizing total RNA isolation, there is an inability to discriminate the population of host mRNAs isolated from the infected cells versus the surrounding uninfected cells. As the percentage of uninfected cells is high *in vivo*, mRNA from uninfected cells likely creates background signal that skews or masks the analysis from infected cells. Discriminating the direct viral impact on infected cells from the subsequent effects on bystander uninfected cells is critical to fully understanding the pathogenesis of a given virus, yet most analyses lack this distinction.

To circumvent this limitation, we have optimized and implemented an innovative mRNP-tagging technique to isolate host mRNA specifically from infected cells following viral infection in cultured cells as well as tissues *in vivo*. The mRNP-tagging technology was originally developed from a functional genomics approach termed *ribonomics*, which examines mRNAs functionally clustered in ribonucleoprotein complexes (1, 2). The mRNP-tagging system takes advantage of the natural interaction of RNA-binding proteins with cellular mRNA to effectively enrich and isolate messages from a specific minority cell type within a heterogeneous environment. One such interaction that has been used in several systems is the well established strong binding of poly(A) binding protein I (PABP) to the poly(A) tail of cellular mRNAs prior to translation (3-8). In the mRNP-tagging technique, a unique version of PABP engineered with an epitope tag, is expressed in a cell- or tissue-specific manner. The cellular mRNA bound to the tagged-PABP is then co-immunoprecipitated using an anti-epitope antibody, enriching the mRNA

from the targeted cell population and separating it from the mRNA of the surrounding cells or tissues (1, 2, 9). Gene profiling methods such as cDNA microarrays or quantitative real-time PCR can then be performed using the enriched mRNA population to assess the gene expression status within the cell or tissue population of interest. This method has been successfully applied to identify tissue-specific mRNA populations in *Caenohabditis elegans* and *Drosophila melanogaster* (10-13), as well as to identify cell type-specific gene expression changes in mixed cell culture models *in vitro* (14).

Here, we have adopted the mRNP-tagging technique to characterize host gene expression changes following infection with Venezuelan equine encephalitis virus (VEE). VEE is an arthropod-borne, single stranded (+)sense RNA virus associated with periodic epidemics and equine epizootics in the Western Hemisphere, and serves as a leading model for the study of alphavirus pathogenesis (15). Numerous studies have underscored the dramatic role of virus genetics and the subsequent host defense response in dictating the course and outcome of VEE infection (16-32). Although infection in the murine model has been well studied for some time, little is known concerning the molecular markers of VEE-induced disease, including the direct effects on host cell gene expression. VEE infection is characterized by two distinct disease phases following infection in humans, horses, and mice: An initial lymphotropic phase characterized by a high serum viremia, followed by invasion of the central nervous system and initiation of a neurotropic phase leading to encephalitis. In horses and mice, progression to the neurotropic phase occurs at very high frequency, whereas progression in humans occurs in

approximately 1% of cases. Previous studies in our laboratory have carefully examined the progression of pathogenesis in the mouse model, utilizing molecularly cloned infectious VEE as well as an extensive panel of mutants blocked at various stages of infection (18, 21, 22, 25, 27, 29). The draining lymph node (DLN), in particular the dendritic cells, was subsequently identified as the initial site of viral replication, with infected Langerhans cells migrating there from the site of inoculation in the footpad (20). It has been hypothesized that the early events within the DLN set the stage for a specific pattern of virus replication and host response that contributes to the pathogenesis of the infecting virus. However, many details of the earliest stages of VEE infection remain largely undefined, with the innate host response likely playing a major role.

To define the molecular profile of the early virus-host interactions central to VEE pathogenesis, we took advantage of several tools. One tool paramount to studying the early events in infection are VEE replicon particles (VRP). VRP are propagation-defective vector particles that undergo only one round of infection, as the structural genes which normally drive the assembly of progeny virions are deleted and replaced with a marker gene of interest (33). As such, VRP replication is limited to the first infected cells, allowing us to model the earliest events of VEE infection. In addition, the application of an mRNP-tagging technology offers an opportunity for a distinct view of the VEE-induced changes in host gene expression. By expressing an epitope tagged version of PABP from VRP, host messages induced specifically within the first round of infected cells can be fractionated from those of the surrounding uninfected cells. Through co-immunoprecipitation with

antibody to the epitope tag, the infected cell host mRNA bound to the VRP-delivered tagged-PABP can be isolated and screened as a discrete mRNA population for changes in host gene expression. This technology enables discrimination of uninfected cells from infected cells, and specifically profiles the changes induced in the infected cell population—a distinction that previously has been difficult to achieve, particularly *in vivo* where the infected cells may be only a small minority in a given tissue (e.g., in the DLN post-VRP infection).

Using VRP to infect primary dendritic cells *in vitro*, and to limit infection to the initially infected cells *in vivo*, we have elucidated gene expression patterns that define the early stages of VEE pathogenesis, including members of the interferon, proinflammatory, and general defense pathways. This analysis revealed multifactorial interactions that occur with the virus infected host, and indicated a two phase innate response with distinct host profiles specific for infected cells and uninfected cells during the course of infection.

This setting also provides a novel means to examine the effects of viral genetic determinants during infection using VEE mutants in relation to wildtype infection. Comparing the host gene response to two differential VEE infections, and determining both the common and unique changes induced by each infection will facilitate a greater understanding of how the host response develops. Therefore, in addition to wildtype VRP, the host response to infection with VRP containing a mutation that attenuates virulent VEE also was explored. This single non-coding substitution of G-to-A in the third nucleotide of the 5' untranslated region (UTR), results in the complete attenuation of the 100% mortality observed in mice infected

with wildtype VEE, and was originally defined as a primary attenuating mutation within the TC-83 vaccine strain of VEE (18, 28). A major role for the innate immune response in the loss of virulence of this nt3A mutant is indicated by its heightened sensitivity to IFN$\alpha\beta$, which appears to be driven by a PKR/RNaseL-independent mechanism (18)(L.J. White and R.E. Johnston, unpublished). The data presented here demonstrate that, consistent with the dramatic phenotypic differences *in vivo*, this mutant displays dramatic differences in host gene expression post-infection in comparison to wildtype VRP infection.

MATERIALS AND METHODS

VEE replicon particles (VRP)

The construction and packaging of VRP using a split helper system have previously been described (33). The replicon plasmid constructs used in this study were *(i)* null replicons that lack any functional transgene sequence downstream of the 26S promoter (null VRP), *(ii)* replicons expressing green fluorescent protein (GFP-VRP) and *(iii)* replicons expressing an N-terminally FLAG-tagged version of poly(A) binding protein I (FLAG-PABP VRP). The production of GFP-VRP and null VRP have been described previously (20, 34). The FLAG-PABP replicon plasmid was generated by the directional cloning of the ORF of PABP I containing an N-terminal FLAG epitope tag (GACTACAAGGACCACGATGACAAG, kindly provided by J.D. Keene (Duke University Medical Center, Durham, NC) (14)), immediately downstream of the 26S mRNA promoter of the pVR21 replicon plasmid.

In addition to the wildtype null- and FLAG-PABP replicon genomes, a mutant genome containing a change from the wildtype nucleotide G at position three to a mutant nucleotide A also was utilized (nt3A mutant). Nt3A mutant null- and FLAG-PABP replicon plasmids were constructed by substituting the 543bp *Xba*I-*Rsr*II fragment from the previously cloned pV5505 replicon plasmid containing the nt3A mutation, for the equivalent fragment in the wildtype constructs (18). The presence of the nt3A mutation was confirmed by sequencing.

All replicon particles used in this study were packaged in the wildtype (V3000) VEE envelope (33). Briefly, the replicon RNA genome containing the VEE nonstructural genes and expressing the heterologous gene from the viral 26S promoter, along with two defective helper RNAs providing the wildtype capsid and glycoprotein genes, but lacking the virus-specific packaging signal, were co-electroporated into BHK-21 cells (ATCC). Due to the lack of encoded viral structural genes in the replicon genome, infectious VRP undergo only one round of infection, and the absence of propagating recombinant virus was confirmed by passage in BHK-21 cells. VRP were concentrated from supernatants by centrifugation through a 20% sucrose cushion and resuspended in PBS. BHK-21 titers were determined either by immunofluorescence (GFP-VRP), or immunocytochemistry (null VRP, FLAG-PABP-VRP) using sera containing antibody to the VEE nonstructural proteins.

Cells and in vitro infections

(i) Infection of L929 cells. L929 murine fibroblasts (ATCC) were maintained at 37°C under 5% CO_2 in complete alpha minimal essential medium (αMEM, Gibco)

containing 10% donor calf serum, 10% tryptose phosphate broth, 2 mM L-glutamine, 100U/ml penicillin and 0.5 mg/ml streptomycin. For VRP infection, 10^6 cells were seeded in 60 mm dishes and incubated overnight. The medium was removed from the monolayer and the cells were infected at a multiplicity of infection (MOI) of 5 (unless otherwise indicated) in 0.2 ml endotoxin-free PBS supplemented with 110 mM Ca^{2+}, 50 mM Mg^{2+}, and 1% vol./vol. donor calf serum. After 1 h of adsorption at 37°C, complete αMEM was added to the monolayer.

(ii) Generation of primary murine BMDCs. Breeding pairs of IFNα/βR+/+ 129Sv/Ev and IFNα/βR-/- mice were kindly provided by Herbert Virgin (Washington University, St. Louis, MO.) and Barbara Sherry (North Carolina State University, Raleigh, N.C.), respectively. Mice were bred under specific pathogen-free conditions in the Department of Laboratory Animal Medicine breeding colony facilities at the University of North Carolina, Chapel Hill. To generate primary immature BMDCs (35, 36), bone marrow cells from femurs and tibia of 8- to 14-week-old mice were aspirated with RPMI-10 medium [RPMI 1640 (Gibco), 10% FBS, 2 mM L-glutamine, 50 uM 2-ME, 100 U/ml penicillin, 100 ug/ml streptomycin sulfate]. Cells were filtered through a 40 um cell strainer, pelleted (1200 rpm, 5 min), and resuspended in ACK lysis buffer (0.15 M NH_4Cl, 0.1 mM Na_2EDTA, 1 mM $KHCO_3$, pH 7.2-7.4). Following lysis of red blood cells at room temp, 10 ml of RPMI-10 media/mouse was added, cells were again pelleted and resuspended in fresh RPMI-10 media for counting. Cells were seeded in 6-well low cluster plates (Corning) in RPMI-10 media supplemented with 20 ng/ml GM-CSF (Peprotech), and incubated at 37°C under 5% CO_2. On day three, RPMI-10 media supplemented with

20 ng/ml GM-CSF and 20 ng/ml IL-4 (Peprotech) was added to each well. On day five, additional RPMI-10 media supplemented with 10 ng/ml GM-CSF and 10 ng/ml IL-4 was added to each well. On day seven, cells were harvested by gently transferring to 50 ml conical tubes, and washing each well with cold PBS. Cells were pelleted (1200 rpm, 10 min at 4°C), and resuspended in RPMI-1H (RPMI 1640, 1% FBS, 10 mM Hepes, 2 mM L-glutamine, 50 uM 2-ME, 100 U/ml penicillin, 100 ug/ml streptomycin sulfate). BMDCs were cryopreserved at 2-5 x 10^6/ml in 90% FBS/10% DMSO.

(iii) Infection of primary BMDCs. Cryopreserved BMDCs were quickly thawed in a 37°C water bath, and gently transferred to a conical tube containing an equal volume of RPMI-10. The volume of RPMI-10 was brought up to 10 ml, and the cells were pelleted. An additional wash with RPMI-10 was completed, and the cells were resuspended in 3 ml RPMI-10 per 2x10^6 cells, supplemented with 5 ng/ml GM-CSF and IL-4. BMDCs were seeded at 2.5 x 10^6 cells/well in hydrated six-well low cluster plates, and allowed to recover overnight at 37°C, 5% CO_2. BMDCs were harvested and pooled with a cold PBS wash of each well. After pelleting, cells were resuspended in RPMI-1H at 10^6 cells/ml, and 10^6 cells/well were seeded in a hydrated six-well low cluster plate. BMDC were infected with VRP at an MOI of 0.5 in 100 ul PBS supplemented with 1% donor calf serum and Ca^+/Mg^+. Following 2hs of absorption at 37°C, 5 ml of RPMI-10 supplemented with 5 ng/ml GM-CSF and IL-4 was added to each well.

Animals and in vivo infections

Seven- to eight-week-old female BALB/c mice were obtained commercially (Charles River Laboratories) and allowed to acclimate for 5-7 days. Mice were inoculated in each rear footpad with 10^6 IU of VRP diluted in 10 ul endotoxin-free PBS containing 1% donor calf serum. Mock-infected animals received diluent alone.

Total RNA isolation

(i) L929 cells. At indicated times post-infection, media was removed and L929 cell monolayers were washed with cold PBS. The UltraSpec RNA Isolation System was used to isolate total RNA, with 1ml of UltraSpec RNA Reagent added to each 60mm dish of L929 cells per manufacturer's protocol (Biotecx).

(ii) Primary BMDCs. At 6 or 12hpi, BMDCs were transferred to a 15 ml conical tube and pelleted (1200 rpm, 10 min at 4°C), during which time each well was washed with cold PBS. The wash was used to resuspend the pelleted cells, followed by a second spin. Total RNA was harvested from BMDC using the RNeasy Mini Kit, according to the manufacturer's protocol (Qiagen).

(iii) Lymph Nodes. At indicated times post infection, mice were euthanized and both draining popliteal lymph nodes were harvested, washed with cold PBS, and pooled together into 200 ul RNA*later* RNA Stabilization Reagent (Qiagen, Ambion). Total RNA was harvested from tissue homogenate prepared using a plastic pestle with a handheld motor and the RNeasy Protect Mini Kit (Qiagen).

mRNA-tag immunoprecipitation and RNA isolation

(i) Antibodies. The mRNP-tagging method as applied to cells and animal tissues infected with VRP was developed from general ribonomics/mRNP-tagging protocols previously described by the Keene laboratory (1, 2, 9, 14). Polyclonal anti-PABP antibody was generously provided by J. Keene (Duke University Medical Center). Additionally, polyclonal anti-PABP H-300 antibody was obtained from Santa Cruz Biotechnology. Monoclonal anti-FLAG M2 antibody was acquired from Sigma-Aldrich.

(ii) Preparation of mRNP lysate from cultured cells. L929 monolayers (10^6 cells total) were washed with cold PBS, followed by lysis of the monolayer with 1ml of polysome lysis buffer [100 mM KCl, 5 mM MgCl2, 10 mM Hepes, pH 7.0, and 0.5% Nonidet P-40 with 1 mM DTT, 100 U/ml RNaseOUT(Invitrogen), 0.2% vanadyl ribonucleoside complex (New England Biolabs), and 1 tablet/10 ml Complete Mini Protease Inhibitor Cocktail Tablet (Roche) added fresh at time of use]. For BMDC lysis, cells were gently pelleted and the media removed. The pellet was washed with PBS and spun again, followed by resuspension and lysis in 500 ul of polysome lysis buffer. Cells were lysed for 10 min, followed by centrifugation at 14,000 x g in a tabletop microfuge for 10min at 4°C to remove cellular debris. The ~1 ml total volume of L929 mRNP lysate (isolated from 10^6 L929 cells) was stored at -80°C in 200 ul working aliquots, while the 500 ul total volume of BMDC mRNP lysate (isolated from 10^6 BMDC cells) was stored at -80°C in 250 ul working aliquots.

(iii) Preparation of mRNP lysate from whole animal tissue (DLN). Freshly dissected DLN were washed with ice-cold PBS. Five DLN were pooled per sample,

and coarsely homogenized in 200 ul polysome lysis buffer (containing RNase and protease inhibitors as described above) using a plastic pestle and hand-held motor. Samples were frozen at -80°C until use. Upon thawing (on ice), the homogenization and lysis was continued to completion (as monitored microscopically), and the lysate spun at 4°C to pellet any remaining tissue/debris. The supernatant was transferred to a fresh tube on ice, and a second round of lysis/ homogenization was completed on the pellet using 100 ul polysome lysis buffer. Upon centrifugation, this supernatant was pooled with the first (~300 ul total) and kept on ice until use.

(iv) mRNP immunoprecipitation. For each immunoprecipitation sample, two 60 ul aliquots of protein beads were prepared; the first aliquot to coat with the specified antibody, and the second to pre-absorb the lysate for removal of non-specific binding. For antibody coating, 60ul Protein-A Sepharose beads (pre-swollen with 12ml PBS/1.5g beads, Sigma) or fast flow Protein-G Sepharose beads (commercially pre-swollen, Sigma) were washed with PBS (10 volumes), followed by a second wash of 10 volumes NT2 buffer (50 mM Tris, pH 7.4, 150 mM NaCl, 1 mM MgCl2, 0.05% Nonidet P-40) tumbled end-over-end for 15 min at room temperature. Beads were resuspended in 10 volumes fresh NT2 buffer supplemented with 5% BSA, and tumbled overnight at 4°C with excess immunoprecipitating antibody (200 ul anti-PABP antibody; 25 ul anti-FLAG antibody). Prior to the immunoprecipitation reaction, the antibody-coated beads were washed with 1 ml NT2 buffer.

To pre-absorb the lysate, a second 60 ul aliquot of beads (per sample) was prepared as described above through the 15 min NT2 buffer wash. These beads were resuspended in 5-10 volumes NT2 buffer supplemented with 100 U/ml

RNaseOUT, 0.2% vanadyl ribonucleoside complex, 2 mM DTT, and 25 mM EDTA. The mRNP lysate was added (200 ul L929 lysate, 250 ul BMDC lysate, or 300 ul DLN lysate), along with 1 ul normal animal serum corresponding to the immunoprecipitating antibody (normal mouse serum for anti-FLAG immunoprecipitation samples; normal rabbit serum for anti-PABP immunoprecipitation samples). Samples were tumbled at room temperature for 1 h to remove any material that would non-specifically bind to the beads. This pre-absorbed lysate was recovered by pelleting the beads (2000 x g, 3 min) and applying the supernatant to the specific antibody-coated beads, along with 5-10 volumes of NT2 buffer supplemented as described above. This immunoprecipitation slurry was tumbled end-over-end at room temperature for 2h.

(v) RNA extraction from immunoprecipitated mRNP complex. Immunoprecipitated samples were centrifuged (5 min at 2000 x g, 4°C) to pellet the beads, and washed four times with ice-cold NT2 buffer (10 bead volumes). Washed beads were resuspended in 600 ul proteinase K digestion buffer (100 mM Tris pH 7.5, 12.5 mM EDTA, 50 mM NaCl, 1% SDS), plus 25 ul of 20 mg/ml proteinase K, and incubated for 30 min in a rotating device at 50°C. 600 ul phenol-chloroform-isoamyl alcohol (Fisher) was added to the beads, which were vortexed for 2 min and then centrifuged for 5 min at 14,000 x g, 4°C. This was followed by extraction with one volume of RNA-grade chloroform (Fisher), and precipitation with 1 volume of isopropanol, 60 ul of 4M ammonium acetate, 3 ul of 1 M $MgCl_2$ and 8 ul of glycogen. The samples were stored at -80^{o}C until use for gene expression analysis. Upon thawing on ice, the samples were spun for 30 min (14,000 x g, 4^{o}C), and the RNA

pellet washed with 100 ul of 80% ethanol. The RNA pellet was resuspended in RNase-free water (Ambion), or hybridization buffer as necessary.

RNase protection assay (RPA)

RNase protection assays were used to determine the relative abundance of specific cellular mRNAs in infected and mock infected L929 cells. ^{32}P-labeled RNA probes were synthesized by use of the RiboQuant *in vitro* transcription kit and a RiboQuant multiprobe custom template set (BD Pharmingen). This custom set included template for the synthesis of radiolabeled probes specific to murine interferon beta (IFNβ) and interferon regulatory gene-1 (IRF-1), as well as mRNAs encoding the murine housekeeping proteins GAPDH and L32. RNA isolated from the mRNP complexes was used as input RNA for the mRNP-tagging samples, using 100% of the isolated RNA by resuspending the RNA pellet directly in hybridization solution. 2 ug of total RNA to be used as input samples for total RNA analysis was isolated as described above. The custom probe set was mixed with each RNA sample, placed in a pre-warmed heat block at 90°C which was immediately turned down to 56°C, and incubated overnight. The RNA-probe mixtures were treated with RNase according to the RiboQuant RPA kit protocol (BD Pharmingen). The protected dsRNA species were electrophoresed on a 4.5% polyacrylamide-8M urea sequencing-sized gel, the gels were dried, and analysis conducted on a Molecular Dynamics Storm phosphorimager with ImageQuant software. Values represent the fold change over mock expression, as normalized to anti-PABP immunoprecipitated

GAPDH housekeeping mRNA levels for the mRNP-tagging samples, or total GAPDH housekeeping RNA levels for total RNA samples.

Fluorescence activated cell sorting (FACS) analysis

To compare the infected cell host message profile generated by the mRNP-tagging approach versus FACS-facilitated sorting, 1.5 x 10^6 L929 cells were mock treated or infected at a low MOI of 0.2 with either FLAG-PABP VRP or GFP-VRP. At 12hpi, cultures were treated in one of 2 ways to generate a profile of host message levels specifically from the infected cells. The cell monolayers that had been infected with FLAG-PABP VRP were lysed, and FLAG-tagged host messages were immunoprecipitated from the infected cells per the mRNP-tagging protocol described above using 100% of the monolayer lysate. A separate anti-PABP immunoprecipitation was completed from both mock- and FLAG-PABP VRP-infected cell lysates to isolate all PABP-associated mRNA and served as the mock reference with normalization to GAPDH signal levels.

To generate a comparative profile of the infected cell host response, cell monolayers that had been infected with GFP-PABP VRP were prepared for FACS-based analysis. The monolayers were trypsinized, washed with media (αMEM supplemented with 2% FBS, 100 U/ml penicillin, and 0.5 mg/ml streptomycin) and resuspended in 700 ul of fresh media. The UNC-CH Flow Cytometry Core Facility provided cell sorting capability using the Cytomation Inc. Modular Flow (MoFlo) FACS system, gating on GFP-positive signal to sort and recover the infected cell population. This GFP-positive cell population was gently pelleted and resuspended

in 0.5 ml polysome lysis buffer. 100% of the resulting lysate was immunoprecipitated with anti-PABP antibody to isolate all PABP-associated messages specifically from the (GFP+ sorted) infected cell population. A separate anti-PABP immunoprecipitation was completed from mock cell lysate and served as the mock reference with normalization to GAPDH signal levels. The host message populations isolated from each technique were analyzed using Taqman real-time PCR (see below).

cDNA synthesis, real-time PCR, and analysis

(i) cDNA synthesis. A one-tube DNase treatment and reverse transcription protocol was used to generate cDNA, using SuperScript III Reverse Transcriptase First Strand cDNA kit (Invitrogen). 0.5-0.75 ug of either mRNA-tag isolated or total RNA served as input RNA for the reaction, using RNase-free water to bring the total volume to 10 ul. This was combined with 1 ul 10 mM dNTP mix (Amersham Biosciences), 4 ul 5X SuperScript III reverse transcriptase buffer, 1 ul 0.1 mM dTT, 1 ul 40 U/ul RNaseOUT (Invitrogen), and 1 ul RQ1 RNase-free DNase (Promega). The samples were DNase treated at 37°C for 30 min, followed by the addition of 1 ul RQ1 Stop Solution (Promega) and heat inactivation of the samples at 65°C for 10 min. Following the addition of random hexamer primers (150 ng, Invitrogen), reverse transcription of the samples was continued in the same tube, according to the SuperScript III protocol (Invitrogen). cDNA samples were stored at -20°C.

(ii) Real-time PCR. Real-time PCR was performed to determine the relative abundance of specific cellular mRNAs in infected and mock treated samples.

Taqman Gene Expression Assays (Applied Biosystems) containing primers and probes for various target host messages were used, with each reaction performed in a 25 ul total volume [5ul cDNA, 12.5 ul TaqMan Universal PCR Master Mix without AmpErase UNG (Applied Biosystems), 1.25 ul probe/primer mix (Applied Biosystems), and 6.25 ul RNase-free water]. The default amplification profile was performed by the ABI Prism 7000 Real-Time PCR System, and the data converted into cycle threshold (C_T) values by the 7000 Sequence Detection Software (v1.2.3, Applied Biosystems). Duplicate samples were amplified from each experimental group with GAPDH serving as the housekeeping control along with each target gene of interest. A negative template control also was performed, with all samples run in parallel on the same plate.

(iii) Total RNA real-time PCR analysis. Real-time PCR results are presented as fold gene expression in the infected sample over that in the mock sample, as normalized to the GAPDH housekeeping gene. During each reaction, a cycle threshold (C_T) value was generated for the target gene of interest (and GAPDH), corresponding to the cycle number at which the fluorescence of the PCR product reached significant levels above the background threshold level. Raw C_T values generated from total RNA samples were analyzed using the well established delta C_T (ΔC_T) method to generate the fold expression results [*User Bulletin*, ABI Prism 7000 Sequence Detection System (Applied Biosystems)]. Briefly, for each cDNA sample, the GAPDH C_T value was subtracted from the C_T value of the target gene (e.g., cytokine) of interest, yielding a ΔC_T value. The ΔC_T value generated for the VRP-infected sample was then subtracted from the ΔC_T value of the mock

sample, yielding a $\Delta\Delta C_T$ value. This widely-used method assumes the target and housekeeping genes were amplified with the same efficiency, thus the increase in host mRNA levels in the infected samples compared to the mock treated samples was calculated as $2^{-(\Delta\Delta CT)}$.

(iv) Real-time PCR analysis of mRNA-tagged samples. Prior to this standard ΔC_T analysis, raw C_T values generated from mRNA-tagged samples were normalized in a manner that was inherently required for this system. The mock signal values were generated from an anti-PABP immunoprecipitation which isolates all PABP-bound messages in the entire cell culture or tissue analyzed. However, the infected sample values were derived using an anti-FLAG immunoprecipitation to specifically isolate the infected-cell minority subset of the population. Therefore, an mRNP-tagging normalization step was utilized to account for two parameters: 1) The disparity in the cell population size of the mock and infected samples assayed by the mRNP-tagging system, and 2) any difference in the immunoprecipitating antibody strength (the polyclonal anti-PABP antibody versus the monoclonal anti-FLAG antibody). To do so, raw GAPDH C_T values were generated from mRNP-tagging samples in the following manner. From FLAG-PABP VRP infected samples, raw GAPDH C_T values were generated from both anti-FLAG and anti-PABP immunoprecipitation-derived cDNA, representing GAPDH expression in the infected cell subset or the entire culture respectively. However from mock samples, raw GAPDH C_T values were solely generated from anti-PABP immunoprecipitation-derived cDNA, thus representing the expression of GAPDH in the entire cell population. Therefore, to normalize the mock control values for comparison to the

infected samples, a ratio of the anti-FLAG GAPDH signal to the anti-PABP GAPDH signal was applied to account for the difference in cell population size and antibody strength(*r*):

$$\text{i)} \qquad \frac{\text{VRP anti-FLAG raw GAPDH } C_T \text{ value}}{\text{VRP anti-PABP raw GAPDH } C_T \text{ value}} = \text{“}r\text{”}$$

This ratio was then applied to the mock anti-PABP raw GAPDH C_T value to generate a normalized mock GAPDH value:

$$\text{ii)} \qquad (r) \times (\text{mock anti-PABP raw GAPDH } C_T \text{ value}) = \textit{Normalized mock GAPDH } C_T$$

This normalized C_T value served as the input mock GAPDH value for the standard ΔC_T analysis, as described above for total RNA.

Affymetrix gene expression arrays and analysis

L929 cells were mock treated or infected at an MOI of 5 with either wildtype or nt3A mutant null-VRP, and total RNA was isolated at 5h p.i. using the UltraSpec reagent protocol as described above. The UNC-CH Functional Genomics Core Facility provided Affymetrix sample preparation and hybridization services, hybridizing the samples to Affymetrix Mouse Expression 430A (*MOE*430A) GeneChip arrays, which include analysis of ~22,600 genes. cDNA was synthesized using 7 ug of total RNA and a custom cDNA kit from Life Technologies using a T7-$(dT)_{24}$ primer for the reaction. Biotinylated cRNA was then generated from the cDNA reaction using the BioArray High Yield RNA Transcript Kit, and the cRNA was fragmented in fragmentation buffer (40 mM Tris-acetate pH 8.1, 100 mM KOAc, 30 mM MgOAc) at 94^{o}C for 35 min. 15 ug of fragmented cRNA was then added to a

hybridization cocktail (0.05 ug/ul fragmented cRNA, 50 pM control oligonucleotide B2, *BioB*, *BioC*, *BioD*, and *cre* hybridization controls, 0.1 mg/ml herring sperm DNA, 0.5 mg/ml acetylated BSA, 100 mM MES, 1M $[Na^+]$, 20 mM EDTA, 0.01% Tween 20). 10 ug of cRNA was used for hybridization. The arrays were hybridized for 16h at 45^oC in the GeneChip Hybridization Oven 640, followed by washing and staining with R-phycoerythrin streptavidin in the GeneChip Fluidics Station 400. The arrays were then scanned with the Hewlett Packard GeneArray Scanner. Affymetrix GeneChip Microarray Suite 5.0 software was used for washing, scanning, and basic analysis, with sample quality assessed by examination of 3' to 5' intensity ratios of certain genes. Expression analysis files created by Microarray Suite were imported into GeneSpring 6.2 (Silicon Genetics) for further gene expression analysis and filtering. Two independent array studies were completed, and gene lists were compiled representing only those genes that were up- or downregulated by greater than 2-fold in replicate analyses.

RESULTS

Establishment of the VRP mRNP-tagging system

An mRNP-tagging technique has been optimized and applied to the isolation of mRNA specifically from infected cells following VRP infection. The fundamental basis of mRNP-tagging relies on the natural interaction of RNA-binding proteins with RNA. Synthesis of a uniquely tagged RNA binding protein in target cells or specific tissues of interest enables the isolation of a specific mRNA population, employing tag-specific antibodies and co-immunoprecipitation to isolate the target mRNAs. To

apply this technique to a virus infection model, a FLAG epitope-tagged version of PABP was delivered specifically to infected cells by engineering the virus itself to express the unique RNA-binding protein. The PABP coding sequence, with the FLAG epitope fused in frame at the 5' end, was cloned directly downstream of the 26S promoter of the VEE replicon plasmid (Fig. 2.1A), and the replicon RNA was packaged into VEE replicon particles to generate FLAG-PABP VRP. Upon infection of BHK and L929 cells, the FLAG-PABP VRP programmed the robust expression of the epitope-tagged version of PABP within 2 -3hpi, as determined by Western blotting and anti-FLAG immunoprecipitation from cell lysates (data not shown). High levels of expression were expected based on the documented high level of transgene expression from the 26S mRNA promoter of VRP (33), a key element for this VRP mRNP-tagging system.

An outline of the VRP mRNP-tagging procedure is shown in Fig. 2.2. Briefly, following infection with FLAG-PABP VRP at low MOI, the FLAG-tagged PABP molecule is synthesized only in the infected cells as the replicon RNA is expressed. At various times post-infection the cells are lysed, releasing PABP-bound messages. After pre-clearing, the lysate is mixed with agarose beads coated with anti-FLAG antibody and blocked with BSA. The mRNA from the infected cells is immunoprecipitated specifically via the FLAG epitope of the PABP bound to the message in the RNP complex, as this form of PABP is only present in VRP-infected cells. The message is subsequently isolated from that complex by proteinase K digestion and phenol-chloroform based extraction. Initial experiments utilized RNase protection assays to detect host messages following the anti-FLAG

immunoprecipitation from infected BHK and L929 cell extracts. These studies verified that the VRP-supplied tagged-PABP was in fact bound to host messages, and that it could be co-immunoprecipitated to isolate mRNA for use in gene expression profiling (data not shown). Additionally, we determined the concentration of immunoprecipitating antibodies that would ensure antibody excess, which was important due to the high level of expression from the VRP (data not shown).

An issue that could complicate the precise nature of the profiling involved in mRNP-tagging systems is the potential for promiscuous exchange or reassortment of endogenous and tagged-PABP among mRNAs in cell extracts. To alleviate concern in this matter, several groups have employed the use of formaldehyde crosslinking to increase the stability of the mRNA – PABP interaction during immunoprecipitation (10-13). However, in studies where this treatment was assessed, it was found that formaldehyde treatment had little to no effect on the level of mRNA enrichment from the target populations (9, 13). Additionally, the degree of crosslinking that is effective, without irreversibly linking the mRNA to the protein and thus dampening RNA recovery, may be difficult to determine. Furthermore, concerns of PABP reassortment were also alleviated by studies demonstrating that mRNA originally bound to PABP in cell lysates was not displaced by competing excess poly(A) RNA, nor by a free pool of PABP (9).

We designed an experiment to address the degree, if any, of PABP reassortment in our system, including whether it may occur intracellularly prior to lysate preparation. L929 cells were pre-treated with actinomycin D (AMD), thereby inhibiting DNA-dependent RNA transcription, and then infected with FLAG-PABP

VRP under continued AMD treatment. The AMD treatment prior to infection prevented new host RNA synthesis, and as such, new host messages were not available for binding with the tagged PABP (as delivered by the VRP). Importantly, AMD does not inhibit alphavirus RNA replication or expression. When host mRNA was isolated from AMD treated cells and analyzed, either a decrease in signal during the length of AMD treatment or a complete absence of host mRNA signal in anti-FLAG immunoprecipitated lysates was observed (data not shown). Therefore, the VRP-supplied tagged-PABP did not reassort with or out-compete endogenous PABP bound to mRNA during infection. These results, along with the data generated from other groups, indicated that PABP reassortment was not a major concern.

Analysis of the message population isolated by VRP mRNP-tagging

The fundamental purpose of applying an mRNP-tagging approach to the examination of the host response during viral infection is to be able to discern changes in host gene expression that occur directly within the infected cells. This is a distinct advantage over traditional profiling techniques when infected cells are the minority in the overall cell population. However, the mRNP-tagging technique does isolate a particular subset of mRNA in the cell, namely those that bind PABP. Therefore, we wanted to verify that this method would yield an mRNA population representative of host transcription following infection. To do so, cells were infected at a high MOI such that the tagging technique would assess the message profile of the same cell population as the more traditional total RNA isolation techniques.

L929 cells, a murine fibroblast cell line, were infected with FLAG-PABP VRP at an MOI of 5. At 6, 12, or 24hpi, RNA was harvested using each of the following three methods: 1) For traditional isolation of total cellular RNA, a commercially available solution of guanidine salts and urea in conjunction with phenol and detergent (UltraSpec reagent) was used. 2) To isolate all poly(A) RNA bound to PABP in the cell population, an anti-PABP immunoprecipitation assay was performed on a separate set of mock and VRP-infected cells. 3) Finally, to isolate poly(A) RNA bound to the FLAG-tagged PABP provided by the FLAG-PABP VRP infection, an anti-FLAG immunoprecipitation assay was performed. RNA isolated from all three techniques was used as input RNA in an RNase Protection Assay designed to analyze the expression profiles of host genes relevant to this study. The infected cell profile of two such genes, IRF-1 and IFNβ, relative to that in mock infected cells is shown in Fig. 2.3, with a comparison of the levels as assayed by the three different RNA isolations. The data shown are representative of two separate experiments, and the specific mRNA signal generated from each isolation technique was normalized to GAPDH signal. During a timecourse of 6, 12, and 24h post infection at a high MOI, the message profiles of these two relevant host genes were similar among the various methods that were used to isolate RNA. Therefore, the mRNP-tagging technique was not limiting in terms of the availability or abundance of RNA screened.

mRNP-tagging provides a sensitive measure of viral-induced host gene expression

While the robust RNA populations examined using the VRP mRNP-tagging system in a high MOI situation are representative of those induced in infected cells, the truly advantageous use of the technique is in low MOI situations, where the number of infected cells are a small minority (i.e., tissues from VRP-infected animals). Therefore it was important to assess the level of sensitivity that could be expected in these low MOI situations. An *in vitro* experiment was designed to model the *in vivo*-like condition of a low frequency infected cell population. At 6hpi, cell lysates were prepared from L929 cells that were either mock infected or infected at an MOI of 5 with FLAG-PABP VRP. The cell lysates were mixed in decreasing ratios of infected cell lysate to uninfected cell lysate, and the mixed lysate was then immunoprecipitated with anti-FLAG antibody, isolating the FLAG-PABP bound mRNA. This mRNA served as template RNA in an RNase Protection Assay, using probes specific for several host mRNAs. The results (Fig. 2.4) for two host mRNAs, IRF-1 and GAPDH, demonstrate that the mRNP-tagging system provides a sensitive measure of VRP-induced host gene expression, as the signal from FLAG-tagged host mRNA immunoprecipitated from the infected cells was detected in samples that contained as little as 1% infected cell lysate. In this particular experiment, the 1% value is approximately equal to 2000 infected cell equivalents. It is worthy to note that RPAs do not include an amplification step, and as such the input RNA is directly assayed. Therefore, a higher degree of sensitivity was to be expected in assessing

a similarly dilute infected cell population using mRNP-tagging combined with methods that include an amplification step, such as real-time PCR.

An alternate strategy to assess host gene expression changes specifically in the infected cell compartment might rely on the sorting of the infected cell population from the uninfected cells (e.g., by FACS), followed by the independent analysis of the RNA isolated from each population. To further assess the level of sensitivity, VRP-induced changes in host gene expression as assessed by the mRNP-tagging method were compared to the host profile derived by a FACS-based method (Fig. 2.5). L929 cells ($2x10^6$) were infected at a low MOI of 0.2 with VRP expressing either GFP (Fig. 2.1) or FLAG-PABP. At 12hpi, GFP expression was used as the basis for FACS-facilitated sorting of the GFP-VRP infected and uninfected cells into the two respective populations. The recovered GFP-positive (infected) cells were lysed, and all PABP-bound host messages were subsequently isolated by anti-PABP immunoprecipitation and RNA isolation. In parallel, the mRNP-tagging assay was used to sort messages from FLAG-PABP VRP infected L929 cells by lysing the entire monolayer, and using anti-FLAG immunoprecipitation to isolate FLAG-tagged PABP-bound messages specifically from the infected cells in the monolayer. To compare host mRNA levels in each of the infected cell populations, mock treated L929 monolayers also were lysed, and the PABP-bound mRNA isolated by immunoprecipitation.

As shown by real-time PCR analysis (Fig. 2.5), a substantial induction of IFNβ, IP-10 and IRF-1 mRNA in the L929 infected cell population over mock treated cells was apparent following analysis of both the FACS-based or mRNP-tagging

techniques. Importantly, in comparing the two methods, the degree of sensitivity in detecting mRNA from the minority population of infected cells using the tagging technique was at least equal to (IFNβ, IRF-1), if not enriched (>5x enrichment in IP-10) in comparison to those generated by the FACS-based method. These results further validate the mRNP-tagging system as a powerful tool for the analysis of changes in host gene expression following viral infection.

Utilizing VRP mRNP-tagging in dendritic cells provides an *in vitro* system for studying early events in VEE pathogenesis.

A major advantage in using VRP as opposed to VEE virus in the mRNP-tagging system is the opportunity they provide to study the earliest events in the course of VEE pathogenesis, as VRP infect and replicate only within the first round of infected cells. We have previously demonstrated that dendritic cells represent an important early target of infection *in vivo*, as VRP target DCs at the site of inoculation following footpad delivery in the mouse model (20), and have likewise been shown to efficiently transduce human DCs *in vitro* (37). Furthermore, several groups have examined DC-tropic properties for other alphaviruses, such as Sindbis virus (38-41) and Ross River virus (35). In light of these previous studies, primary murine bone marrow dendritic cells were chosen as an *in vitro* model system to study early VRP-induced gene expression patterns.

To compare the host response profile following traditional total RNA isolation of BMDCs versus that generated using the mRNP-tagging system, primary DCs isolated from 129sv/ev mice were infected at an MOI of 0.5 with FLAG-PABP VRP.

At this MOI, it is estimated that less than 5% of the cells are infected (T.P. Moran and R.E. Johnston, personal communication). At 6hpi, RNA was isolated from mock treated and VRP-infected BMDC by either 1) preparing cell lysates for isolation of PABP and FLAG-PABP bound mRNAs by immunoprecipitation, or 2) adding UltraSpec reagent for isolation of total RNA. The mRNP-tagging method specifically isolated mRNA from the infected cells using the bound FLAG-tagged PABP marker, and this population of mRNA was compared to endogenously PABP-bound messages in the mock BMDC culture. In contrast, the traditional RNA isolation lacked this discrimination, and therefore total cellular RNA was isolated from the entire infected and mock treated BMDC cultures for comparison.

As shown in Fig. 2.6 (black bars), the gene expression profiles (IFNβ, IP-10, IL-6) evaluated specifically from the infected cells of the BMDC culture using the mRNP-tagging technique were dramatically enhanced in comparison to profiles generated using total RNA isolated from the entire population of infected and uninfected DCs. The fold induction over mock of IFNβ, IP-10 and IL-6 mRNA in the infected BMDC cultures were found to be approximately 20 to 200 fold higher than that measured by total RNA (comparing the black bars in Fig. 2.6). It is likely that the high proportion of uninfected cells in the low MOI environment masked the signal from the minority of infected cells when assayed from the total RNA samples. Additionally, it is possible that fundamental differences existing between the infected and uninfected cell responses contributed to the observed difference in these gene profiles assayed by the two methods. All three of the evaluated defense response genes were induced to high levels in the infected DCs at this early timepoint of 6h

post-infection, suggesting that the host innate response is rapidly initiated following VRP infection of BMDCs. Although this rapid response could be detected in the DC culture as a whole using the total RNA analysis, the mRNP-tagging method was required to reveal the full extent of this early defense response within the infected cell population.

In the absence of IFNAR signaling, the defense response in infected BMDCs is greatly diminished.

The contribution of the IFNαβ system in determining the outcome and severity of VEE disease has been described for over 30 years (42, 43). Therefore, in seeking to further characterize the initial stages of VEE pathogenesis, the interferon response was a primary target for study. The host response to infection in primary BMDC isolated from IFNαβ receptor knockout (IFNαβR-/-) animals also was analyzed in the previous experiment, with the same sample groups isolated and analyzed at 6h post-infection as described above. We hypothesized that in a system lacking IFNαβ receptor signaling, the mRNP-tagging method of specifically profiling the infected cell response should detect a diminished induction in interferon-stimulated genes (ISGs), as the positive autocrine feedback signaling within these cells should be crippled in the absence of the IFNαβ receptor. In this manner, the IFNαβR-/- BMDC also provided another model system for substantiating the VRP mRNP-tagging technique.

As demonstrated in Fig. 2.6, the ISG response in the infected IFNαβR-/- BMDC (stippled bars) as measured by the mRNP-tagging assay was much

diminished in comparison to the response in wildtype BMDC (black bars). The induction of IFNβ and IP-10 in the receptor knockout BMDC was diminished by 200-2000 fold respectively, in comparison to levels of induction in the wildtype BMDCs. The IL-6 response also was reduced specifically in the infected cells of the IFNαβR-/- BMDC culture as compared to the wildtype IFNαβR+/+ BMDC culture, with the induction of IL-6 message measured by the mRNP-tagging assay at only background levels in comparison to mock treated IFNαβR-/- BMDC culture. Therefore, the host response in the absence of IFNαβ receptor signaling did in fact demonstrate a diminished induction of interferon-stimulated genes specifically within VRP-infected cells.

In contrast to the infected cell response, when the same cultures were globally assayed for changes in gene expression using total RNA analysis, the loss of the IFNαβ receptor in the culture overall appeared to have little effect on interferon-stimulated gene induction at this early time post-infection (Fig. 2.6). As compared to mock treated cells, the induction of IP-10 and IL-6 mRNA was similar in wildtype and interferon receptor knockout BMDC when measured by total RNA at 6hpi. Additionally, IFNβ total RNA message levels were found to be approximately five fold higher in the IFNαβR-/- BMDC culture in comparison to the wildtype BMDC culture, following VRP infection. This enhancement may be due in part to IFNαβ receptor-independent signaling induced in the uninfected cell majority by cytokines and/or dsRNA released into the BMDC culture media following VRP infection. However, it is clear from the total RNA profile of the IFNαβR-/- BMDCs, that in this low MOI infection, the high background of uninfected cells in the culture masked the

dramatic effect of the receptor knockout on host gene expression in the infected cell population. This decreased host response of IFNαβ, IP-10 and IL-6 message in the infected IFNαβR-/- cells would have gone undetected had the mRNP-tagging system not been utilized.

Comparison of the early host defense response to wildtype and IFN-sensitive VEE *in vitro*.

As an initial approach, Affymetrix DNA microarray analysis was used to globally define changes in the host gene expression profile following VRP infection. Null-VRP were utilized for infection in the array analysis because they lack a transgene downstream of the 26S subgenomic promoter (Fig. 2.1C), thus eliminating any effect on host gene expression that an exogenous gene driven from a replicon might otherwise have imposed. In addition, the host response to null-VRP containing a mutation at nucleotide position 3 in the 5' UTR region was compared to wildtype null-VRP.

Previous studies have described characteristics of the nt3A mutation (18, 28), the most prominent being avirulence of this mutant *in vivo*. Infection of mice with VEE harboring the nt3A point mutation results in 0% mortality, which is in stark contrast to the 100% mortality experienced in the mouse model following wildtype VEE infection (18). This attenuation was attributed largely to a heightened sensitivity of the mutant to the host interferon response, mediated by a pathway other than PKR, RNaseL, and Mx (L.J. White and R.E. Johnston, unpublished), and importantly not due to any defect in replication (18). The array studies presented

here included differential analysis of the changes in host gene expression following wildtype and nt3A mutant null-VRP for two main purposes: 1) To elucidate potential host factors and pathways involved in the increased IFN sensitivity of the nt3A mutant, and 2) by analyzing genes similarly and differentially regulated by the two infections, to better understand the hallmark effects that virulent VEE induces in host cells during the early stages of infection.

Total RNA was isolated at 5hpi from L929 cells that had been mock treated, or infected with either wildtype or nt3A mutant null-VRP (MOI=5). The samples were subsequently analyzed for changes in host gene expression using the Affymetrix Mouse Expression 430A GeneChip technology. Data from two independent array experiments were analyzed to determine genes induced or repressed during each infection, as compared to mock treated cells. Only those genes that were modulated in both array experiments are reported (Fig. 2.7, Table 2.1, Supplemental Fig. 2.1, Supplemental Table 2.1). At the early time of 5h post-infection, there was an abundant host response to infection with either wildtype or nt3A mutant VRP. Analysis of messages that were differentially modulated during each infection by >2-fold over mock treated cells demonstrated a striking population of mRNAs that were uniquely affected by the two separate infections (Fig. 2.7). Of the 125 genes reproducibly upregulated by >2-fold following wildtype infection, only 55 of these genes were also upregulated following nt3A mutant infection, during which an additional 10 distinct genes were induced. Similarly, of the 332 genes reproducibly downregulated by >2-fold by wildtype VRP, only 20 of these genes were also downregulated following nt3A mutant infection. Twelve genes were uniquely

repressed by >2-fold by nt3A mutant VRP infection. When the analysis was restricted to the more rigorous parameter of modulation by >4-fold over mock expression, unique populations of messages up- or downregulated following each infection were again revealed (shown in parentheses, Fig. 2.7), suggesting that infection with the nt3A mutant may modulate pathways of the host response that differ from those affected by wildtype VRP infection. It may be important to note however, that a large number of genes were modulated, just not in a reproducible manner. This was particularly true of unique as well as shared sets of genes downregulated following infection by wildtype and nt3A mutant VRP, supportive of the global but perhaps nonspecific shutoff of host transcription that occurs following alphavirus infection (15, 44, 45).

In light of the interferon sensitivity phenotype and *in vivo* attenuation of the nt3A mutant, genes belonging to interferon-related, proinflammatory, and host defense response pathways were examined specifically, under a general hypothesis that nt3A-containing VRP might induce a more robust response in these pathways. However, when the fold induction of messages belonging to these gene categories were examined, the levels of expression following nt3A mutant VRP infection were found to be at or below levels following wildtype infection (Table 2.1, Supplemental Table 2.1). Two independent array studies were completed, and gene lists were compiled representing only those genes that were up- or downregulated by greater than 2-fold in both replicate analyses. The fold induction (over mock) in message levels of IFNβ, Oasl1, Isgf3g/IRF-9, ifit1/p56, IP-10, IL-6, and a multitude of other ISGs were found to be lower at 5h following infection with nt3A mutant VRP than

with wildtype VRP. The same was true for proinflammatory and host defense response mediators, including Rantes, GROα, MIP2α, Socs2, and TLR2. Therefore, although VEE virus harboring the nt3A mutation is up to 100-fold more sensitive than wildtype virus to the interferon-induced antiviral state in cultured cells (18), it does not appear that this is due to the induction of a more robust interferon-stimulated gene response to the mutant early after infection *in vitro*.

In vivo, the combination of mRNP-tagging and traditional profiling reveals dynamic multifactorial interactions in the DLN.

Previous studies by our group and others have examined the succession of events characteristic of VEE pathogenesis in the mouse model. Following inoculation in the footpad, Langerhans-like cells infected at the site of inoculation in the footpad subsequently migrate to the popliteal draining lymph node (DLN), which is the initial site of viral replication (20). It has been hypothesized, based on these observations, that the early events within the DLN set the stage for the specific pattern of virus replication and host response that are hallmarks of VEE pathogenesis. However, many details of the earliest lymphotropic stages of VEE infection *in vivo* remain largely unknown. Seeking to focus on the early interactions of virus and host in the DLN, as well as returning to the system where the most compelling data on the nt3A mutation has been described, we extended our characterization of the host response to the mouse model. VRP were again chosen as a tool to limit infection to the initially targeted cells, and the mRNP-tagging technology was employed to analyze the early host response. As the infected cell

population within the DLN post-footpad inoculation is by far a minority, we hypothesized that combining total RNA profiling with the tagging system would generate a more comprehensive view of the host response post-infection *in vivo.* Additionally, the comparison of the nt3A mutant profile to that of wildtype VRP *in vivo* rather than in a fibroblast cell line was expected to more accurately elucidate mediators contributing to the attenuated nt3A mutant phenotype demonstrated *in vivo*.

Adult BALB/c mice were inoculated in each rear footpad with 10^6 IU of either wildtype or nt3A mutant FLAG-PABP-VRP. At 6h and 9hpi, the popliteal DLNs were removed, pooled, and either total RNA or RNA specifically from the infected cells was isolated by anti-FLAG immunoprecipitation. cDNA was synthesized from each RNA sample, and Taqman real-time PCR was performed to analyze several target host genes. Two independent DLN samples were analyzed from each group, with GAPDH serving as the internal housekeeping control gene, and the results were averaged. The expression profiles of four host messages (IFNβ, IP-10, GM-CSF, and IL-6) characterized from the DLN post-infection are shown in Fig. 2.8. Two distinct views of the response to infection in the DLN were revealed: The profile generated from the traditional total RNA isolation grants a view of the overall response to infection in the DLN as a whole, including both the infected and uninfected cell response. The mRNP-tagging profile of each gene reveals the host response to infection specifically within the infected cells of the DLN, granting a view of the impact of infection directly within the infected cells of the DLN.

First, examining the response to infection over time within the infected cells, an early robust expression of IFNβ, IP-10 and GM-CSF was exhibited in the anti-FLAG isolated RNA at 6hpi, which waned by 9hpi. This suggests a very rapid response to VRP infection within infected cells of the DLN. While the response was waning between 6 and 9hpi within the infected cells, the total RNA profile of the DLN demonstrated that the response in the organ as a whole was increasing during this time interval. By 9hpi, the majority of the IFNβ, IP-10, and GM-CSF host response appears to have shifted to the surrounding uninfected cells of the DLN. This is likely due to a robust activation of the innate immune response directly within the infected cells, initiated by binding, entry, and replication of the VRP, which then induces mediators (e.g., cytokines) that are released into the surrounding environment of the DLN and activate a paracrine response in neighboring uninfected cells. This detailed view of events occurring at early times post-infection has been difficult, if not impossible, to examine previously, and suggests a much more intricate induction of innate responses than that apparent from total RNA analysis.

The IL-6 host response presents an interesting scenario, as there was a complete lack of signal detected at 6hpi in the infected cells of the DLN as measured by the mRNP-tagging system (Fig. 2.8, asterisk). However there was a robust IL-6 response measured at 6hpi from the total RNA isolated from the entire DLN. This suggests that the infected cells of the DLN are not the main producers of IL-6 initially following VRP infection. Instead, the uninfected bystander cells may be particularly poised to respond to paracrine signals from infected neighboring cells, resulting in IL-6 expression. By 9hpi, IL-6 expression was detected in both the infected cell

population as well as in the DLN as a whole, indicating a continuation of the dynamic interplay between the infected and uninfected cells in this environment. This two phase innate response would have otherwise gone undetected had the mRNP-tagging technique not been integrated with the traditional profiling.

Assessing the host defense response *in vivo* to wildtype versus nt3A mutant VRP infection (Fig. 2.8, black versus grey bars), this integrative approach continued to offer two distinct views of the innate response. Looking globally within the DLN as a whole, the IFNβ, IP-10, GM-CSF and IL-6 responses were similar at 6h and 9h following wildtype and nt3A mutant VRP infection. However, evaluation of the infected cells of the DLN by the mRNP-tagging method demonstrated a less robust host response following nt3A mutant VRP in comparison to wildtype infection. The results generated *in vivo*, specifically from the infected cells of the DLN, mirrored the results from the *in vitro* Affymetrix GeneChip experiment, in which a high MOI was used to ensure infection of nearly 100% of cultured cells. As was also described *in vitro*, it does not appear that the interferon sensitivity of the attenuated nt3A mutant can be attributed to a more robust induction of the innate host defense response *in vivo,* at least not within 6-9h in the DLN. Here, the mRNP-tagging technique allowed the specific profiling of infected cells in the naturally low MOI environment *in vivo*. Altogether, this integrative approach allowed a uniquely multifaceted examination of the VRP-infected host. The total RNA profiling and mRNP-tagging approaches are together far more informative than either alone.

DISCUSSION

Here we have introduced an innovative approach for assessing gene expression changes following viral infection *in vitro* and *in vivo*, addressing a critical parameter that has been difficult, if not impossible, to address previously. By distinguishing changes in the host transcriptional program of infected cells from that of uninfected bystander cells, the mRNP-tagging technology provides an important advancement in gene expression profiling, and promises to increase our understanding of the host response to virus infection, particularly *in vivo*.

Characterization of the VRP mRNP-tagging approach has demonstrated several key aspects of the system. First and foremost is the ability of the system to effectively target and isolate mRNA from the infected cell population. In high MOI cell culture experiments, where all cells are infected, the gene expression profiles generated from total RNA and RNA isolated by mRNP-tagging were similar. Additionally, in low MOI cell culture experiments, where only a minority of cells are infected, the RNA profiles generated from the infected cell population isolated by FACS were similar to the gene expression profiles isolated by the mRNP-tagging technique without prior cell sorting. These results demonstrate that mRNP-tagging yields profiles that are representative of infected cells, even when they are the minority cell population.

An equally important aspect of the mRNP-tagging system is that the method is sensitive. In mixing experiments, where the infected cell signal was diluted with mock lysate, the mRNP-tagging approach detected a unique transcriptional profile when as few as 1% of the cultured cells were infected. Moreover, the sensitivity of

directly isolating infected cell mRNA via the mRNP-tagging approach proved to be as great, or even enhanced in comparison to analysis of message levels when isolated from infected cells following a commonly utilized FACS-based approach. This ability to effectively analyze a small minority of infected cells, such that the mRNA signal from infected cells is no longer masked by the background of uninfected cells, is a property well suited for application *in vivo*. Additionally, the VRP mRNP-tagging technique allows this level of specificity without harsh treatment of the infected cell populations prior to RNA isolation. This is in contrast to FACS analysis, which commonly requires physical manipulation of cultured cells or tissues (e.g., trypsinization, collagenase digestion), and may result in cellular damage to delicate cell types analyzed post-infection, such as the shearing of fragile dendrites from the cell body of DCs. This physical manipulation may affect the host gene expression profile of cells, similar to the profound effects various isolation techniques can have on the maturation and function of DCs (46). However, since the VRP mRNP-tagging system isolates mRNA from infected cells following lysis directly in the culture vessel or from intact tissue, the cells are not distressed prior to message isolation and may more accurately reflect the host transcriptional program at the time of isolation. Furthermore, given the well-established roles for PABP in translation initiation and mRNA stability (5, 7, 8, 47), PABP-associated mRNA may actually be more representative of the cell's actively translated message population or the proteome. Therefore, the VRP mRNP-tagging system may provide a more accurate view of the biological state of the cell post-infection (1, 13).

Application of the mRNP-tagging method has revealed several important insights into the host innate response to virus infection. First, the host response is dramatically different in infected and uninfected cells within the same *in vitro* cell culture or the same tissue *in vivo,* varying in quantitative, qualitative and temporal terms. Quantitatively, the level of response in each population varied by gene, indicating that the transcriptional programs of infected and uninfected cells within the same culture or tissue are uniquely affected. On a gene by gene basis, comparing the infected cell profile generated by the mRNP-tagging system to the total RNA profile generated from the entire culture or tissue allows the relative contribution of the infected versus uninfected cell populations to be teased apart. In the case where a small percentage of primary BMDC were infected *in vitro*, the induction of IFNβ, IP-10 and IL-6 in infected cells as measured by the mRNP-tagging system was up to 200 times that indicated in the total RNA sample for the entire culture. Similarly, at 6h in the DLN following infection *in vivo*, induction of GM-CSF mRNA in the infected cell population was nearly 80 times that in the total RNA sample from the entire lymph node. These results suggest that the infected cells are the primary source of the IL-6 and GM-CSF response to VRP infection at 6h in BMDC cultures and the DLN, respectively.

In the above instance, had the mRNP-tagging system not been utilized, the induction of both of these genes would likely have been overlooked due to the low total RNA induction measured from the culture as a whole. Therefore, at particular times the level of response in the infected and uninfected cell populations can differ so extensively that their analysis becomes qualitatively different. In other words, a

response that is robust in one population may be completely absent in the other, and in this regard, the host response will appear to be quite different when evaluating infected cells alone rather than the entire culture or tissue.

Temporally, the combination of the mRNP-tagging approach and total RNA analysis offered a unique vantage point into the kinetics of the infected and uninfected cell responses. In the DLN, this analysis demonstrated two phases of the innate host response. The first apparent phase was a rapid response in the infected cells of the DLN, including the robust activation of several host defense genes (IFNβ, IP-10, and GM-CSF) at 6h following footpad inoculation. While this infected cell response was waning by 9h post-infection, an apparent second phase of response was mounting in the surrounding uninfected cells of the DLN, with induction of the same defense genes increasing from 6h to 9h post-infection. In fact, a similar rapid onset of the host innate response has been described previously following virulent VEE infection, with cytokine RNA levels in the DLN of infected mice peaking at 6-12h following footpad inoculation, and waning by 24-48h (48). However, the use of VRP and the application of the mRNP-tagging system in our study provided the ability to distinguish the events specifically occurring within the first round of infected cells *in vivo* from the effects on the uninfected bystander cells of the DLN, revealing the unique kinetic response to infection occurring in each population.

Several signaling events are likely to contribute to the kinetics of this two phase activation, highlighting another important insight gained using this system. In the heterologous environment that exists following infection *in vivo*, autocrine and paracrine mediators are induced in the first infected cells that drive the host

transcription profile of infected and uninfected cells, respectively. Replicon particle binding, entry, and replication provide a multitude of signals to initiate the early host defense response directly within the infected cells. It is likely that the rapid innate activation of the infected cell population leads to the secretion of cytokines and other soluble immune modulators. A portion of these mediators then initiate the cell signaling events in uninfected bystander cells that are responsible for the strong response in the DLN at later times post-infection. This would undoubtedly include the activation of cells which have homed to the DLN as an active site of viral infection. In fact, a large influx of cells to the DLN has been observed following footpad VRP inoculation, resulting in a visible increase in node size, and includes cells of the proinflammatory response as well as antigen presenting cells (e.g., T-cells, B-cells, and DCs) (J.M. Thompson, A.C. Whitmore, J.L. Konopka, T.P. Moran and R.E. Johnston, unpublished data). These recruited cells would remain uninfected, but would be susceptible to the primed environment of the DLN, and likely contribute to the induction of the second phase of the host innate response in the uninfected cells of the DLN.

Our results highlight the role of the innate immune response during VEE infection, particularly the interferon response. Evidence for the interferon system as a major factor in controlling VEE replication and spread *in vivo* has been well established (18, 19, 23, 35, 42, 43, 49-51). Infection with VEE results in tremendous levels of soluble, biologically active interferon in the serum, measured at up to 80,000 IU/ml following virulent wildtype VEE infection (18). In the absence of interferon signaling *in vivo*, a significantly shorter average survival time has been

documented following VEE infection in mice lacking the IFNαβ receptor (30h) in comparison to wildtype mice (7.7 days), with a 10,000-fold increase in virus titers (18). When signaling through the IFNαβ receptor was specifically investigated in BMDC, the role of the interferon response in autocrine and paracrine signaling of infected and uninfected cells was further elucidated. While ablating the IFNαβ receptor had no apparent effect on the total RNA induction of IFNβ, IP-10, and IL-6 genes in the BMDC culture as a whole, a dramatically reduced induction of each of these host response genes was observed in the infected BMDC population by mRNP-tagging analysis. This strongly suggests that autocrine signaling through the IFNαβ receptor plays a critical role in the high level of interferon stimulated gene induction seen in the infected cell population. Conversely, the induction of these host response genes apparently was not reduced in the majority uninfected cell population. This suggests that interferon-mediated signaling through the IFNαβ receptor is not the primary paracrine mediator leading to the induction of these particular host response genes in uninfected bystander cells. This is consistent with previous findings that levels of serum IFNαβ are not reduced at early times after VRP infection of IFNαβR-/- mice compared to wildtype controls (18).

Taken together, the data presented here highlight an important additional observation. Namely, reductionist *in vitro* approaches do not always recapitulate what is occurring *in vivo*. Often, high multiplicity infections of largely homogenous culture cells are utilized *in vitro* to draw conclusions about what occurs in naturally low multiplicity infections of complex heterogeneous tissues *in vivo*. However, the data presented here strongly argue that the naturally heterogeneous environment of

infected and uninfected cells existing during infection *in vivo* must be appreciated in order to understand the dynamic interactions occurring between these populations. For example, in cultured BMDC, IL-6 was highly induced in VRP infected cells at 6h post-infection. However, this did not appear to be the case *in vivo* where induction of IL-6 mRNA was first documented in the uninfected bystander population. Using a combination of high and low multiplicities of infection, and contrasting how the infected cell responds with and without neighboring bystander cells will likely facilitate a better understanding of what cell-cell interactions or signaling events regulate the innate response to VEE pathogenesis.

Finally, large differences in the host responses to wildtype and mutant VRP infection were revealed in this study. A single non-coding substitution of G-to-A in the third nucleotide of the VEE 5' UTR results in a mutant virus that is up to 100-fold more sensitive to the interferon-induced antiviral state, rendering this nt3A mutant virus completely avirulent in mice (18). It has been hypothesized that these properties of the nt3A virus may increase the induction and/or activation of IFN$\alpha\beta$-related antiviral effectors early in infection. In fact, both wildtype and nt3A mutant VRP infection mounted a substantial early host response, and unique subsets of host genes were induced and repressed following each infection. Surprisingly, the induction of interferon, proinflammatory, and host defense response genes were actually reduced following nt3A mutant VRP infection in comparison to infection with wildtype VRP. This was demonstrated following high multiplicity infection of cultured cells, as well as in the DLN following infection *in vivo*. Importantly, the mRNP-

tagging technique was required to detect this differential induction *in vivo* in the minority of infected cells.

These results strongly suggest that the documented attenuation of the nt3A mutant is not a function of a more robust induction of antiviral effectors at this early time in infection. However, it does not prove that other IFN-mediated host factors not yet included in our analyses are involved. Other aspects of infection that have been explored (e.g., replication kinetics, host translation shutoff, induction of apoptosis) have not identified a clear attenuating mechanism for the nt3A mutant [J.L. Konopka and L.J. White, unpublished]. However, a recent study examining the response to Sindbis virus infection in systems triply deficient in PKR, RNaseL, and Mx identified several candidate interferon-stimulated genes as important antiviral mediators within this alternative pathway (41). A more extensive kinetic examination of the induction of antiviral effectors following nt3A mutant VEE infection, including these new candidate gene families, may be required, as well as further studies into the subsequent activation of such molecules.

The VRP mRNP-tagging system suggests a multitude of future studies that promise unique perspective on the highly coordinated host response to viral infection. A critical future application of the VRP mRNP-tagging system is the analysis of the host response to infection within the brain, where the most extensive pathogenesis is observed following VEE virus infection. Alphavirus CNS pathogenesis has been studied extensively in several model systems. Much of the pathology associated with alphavirus induced disease in the CNS is a direct result of the host's own immune response to the infection. However, unique to VEE,

extensive pathology within the CNS is observed even in the absence of the adaptive immune response (52), suggesting that multiple parameters contribute to VEE-induced disease in the brain. In addition, although there is strong evidence of apoptosis occurring in the brain of VEE-infected animals (53, 54), the relative contribution of death induced directly in infected versus bystander neurons remains to be fully addressed—a distinction shown to be critical following infection with neuroadapted Sindbis virus (55, 56). The use of the mRNP-tagging system in the context of such studies may facilitate a deeper understanding of VEE-induced neurodegeneration.

Additional future studies may include the application of the mRNP-tagging system in the context of VEE virus infection. Recombinant viral constructs encoding double 26S subgenomic promoters have been utilized previously, allowing the expression of the viral structural genes as well as a marker gene of interest (20). Therefore, it is feasible to utilize mRNP-tagging in the context of a propagating VEE infection, in which a double promoter virus expresses the FLAG-PABP marker from a second subgenomic promoter. This would facilitate the characterization of the host response to VEE infection downstream of the DLN, including the impacts of virus budding as well as cell-to-cell spread during infection.

This VRP mRNP-tagging system could also be developed using RNA-binding proteins other than PABP, and may identify subsets of functionally related mRNAs representing post-transcriptional RNA-operons in infected cells (1). For instance, utilizing proteins like HuR that activate mRNAs encoding immediate early gene

transcripts, such as cytokines and chemokines, would be of particular interest in the development of future mRNP-tagging systems (57).

The application of mRNP-tagging technology to the study of the host response to viral infection opens avenues of investigation that have previously been difficult to navigate. A better understanding of virus-host interactions may subsequently facilitate the design of improved therapeutics and vaccines. More specifically, gaining a clear profile of the host response to VEE infection promises to further our understanding of the specific virus-host interactions that define alphavirus pathogenesis *in vivo*.

ACKNOWLEDGMENTS

We thank Nancy Davis and Clayton Beard for critical reading of the manuscript, and the entire Carolina Vaccine Institute for stimulating discussions. This work was supported by the National Institutes of Health (NIH) Public Health Service Grant R01-AI51990 (to R.E.J.), and the NIH Predoctoral Training Grant T32-AI07419.

REFERENCES

1. Tenenbaum, S. A., C. C. Carson, P. J. Lager, and J. D. Keene. 2000. Identifying mRNA subsets in messenger ribonucleoprotein complexes by using cDNA arrays. *Proceedings of the National Academy of Sciences* 97:14085-14090.

2. Tenenbaum, S. A., P. J. Lager, C. C. Carson, and J. D. Keene. 2002. Ribonomics: identifying mRNA subsets in mRNP complexes using antibodies to RNA-binding proteins and genomic arrays. *Methods* 26:191-198.

3. Deo, R. C., J. B. Bonanno, N. Sonenberg, and S. K. Burley. 1999. Recognition of Polyadenylate RNA by the Poly(A)-Binding Protein. *Cell* 98:835-845.

4. Bernstein, P., and J. Ross. 1989. Poly(A), poly(A) binding protein and the regulation of mRNA stability. *Trends in Biochemical Sciences* 14:373-377.

5. Burd, C. G., and G. Dreyfuss. 1994. Conserved structures and diversity of functions of RNA-binding proteins. *Science* 265:615-621.

6. Gorlach, M., C. G. Burd, and G. Dreyfuss. 1994. The mRNA Poly(A)-Binding Protein: Localization, Abundance, and RNA-Binding Specificity. *Experimental Cell Research* 211:400-407.

7. Sonenberg, N., and T. E. Dever. 2003. Eukaryotic translation initiation factors and regulators. *Current Opinion in Structural Biology* 13:56-63.

8. Imataka, H., A. Gradi, and N. Sonenberg. 1998. A newly identified N-terminal amino acid sequence of human eIF4G binds poly(A)-binding protein and functions in poly(A)-dependent translation. *Embo J* 17:7480-7489.

9. Penalva, L. O., S. A. Tenenbaum, and J. D. Keene. 2004. Gene expression analysis of messenger RNP complexes. *Methods Mol Biol* 257:125-134.

10. Roy, P. J., J. M. Stuart, J. Lund, and S. K. Kim. 2002. Chromosomal clustering of muscle-expressed genes in Caenorhabditis elegans. *Nature* 418:975-979.

11. Kunitomo, H., H. Uesugi, Y. Kohara, and Y. Iino. 2005. Identification of ciliated sensory neuron-expressed genes in Caenorhabditis elegans using targeted pull-down of poly(A) tails. *Genome Biology* 6:R17.

12. Pauli, F., Y. Liu, Y. A. Kim, P.-J. Chen, and S. K. Kim. 2006. Chromosomal clustering and GATA transcriptional regulation of intestine-expressed genes in C. elegans. *Development* 133:287-295.

13. Yang, Z., H. J. Edenberg, and R. L. Davis. 2005. Isolation of mRNA from specific tissues of Drosophila by mRNA tagging. *Nucl. Acids Res.* 33:e148-.

14. Penalva, L., M. Burdick, S. Lin, H. Sutterluety, and J. Keene. 2004. RNA-binding proteins to assess gene expression states of co-cultivated cells in response to tumor cells. *Molecular Cancer* 3:24.

15. Griffin, D. E. 2001. Alphaviruses. In *Fields virology, 4th ed.* D. M. Knipe, B. N. Fields, and P. M. Howley, eds. Lippincott Williams & Wilkins, Philadelphia, Pa. . 917-962.

16. Anishchenko, M., R. A. Bowen, S. Paessler, L. Austgen, I. P. Greene, and S. C. Weaver. 2006. Venezuelan encephalitis emergence mediated by a phylogenetically predicted viral mutation. *PNAS* 103:4994-4999.

17. Greene, I. P., S. Paessler, L. Austgen, M. Anishchenko, A. C. Brault, R. A. Bowen, and S. C. Weaver. 2005. Envelope Glycoprotein Mutations Mediate Equine Amplification and Virulence of Epizootic Venezuelan Equine Encephalitis Virus. *J. Virol.* 79:9128-9133.

18. White, L. J., J. g. Wang, N. L. Davis, and R. E. Johnston. 2001. Role of Alpha/Beta Interferon in Venezuelan Equine Encephalitis Virus Pathogenesis: Effect of an Attenuating Mutation in the 5' Untranslated Region. *The Journal of Virology* 75:3706.

19. Powers, A. M., A. C. Brault, R. M. Kinney, and S. C. Weaver. 2000. The Use of Chimeric Venezuelan Equine Encephalitis Viruses as an Approach for the Molecular Identification of Natural Virulence Determinants. *The Journal of Virology* 74:4258-4263.

20. MacDonald, G. H., and R. E. Johnston. 2000. Role of Dendritic Cell Targeting in Venezuelan Equine Encephalitis Virus Pathogenesis. *The Journal of Virology* 74:914-922.

21. Bernard, K. A., W. B. Klimstra, and R. E. Johnston. 2000. Mutations in the E2 Glycoprotein of Venezuelan Equine Encephalitis Virus Confer Heparan Sulfate Interaction, Low Morbidity, and Rapid Clearance from Blood of Mice. *Virology* 276:93-103.

22. Aronson, J. F., F. B. Grieder, N. L. Davis, P. C. Charles, T. Knott, K. Brown, and R. E. Johnston. 2000. A Single-Site Mutant and Revertants Arising in Vivo Define Early Steps in the Pathogenesis of Venezuelan Equine Encephalitis Virus. *Virology* 270:111-123.

23. Spotts, D. R., R. M. Reich, M. A. Kalkhan, R. M. Kinney, and J. T. Roehrig. 1998. Resistance to Alpha/Beta Interferons Correlates with the Epizootic and

Virulence Potential of Venezuelan Equine Encephalitis Viruses and Is Determined by the 5' Noncoding Region and Glycoproteins. *The Journal of Virology* 72:10286-10291.

24. Grieder, F. B., and H. T. Nguyen. 1996. Virulent and attenuated mutant Venezuelan equine encephalitis virus show marked differences in replication in infection in murine macrophages. *Microbial Pathogenesis* 21:85-95.

25. Grieder, F. B., N. L. Davis, J. F. Aronson, P. C. Charles, D. C. Sellon, K. Suzuki, and R. E. Johnston. 1995. Specific Restrictions in the Progression of Venezuelan Equine Encephalitis Virus-Induced Disease Resulting from Single Amino Acid Changes in the Glycoproteins. *Virology* 206:994-1006.

26. Davis, N. L., K. W. Brown, G. F. Greenwald, A. J. Zajac, V. L. Zacny, J. F. Smith, and R. E. Johnston. 1995. Attenuated Mutants of Venezuelan Equine Encephalitis Virus Containing Lethal Mutations in the PE2 Cleavage Signal Combined with a Second-Site Suppressor Mutation in E1. *Virology* 212:102-110.

27. Davis, N. L., F. B. Grieder, J. F. Smith, G. F. Greenwald, M. L. Valenski, D. C. Sellon, P. C. Charles, and R. E. Johnston. 1994. A molecular genetic approach to the study of Venezuelan equine encephalitis virus pathogenesis. *Arch Virol Suppl* 9:99-109.

28. Kinney, R. M., G. J. Chang, K. R. Tsuchiya, J. M. Sneider, J. T. Roehrig, T. M. Woodward, and D. W. Trent. 1993. Attenuation of Venezuelan equine encephalitis virus strain TC-83 is encoded by the 5'-noncoding region and the E2 envelope glycoprotein. *The Journal of Virology* 67:1269-1277.

29. Davis, N. L., N. Powell, G. F. Greenwald, L. V. Willis, B. J. Johnson, J. F. Smith, and R. E. Johnston. 1991. Attenuating mutations in the E2 glycoprotein gene of Venezuelan equine encephalitis virus: construction of single and multiple mutants in a full-length cDNA clone. *Virology* 183:20-31.

30. Johnston, R. E., and J. F. Smith. 1988. Selection for accelerated penetration in cell culture coselects for attenuated mutants of Venezuelan equine encephalitis virus. *Virology* 162:437-443.

31. Johnson, B. J., R. M. Kinney, C. L. Kost, and D. W. Trent. 1986. Molecular determinants of alphavirus neurovirulence: nucleotide and deduced protein sequence changes during attenuation of Venezuelan equine encephalitis virus. *J Gen Virol* 67 (Pt 9):1951-1960.

32. Wang, E., A. C. Brault, A. M. Powers, W. Kang, and S. C. Weaver. 2003. Glycosaminoglycan Binding Properties of Natural Venezuelan Equine Encephalitis Virus Isolates. *J. Virol.* 77:1204-1210.

33. Pushko, P., M. Parker, G. V. Ludwig, N. L. Davis, R. E. Johnston, and J. F. Smith. 1997. Replicon-Helper Systems from Attenuated Venezuelan Equine Encephalitis Virus: Expression of Heterologous Genes in Vitro and Immunization against Heterologous Pathogens in Vivo. *Virology* 239:389-401.

34. Thompson, J. M., A. C. Whitmore, J. L. Konopka, M. L. Collier, E. M. B. Richmond, N. L. Davis, H. F. Staats, and R. E. Johnston. 2006. Mucosal and systemic adjuvant activity of alphavirus replicon particles. *PNAS* 103:3722-3727.

35. Shabman, R. S., T. E. Morrison, C. Moore, L. White, M. S. Suthar, L. Hueston, N. Rulli, B. Lidbury, J. P. Y. Ting, S. Mahalingam, and M. T. Heise. 2007. Differential Induction of Type I Interferon Responses in Myeloid Dendritic Cells by Mosquito and Mammalian-Cell-Derived Alphaviruses. *J. Virol.* 81:237-247.

36. Serody, J. S., E. J. Collins, R. M. Tisch, J. J. Kuhns, and J. A. Frelinger. 2000. T Cell Activity After Dendritic Cell Vaccination Is Dependent on Both the Type of Antigen and the Mode of Delivery. *J Immunol* 164:4961-4967.

37. Moran, T. P., M. Collier, K. P. McKinnon, N. L. Davis, R. E. Johnston, and J. S. Serody. 2005. A Novel Viral System for Generating Antigen-Specific T Cells. *J Immunol* 175:3431-3438.

38. Gardner, J. P., I. Frolov, S. Perri, Y. Ji, M. L. MacKichan, J. zur Megede, M. Chen, B. A. Belli, D. A. Driver, S. Sherrill, C. E. Greer, G. R. Otten, S. W. Barnett, M. A. Liu, T. W. Dubensky, and J. M. Polo. 2000. Infection of Human Dendritic Cells by a Sindbis Virus Replicon Vector Is Determined by a Single Amino Acid Substitution in the E2 Glycoprotein. *J. Virol.* 74:11849-11857.

39. Ryman, K. D., W. B. Klimstra, K. B. Nguyen, C. A. Biron, and R. E. Johnston. 2000. Alpha/Beta Interferon Protects Adult Mice from Fatal Sindbis Virus Infection and Is an Important Determinant of Cell and Tissue Tropism. *J. Virol.* 74:3366-3378.

40. Klimstra, W. B., E. M. Nangle, M. S. Smith, A. D. Yurochko, and K. D. Ryman. 2003. DC-SIGN and L-SIGN Can Act as Attachment Receptors for Alphaviruses and Distinguish between Mosquito Cell- and Mammalian Cell-Derived Viruses. *J. Virol.* 77:12022-12032.

41. Ryman, K. D., K. C. Meier, E. M. Nangle, S. L. Ragsdale, N. L. Korneeva, R. E. Rhoads, M. R. MacDonald, and W. B. Klimstra. 2005. Sindbis Virus Translation Is Inhibited by a PKR/RNase L-Independent Effector Induced by Alpha/Beta Interferon Priming of Dendritic Cells. *The Journal of Virology* 79:1487-1499.

42. Jordan, G. W. 1973. Interferon sensitivity of Venezuelan equine encephalomyelitis virus. *Infect Immun* 7:911-917.

43. Jahrling, P. B., E. Navarro, and W. F. Scherer. 1976. Interferon induction and sensitivity as correlates to virulence of Venezuelan encephalitis viruses for hamsters. *Arch Virol* 51:23-35.

44. Gorchakov, R., E. Frolova, and I. Frolov. 2005. Inhibition of Transcription and Translation in Sindbis Virus-Infected Cells. *J. Virol.* 79:9397-9409.

45. Garmashova, N., R. Gorchakov, E. Volkova, S. Paessler, E. Frolova, and I. Frolov. 2007. The Old World and New World Alphaviruses Use Different Virus-Specific Proteins for Induction of Transcriptional Shutoff. *J. Virol.* 81:2472-2484.

46. Swanson, K. A., Y. Zheng, K. M. Heidler, Z.-D. Zhang, T. J. Webb, and D. S. Wilkes. 2004. Flt3-Ligand, IL-4, GM-CSF, and Adherence-Mediated Isolation of Murine Lung Dendritic Cells: Assessment of Isolation Technique on Phenotype and Function. *J Immunol* 173:4875-4881.

47. Mangus, D., M. Evans, and A. Jacobson. 2003. Poly(A)-binding proteins: multifunctional scaffolds for the post-transcriptional control of gene expression. *Genome Biology* 4:223.

48. Grieder, F. B., B. K. Davis, X. D. Zhou, S. J. Chen, F. D. Finkelman, and W. C. Gause. 1997. Kinetics of Cytokine Expression and Regulation of Host Protection Following Infection with Molecularly Cloned Venezuelan Equine Encephalitis Virus. *Virology* 233:302-312.

49. Anishchenko, M., S. Paessler, I. P. Greene, P. V. Aguilar, A.-S. Carrara, and S. C. Weaver. 2004. Generation and Characterization of Closely Related Epizootic and Enzootic Infectious cDNA Clones for Studying Interferon Sensitivity and Emergence Mechanisms of Venezuelan Equine Encephalitis Virus. *J. Virol.* 78:1-8.

50. Schoneboom, B. A., J. S. Lee, and F. B. Grieder. 2000. Early Expression of IFN-alpha/beta and iNOS in the Brains of Venezuelan Equine Encephalitis Virus-Infected Mice. *Journal of Interferon & Cytokine Research* 20:205-216.

51. Grieder, F. B., and S. N. Vogel. 1999. Role of Interferon and Interferon Regulatory Factors in Early Protection against Venezuelan Equine Encephalitis Virus Infection. *Virology* 257:106-118.

52. Charles, P. C., J. Trgovcich, N. L. Davis, and R. E. Johnston. 2001. Immunopathogenesis and Immune Modulation of Venezuelan Equine Encephalitis Virus-Induced Disease in the Mouse. *Virology* 284:190-202.

53. Schoneboom, B. A., K. M. K. Catlin, A. M. Marty, and F. B. Grieder. 2000. Inflammation is a component of neurodegeneration in response to Venezuelan equine encephalitis virus infection in mice. *Journal of Neuroimmunology* 109:132-146.

54. Jackson, A. C., and P. R. John. 1997. Apoptotic cell death is an important cause of neuronal injury in experimental Venezuelan equine encephalitis virus infection of mice. *Acta Neuropathologica* V93:349-353.

55. Darman, J., S. Backovic, S. Dike, N. J. Maragakis, C. Krishnan, J. D. Rothstein, D. N. Irani, and D. A. Kerr. 2004. Viral-Induced Spinal Motor Neuron Death Is Non-Cell-Autonomous and Involves Glutamate Excitotoxicity. *J. Neurosci.* 24:7566-7575.

56. Carmen, J., Genevieve Gowing Jean-Pierre Julien Douglas Kerr. 2006. Altered immune response to CNS viral infection in mice with a conditional knock-down of macrophage-lineage cells. *Glia* 54:71-80.

57. Keene, J. D., and S. A. Tenenbaum. 2002. Eukaryotic mRNPs may represent posttranscriptional operons. *Mol.Cell* 9:1161-1167.

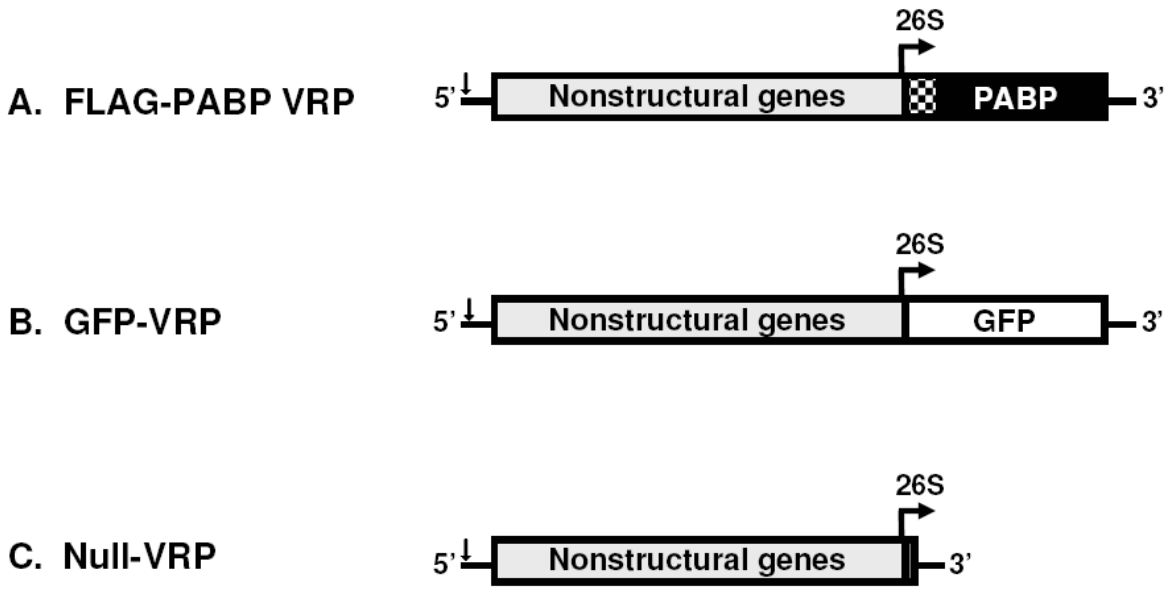

Figure 2.1. VEE replicon constructs. The VEE replicon genome encodes the viral nonstructural genes, the authentic 5' and 3' UTR, as well as a cloning cassette downstream of the 26S subgenomic promoter for transgene insertion. Schematic representation of the replicon constructs used in this study are shown above: (A) FLAG-PABP VRP, expressing an N-terminally FLAG-tagged version of PABP (FLAG epitope denoted by checkered shading); (B) GFP-VRP, expressing green fluorescent protein; and (C) Null-VRP, encoding the replicon genome devoid of functional transgene sequence. Additional FLAG-PABP VRP and null-VRP genome constructs containing a change from wildtype ntG at position three to ntA were also utilized (position within the 5'UTR denoted by the small arrow). All replicon particles used in this study were packaged in the wildtype (V3000) envelope.

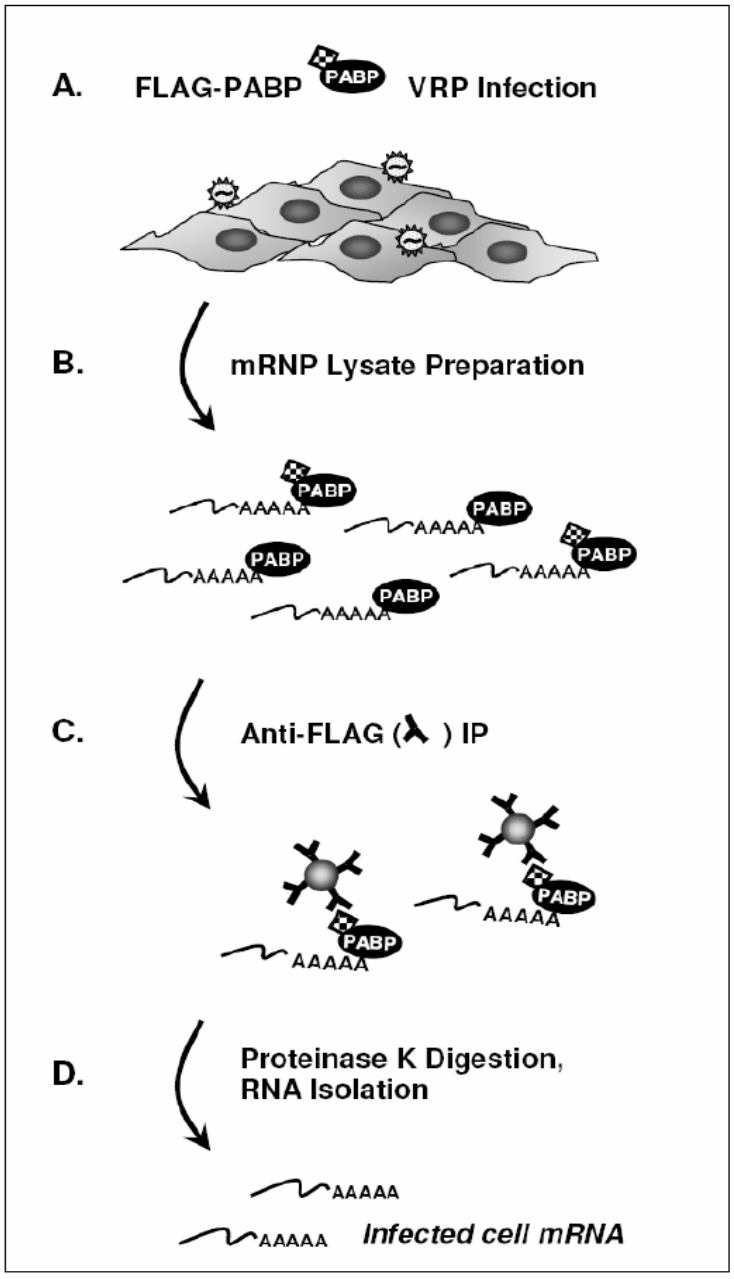

Figure 2.2. The VRP mRNP-tagging system. Flowchart illustrating the VRP ribonomics mRNA-tagging method of isolating mRNA specifically from infected cells. (A) Cells are infected with FLAG-PABP VRP, delivering the unique epitope-tagged version of PABP only to infected cells. (B) At various times post-infection, cytoplasmic lysates are prepared, containing the cellular mRNP complexes. (C) Anti-FLAG antibody-coated agarose beads are added in excess to the lysate, coimmunoprecipitating the mRNA bound by FLAG-PABP, and thus fractionating the mRNA in the infected cells from the mRNA in the surrounding uninfected cells. (D) The immunoprecipitated mRNA-PABP complex is dissociated using proteinase K digestion, and the infected cell mRNA is isolated by standard RNA extraction and precipitation.

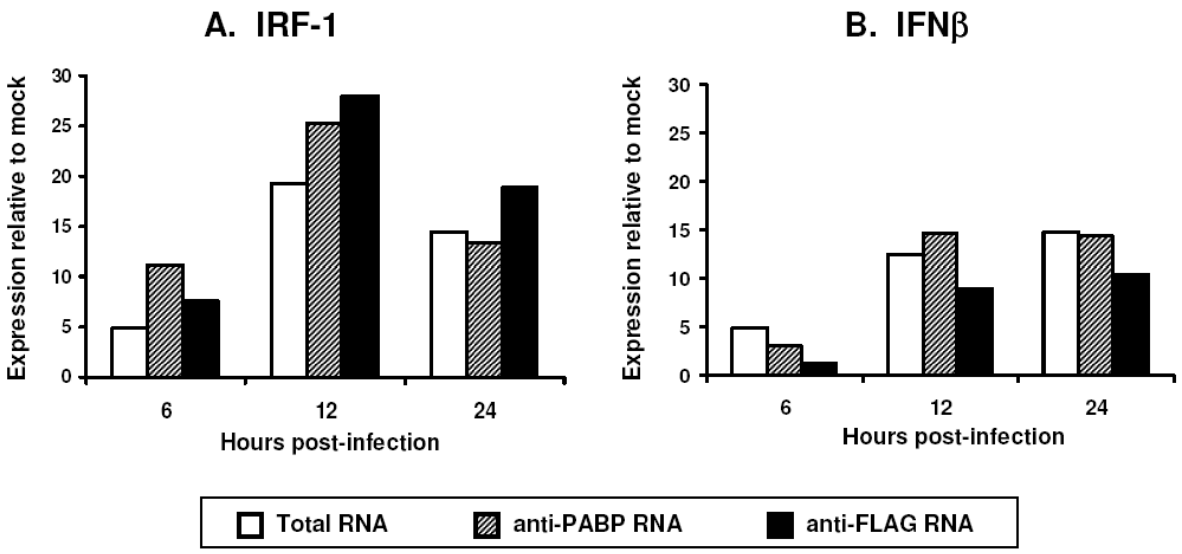

Figure 2.3. RNA profile comparison following high MOI infection. Changes in host gene expression were assessed following VRP infection, using RNA isolated by three distinct methods. 10^6 L929 cells were mock treated or infected with FLAG-PABP VRP (MOI=5). At 6, 12, or 24h, cellular RNA was harvested by three separate methods: (i) Total RNA from mock and VRP-infected cells was isolated using UltraSpec reagent. (ii) All mRNA bound to PABP in lysates prepared from mock and VRP-infected cultures were isolated by anti-PABP immunoprecipitation. (iii) mRNA from infected cells was specifically isolated by anti-FLAG immunoprecipitation, recovering the mRNA bound to the FLAG-PABP in VRP-infected lysates. The isolated RNA populations served as input RNA in an RNase protection assay to analyze the expression profile of several host genes. The fold induction of (A) IRF-1 and (B) IFNβ, relative to expression in mock treated cells, are shown above comparing the profiles generated from the distinct RNA isolations. The data are a representative of two separate experiments, with the signal generated from each sample internally normalized to GAPDH signal.

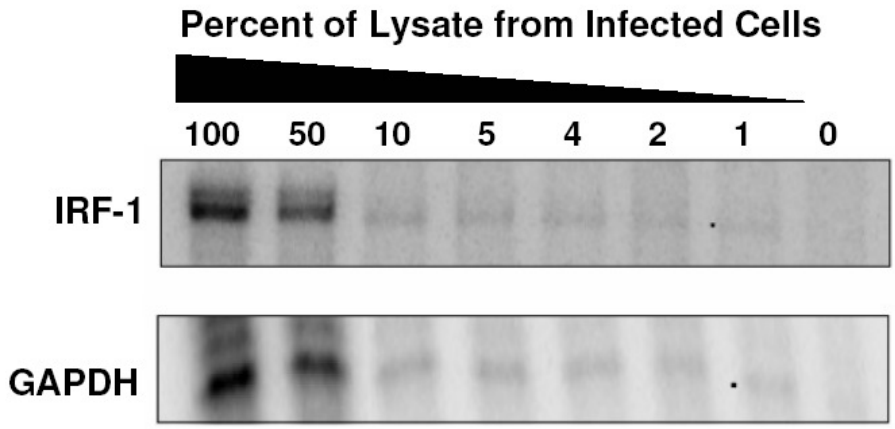

Figure 2.4. Sensitivity of the VRP mRNP-tagging system. To assess the level of ribonomics sensitivity, an *in vitro* experiment was performed to model the *in vivo*-like condition of a diluted infected cell population. At 6hpi, cell lysates (1 ml) were prepared from 10^6 L929 cells that had been infected with FLAG-PABP VRP (MOI=5). The resulting lysates were mixed in decreasing ratios of infected lysate to mock lysate, to a total volume of 200 µl. Anti-FLAG immunoprecipitation was performed to isolate RNA from the infected cell portion of this mixed lysate. To assess the mRNA signal recovered from the infected cells, an RNase protection assay was used to detect several host mRNAs, two of which are shown above (IRF-1, GAPDH). Signal from infected cell RNA within the mixed lysate was detected in samples comprised of as little as 1% infected cell lysate (highlighted by the small dots), a value approximately equal to $2x10^3$ infected cells.

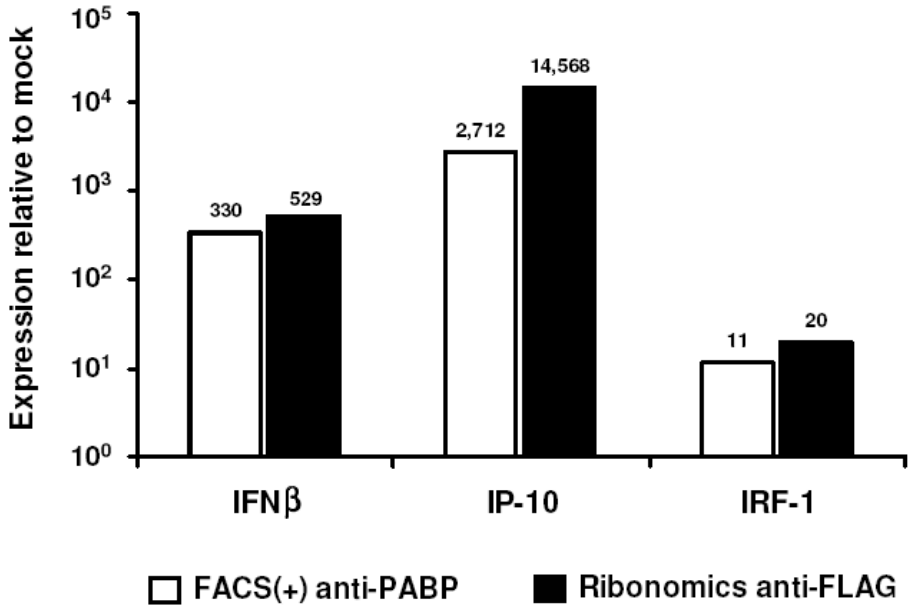

Figure 2.5. Infected cell gene expression profiles generated by mRNP-tagging versus FACS-based assays. The ribonomics approach and a FACS-based method of sorting infected cells were compared. 1.5 x 10^6 L929 cells were infected with either GFP-VRP or FLAG-PABP VRP (MOI=0.2). 12h after GFP-VRP infection, infected cells were sorted and recovered based on GFP expression via FACS. The recovered GFP-positive (infected) cells were lysed, and all PABP-bound host messages were isolated by anti-PABP immunoprecipitation. In parallel, 12h after FLAG-PABP VRP infection, the ribonomics assay was used to directly sort the mRNA from infected cells by anti-FLAG immunoprecipitation. To evaluate and compare host gene expression in the infected cell populations, two independent samples were analyzed for IFNβ, IP-10, and IRF-1 expression by Taqman real time PCR. The results were normalized to GAPDH signal, compared to PABP-bound mRNA from mock infected cells, and averaged.

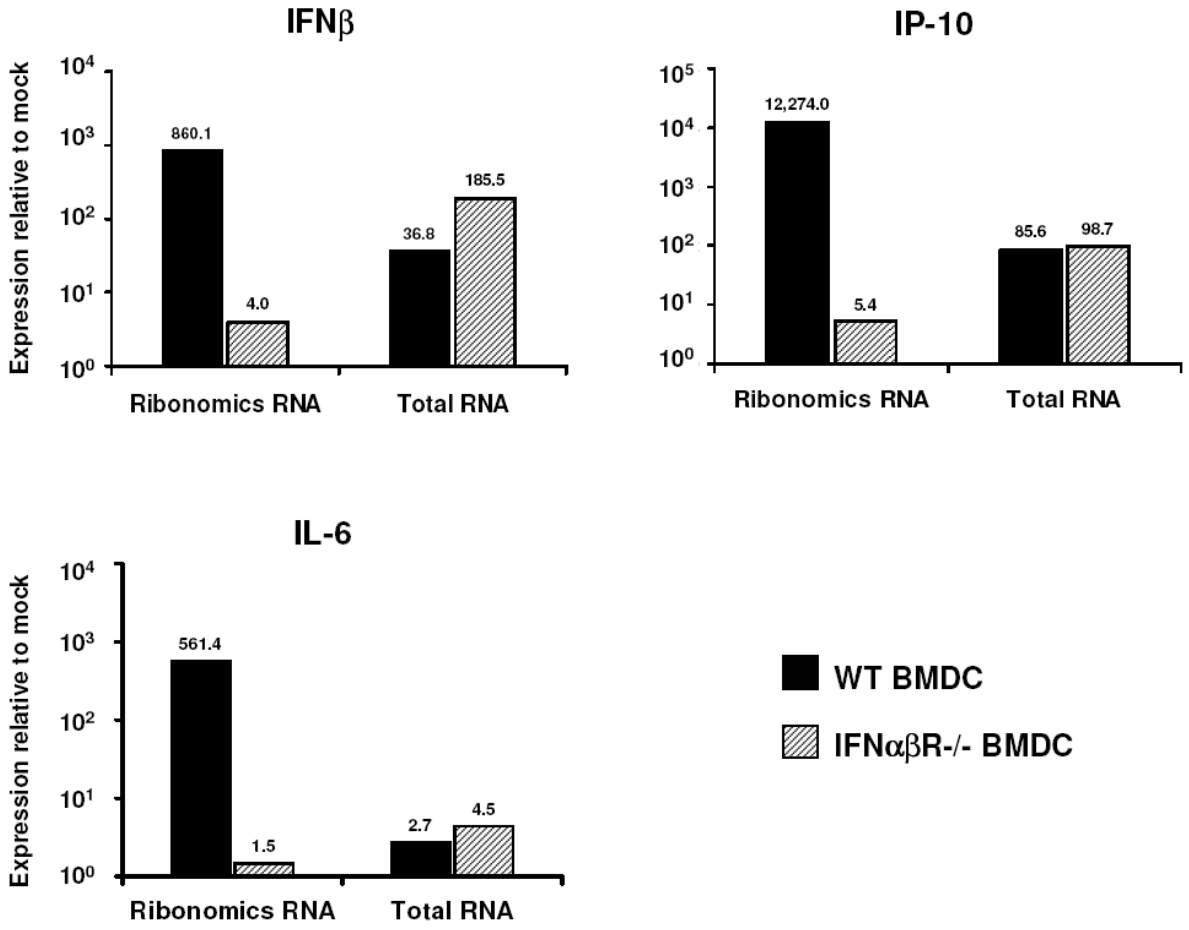

Figure 2.6. Role of interferon signaling in VRP-induced host gene expression in infected versus bystander BMDC. 10^6 BMDC generated from wildtype 129sv/ev mice (black bars) were infected with FLAG-PABP VRP at a low MOI (0.5). At 6h, RNA was isolated from mock and VRP-infected BMDC by either 1) preparing cell lysates for isolation of FLAG-PABP-bound mRNA via anti-FLAG immunoprecipitation, or 2) using UltraSpec reagent to isolate total cellular RNA. The ribonomics method specifically isolated mRNA from the minority of infected BMDC via the bound FLAG-PABP. Conversely, total RNA extraction was used to isolate cellular RNA from the entire VRP-infected BMDC culture, with the majority of the population being DCs that had not been infected. To examine the contribution of signaling through the IFNab receptor, the same analysis was carried out in BMDC derived from IFNαβR-/- mice (hatched bars). cDNA was generated from each RNA isolation, and assessed for changes in host gene expression by Taqman real-time PCR. Two independent samples were normalized to GAPDH signal, analyzed in comparison to mock infected BMDC, and averaged.

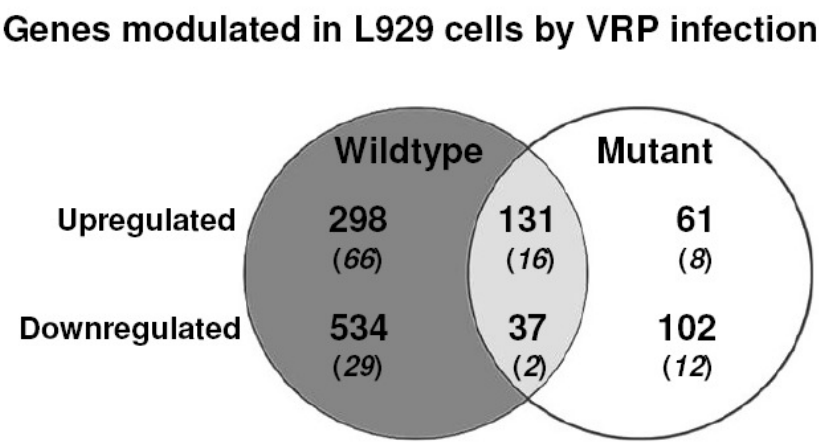

Figure 2.7. Differential regulation of the host response following wildtype and interferon-sensitive VRP infection. Affymetrix DNA microarray analysis was used to define global changes in host gene expression following wildtype and nt3A mutant null-VRP infection. Total RNA was isolated at 5hpi from L929 cells that had been mock or null-VRP infected (MOI=5). Samples were analyzed for changes in host gene expression by the Affymetrix Mouse Expression 430A GeneChip technology. Data from two independent array experiments were analyzed and filtered to uncover genes induced or repressed during each infection in comparison to mock treated cells. Venn diagram assessment of genes that were modulated during infection by >2-fold over mock treated cells revealed populations of mRNAs that were uniquely modulated by each infection. A similar analysis of genes modulated >4-fold (in parentheses) over mock continued to reveal uniquely regulated genes.

Table 2.1. Modulation of host interferon, inflammatory, and defense response gene expression profiles following VRP infection of L929 cells*

Affymetrix Probe ID	Genbank ID	Gene Symbol	Alternative Symbol	Description	Experiment #1 (Fold Induction)		Experiment #2 (Fold Induction)	
					WT VRP v. Mock	nt3A VRP v. Mock	WT VRP v. Mock	nt3A VRP v. Mock
1422305_at	NM_010510	IFNβ		interferon beta; antiviral/host defense response; ISG	3.0	1.3	4.2	1.9
1421322_a_at	NM_008394	ISGF3G	IRF-9, p48	IFN-dependent positive acting transcription factor 3 gamma; host defense response; ISG	5.0	2.2	7.3	2.4
1418580_at	BC024872	RTP4	IFRG28	28kD interferon alpha responsive protein; receptor transporting protein 4; ISG	24.1	1.0	182.9	1.0
1450783_at	NM_008331	IFIT1	p56; GARG-16	IFN-induced protein with tetratricopeptide repeats 1; host defense response; ISG	2.2	1.0	3.4	1.0
1422476_at	NM_023065	IFI30	IP30, GILT	interferon gamma inducible protein 30; ISG	-2.2	-1.3	-3.1	-1.4
1450297_at	NM_031168	IL-6		interleukin 6; immune modulation; inflammatory response; ISG	3.1	1.5	5.2	2.9
1424339_at	AB067533	OASL1		2'-5' oligoadenylate synthetase-like 1; immune response; ISG	7.5	2.9	8.9	1.8
1420380_at	AF065933	CCL2	MCP-1; JE	chemokine (C-C motif) ligand 2; immune modulation; chemotaxis; inflammatory response; ISG	2.4	1.2	2.5	1.3
1418126_at	NM_013653	CCL5	RANTES	chemokine (C-C motif) ligand 5; immune modulation; chemotaxis; inflammatory response; ISG	5.3	1.0	30.5	1.0
1418930_at	NM_021274	CXCL10	IP-10; IFI10	chemokine (C-X-C motif) ligand 10; immune modulation; chemotaxis; inflammatory response; ISG	16.7	1.0	23.0	13.0
1448306_at	NM_010907	NFKBIA	IkappaBa; MAD3	nuclear factor of kappa light chain enhancer in B-cells inhibitor; host defense response; signaling; ISG	2.2	1.1	4.0	1.0
1421228_at	AF128193	CCL7	MCP-3	chemokine (C-C motif) ligand 7; immune modulation; chemotaxis; inflammatory response	3.0	2.2	2.9	2.1
1419209_at	NM_008176	CXCL1	GROa	chemokine (C-X-C motif) ligand 1; immune modulation; inflammatory response	11.3	4.7	11.1	3.0
1449984_at	NM_009140	CXCL2	MIP2a; GROb	chemokine (C-X-C motif) ligand 2; immune modulation; chemotaxis; inflammatory response	3.2	2.0	3.7	1.0
1449109_at	NM_007706	SOCS2	STAT12; SSI-2	suppressor of cytokine signaling 2; STAT-induced STAT inhibitor 2	2.1	1.4	2.6	1.4
1456212_x_at	BB831725	SOCS3	SSI-3	suppressor of cytokine signaling 3; STAT-induced STAT inhibitor 3	2.4	2.3	2.3	1.4
1419132_at	NM_011905	TLR2		toll-like receptor 2; innate immune response	2.1	1.5	3.7	1.4
1450829_at	NM_009397	TNFAIP3	A20	tumor necrosis factor, alpha-induced protein 3; apoptosis; ubiquitin cycle	3.4	1.8	3.2	2.0
1421207_at	AF065917	LIF		leukemia inhibitory factor; cytokine activity, immune response	2.2	1.0	7.5	2.3
1437270_a_at	BB825816	BSF3	CLCF1	B-cell stimulating factor 3; cytokine activity; signaling	2.3	3.0	3.7	2.6
1417625_s_at	BC015254	CMKOR1	CXCR7	chemokine orphan receptor 1; chemokine (C-X-C motif) receptor 7; chemotaxis; defense response	2.8	2.2	2.3	2.0
1435476_a_at	BM224327	Fcgr2b	Fc gamma RIIB	Fc receptor, IgG low affinity IIb; defense response	2.5	2.5	2.1	1.6

* L929 cells were mock treated or infected with either wildtype or nt3A mutant null-VRP (MOI=5). At 5hpi, total RNA was isolated and served as the target for Affymetrix GeneChip analysis to characterize the global host response to each infection (MOE430A GeneChip). Two independent array experiments were completed, and gene lists were compiled representing only those genes that were up- or downregulated by greater than 2-fold in replicate analyses. ISG=interferon-stimulated gene.

A. Ribonomics RNA Analysis

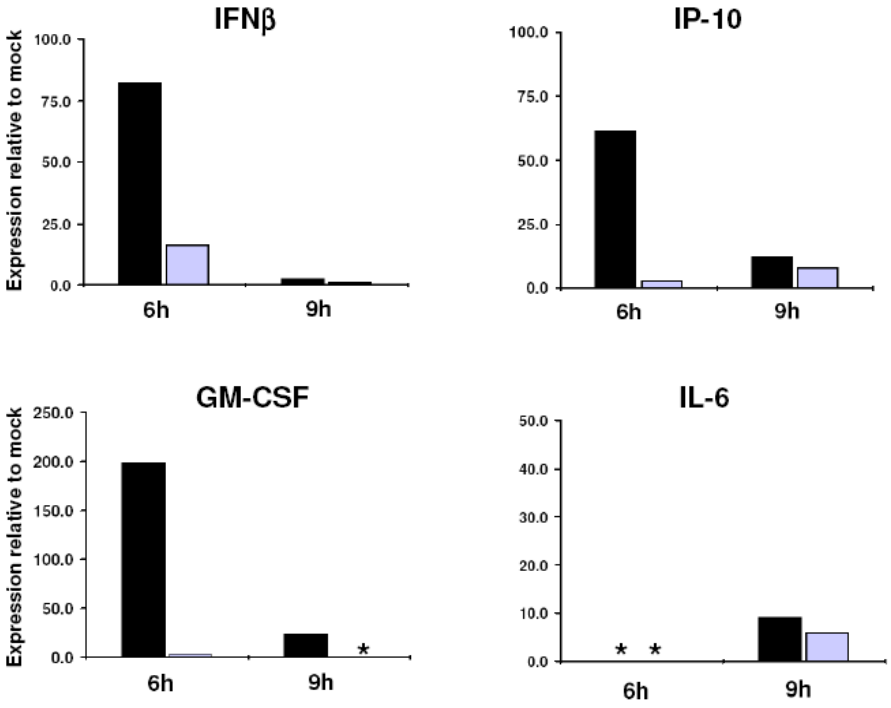

B. Total RNA Analysis

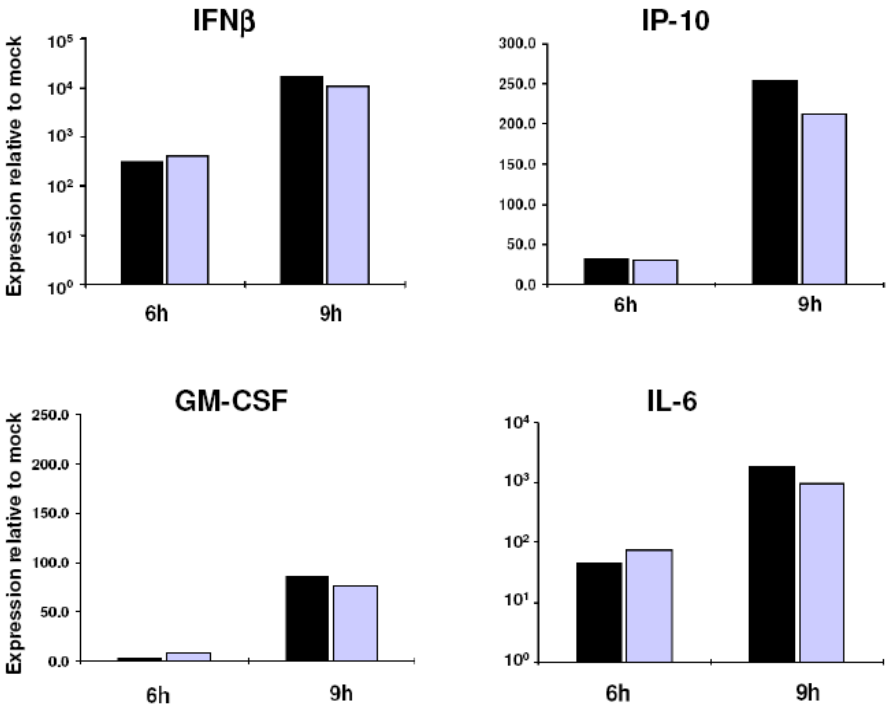

Figure 2.8. *In vivo,* the combination of traditional and ribonomics profiling uncovers dynamic changes in host gene expression within the DLN. Adult female Balb/c mice were inoculated in both rear footpads with 10^6 IU of wildtype or nt3A mutant FLAG-PABP VRP. Mock treated animals were inoculated with diluent alone. At 6 and 9h, the popliteal DLNs were removed and washed with PBS. To isolate RNA from the entire cellular population of the DLN, both DLNs were pooled, homogenized, and total RNA extracted. For isolation of mRNA specifically from the infected cells of the DLN, the ribonomics mRNA tagging technique was used: Five DLNs were pooled per sample and homogenized in lysis buffer, followed by anti-FLAG immunoprecipitation. cDNA was synthesized from each RNA sample, and Taqman real-time PCR was performed against several target host genes. Two independent pools were analyzed from each group, with GAPDH serving as the internal housekeeping control gene, and the results were averaged. Asterisks indicate samples from infected DLN that had no detectable signal following anti-FLAG immunoprecipitation. Ribonomics profiling in conjunction with traditional profiling reveals two distinct, comprehensive views of the response to infection within this target tissue *in vivo*.

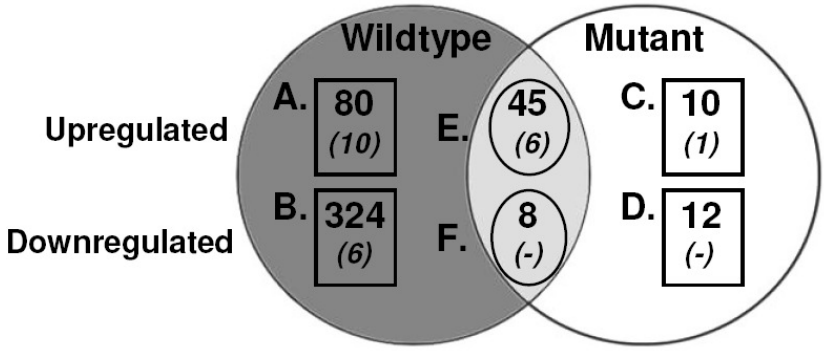

Supplemental Fig. 2.1. Differential regulation of the host response following wildtype and interferon-sensitive VRP infection. Affymetrix DNA microarray analysis was used to define global changes in host gene expression following wildtype and nt3A mutant null-VRP infection. Total RNA was isolated at 5hpi from L929 cells that had been mock or null-VRP infected (MOI=5). Samples were analyzed for changes in host gene expression by the Affymetrix Mouse Expression 430A GeneChip technology. Data from two independent array experiments were analyzed and filtered to uncover genes induced or repressed during each infection in comparison to mock treated cells. Venn diagram assessment of genes that were modulated during infection by >2-fold over mock treated cells revealed populations of mRNAs that were uniquely modulated by each infection. A similar analysis of genes modulated >4-fold (in parentheses) over mock continued to reveal uniquely regulated genes. This data corresponds to the same data in Fig. 2.7, except here groups (A-F) were assigned in order to designate the unique or common gene sets modulated during infection. The individual genes belonging to each of these groups is listed in Supplemental Table 2.1.

Supplemental Table 2.1. Affymetrix Gene Expression Profiling of VRP Infected L929 Cells

Group A: Genes upregulated by greater than two-fold over mock, only in wildtype VRP infected cells

Affymetrix Probe ID	Genbank ID	Gene Symbol	Description
1422999_at	NM_016896	Map3k14	mitogen-activated protein kinase kinase kinase 14; protein phosphorylation
1422916_at	NM_020013	Fgf21	fibroblast growth factor 21
1423100_at	AV026617	Fos	FBJ osteosarcoma oncogene
1423702_at	BC003830	H1f0	H1 histone family, member 0; nucleosome assembly
1423905_at	BB049138	D7Ertd458e	unknown
1422305_at	NM_010510	IFNβ	interferon beta, fibroblast; defense response
1425837_a_at	AF199491	Ccrn4l	CCR4 carbon catabolite repression 4-like (S. cerevisiae); rhythmic behavior
1425868_at	BC019122		MRNA similar to H2B histone family, member J
1426065_a_at	BC012955	Ifld2	induced in fatty liver dystrophy 2; apoptosis
1426930_at	AV327653		unknown
1427013_at	AJ245857	Car9	carbonic anhydrase 9; metabolism
1426464_at	W13191	Nr1d1	nuclear receptor subfamily 1, group D, member 1
1426681_at	BQ177034	B230379M23Rik	unknown
1424866_at	BC021474	Usp43	ubiquitin specific protease 43
1424339_at	AB067533	Oasl1	2'-5' oligoadenylate synthetase-like 1
1424518_at	BC020489	LOC223672	unknown
1417612_at	BF147705	Ier5	immediate early response 5
1417625_s_at	BC015254	Cmkor1	chemokine orphan receptor 1; chemotaxis; defense response
1417263_at	M94967	Ptgs2	prostaglandin-endoperoxide synthase 2; oxidative stress response
1417395_at	BG069413	Klf4	Kruppel-like factor 4 (gut)
1417394_at	BG069413	Klf4	Kruppel-like factor 4 (gut)
1418191_at	NM_011909	Usp18	ubiquitin specific protease 18
1418072_at	NM_023422	Hist1h2bc	histone 1, H2bc; nucleosome assembly
1418126_at	NM_013653	Ccl5; RANTES	chemokine (C-C motif) ligand 5; chemotaxis; inflammatory immune response
1416129_at	NM_133753	1300002F13Rik	unknown
1416029_at	NM_013692	Tieg1	TGFB inducible early growth response 1; transcription factor
1415997_at	AF173681	Txnip	thioredoxin interacting protein; oxidative stress response
1415899_at	NM_008416	Junb	Jun-B oncogene; transcription factor
1417065_at	NM_007913	Egr1	early growth response 1; transcription factor
1416691_at	NM_019581	Gtpbp2	GTP binding protein 2; translation elongation
1416690_at	NM_019581	Gtpbp2	GTP binding protein 2; translation elongation
1416693_at	NM_013519	Foxc2	forkhead box C2; transcription factor
1420352_at	NM_133731	Prss22	protease, serine, 22; proteolysis and peptidolysis
1420380_at	AF065933	Ccl2	chemokine (C-C motif) ligand 2
1421252_a_at	NM_013597	Mef2a	myocyte enhancer factor 2A; transcription factor
1421155_at	NM_080445	B3galt6	glycosaminoglycan biosynthesis; protein amino acid glycosylation
1421207_at	AF065917	Lif	leukemia inhibitory factor; cytokine; immune response
1420909_at	NM_009505	Vegfa	vascular endothelial growth factor A
1420958_at	NM_025575	2610042O14Rik	unknown

1418936_at	BC022952	Maff	transcription factor
1418930_at	NM_021274	Cxcl10; IP-10	chemokine (C-X-C motif) ligand 10; chemotaxis; inflammatory immune response
1419132_at	NM_011905	Tlr2	toll-like receptor 2; pathogen recognition
1418580_at	BC024872	28kD interferon alpha responsive protein; rtp4	receptor transporting protein 4
1418687_at	NM_018790	Arc	cytoskeletal-associated protein; actin binding
1418739_at	NM_013731	Sgk2	serum/glucocorticoid regulated kinase 2; protein phosphorylation
1419611_at	BC023403	4632415L05Rik	unknown
1419619_at	NM_028770	Krt80	keratin 80
1450829_at	NM_009397	Tnfaip3	tumor necrosis factor, alpha-induced protein 3; ap0ptosis
1450783_at	NM_008331	Ifit1; p56; ISG56	interferon-induced protein with tetratricopeptide repeats 1; interferon defense response
1450522_a_at	NM_008197	H1f0	H1 histone family, member 0; nucleosome assembly
1451491_at	BC016225	4930556P03Rik	unknown
1451382_at	BC025169	1810008K03Rik	unknown
1451340_at	BC027152	Arid5a	modulator recognition factor I
1451273_x_at	BC025546	BC025546	unknown
1449300_at	NM_030249	BC003236	unknown
1449109_at	NM_007706	Socs2	suppressor of cytokine signaling 2; regulation of immune response; neuron differentiation
1450297_at	NM_031168	Il6	interleukin 6; acute-phase immune response
1450253_a_at	U11548	Map3k4; MTK1; Mekk4	mitogen activated protein kinase kinase kinase 4; protein phosphorylation
1449731_s_at	AI462015	Nfkbia; IkappaBα	nuclear factor of kappa light chain gene enhancer in B-cells inhibitor, alpha; signal transduction
1449984_at	NM_009140	Cxcl2; GRO2; MIP-2α	chemokine (C-X-C motif) ligand 2; chemotaxis; inflammatory immune response
1456174_x_at	AV309418		similar to cytoplasmic protein Ndr1
1456212_x_at	BB831725		unknown
1459902_at	AI510297	2700007P21Rik	unknown
1459478_at	BG063235		unknown
1453678_at	AK007371	Mbd1	methyl-CpG binding domain protein 1; DNA methylation
1452540_a_at	M25487	Hist1h2bp	histone 1, H2bp
1434831_a_at	BB364488	Foxo3	forkhead box O3; transcription regulation
1427683_at	X06746	Egr2	early growth response 2
1427816_at	U14648	Sfrs2; MRF-1	putative myelin regulatory factor 1; transcription factor
1427182_s_at	BQ032363	D18Ertd653e	unknown
1427372_at	BM119774	Cyp27b1	cytochrome P450, family 27, subfamily b, polypeptide 1
1445116_at	BG065809		unknown
1439372_at	AV215710		similar to Smt3A
1448306_at	NM_010907	Nfkbia; IkappaBα	nuclear factor of kappa light chain gene enhancer in B-cells inhibitor, alpha; signal transduction
1448398_s_at	NM_009079	Rpl22	ribosomal protein L22
1448437_a_at	NM_019581	Gtpbp2	GTP binding protein 2; translation elongation
1436506_a_at	AW988981		unknown
1435174_at	AW546080	C230004D03Rik	unknown
1435476_a_at	BM224327	Fcgr2b	Fc receptor, IgG, low affinity IIb
1438366_x_at	BB144743	Clcn3	chloride channel 3

Group B: Genes downregulated by greater than four-fold of mock, only in wildtype VRP infected cells*

Affymetrix Probe ID	Genbank ID	Gene Symbol	Description
1424118_a_at	BC027121	2600017H08Rik	unknown
1419498_at	NM_025655	2010002A20Rik	unknown
1449859_at	NM_025872	CGI-141 protein	vesicle-mediated transport
1439466_s_at	BB001490		similar to G10 protein homolog (edg2)
1448373_at	NM_026310	Mrpl18	mitochondrial ribosomal protein L18
1448493_at	NM_026420	Paip2	polyadenylate-binding protein-interacting protein 2

*Due to the large number of genes downregulated by greater than two-fold in this group, only those modulated by >four-fold are listed

Group C: Genes upregulated by greater than two-fold over mock, only in nt3A mutant VRP infected cells

Affymetrix Probe ID	Genbank ID	Gene Symbol	Description
1423006_at	NM_008842	Pim1	proviral integration site 1; protein phosphorylation
1427126_at	M12573	Hspa1a	heat shock protein 1A; anti-apoptotic; inhibition of caspase activation
1425601_a_at	BC013820	Rtkn	rhotekin; signal transduction
1425362_at	BC003330	Hrbl	HIV-1 Rev binding protein-like
1417409_at	NM_010591	Jun	Jun oncogene; transcription factor
1417856_at	NM_009046	Relb	avian reticuloendotheliosis viral (v-rel) oncogene related B; transcription factor; dendritic cell differentiation
1419149_at	NM_008871	Serpine1	serine (or cysteine) proteinase inhibitor, clade E, member 1; regulation of angiogenesis
1453589_a_at	BI737178		similarity to Cadherin-11 precursor
1433675_at	BQ177137		unknown
1427886_at	BC028835	9830109N13Rik	nuclear pore membrane protein 121

Group D: Genes downregulated by greater than two-fold of mock, only in nt3A mutant VRP infected cells

Affymetrix Probe ID	Genbank ID	Gene Symbol	Description
1426171_x_at	U10095	Klra7	killer cell lectin-like receptor, subfamily A, member 7; cell adhesion; defense response
1427067_at	AJ404329	4933439F18Rik	unknown
1426478_at	AA124924	Rasa1	RAS p21 protein activator 1
1417565_at	AK007421	Abhd5	abhydrolase domain containing 5
1417095_a_at	NM_015765	Hsp70-4	heat shock protein 4; proteolysis and peptidolysis
1421141_a_at	BG962849	Foxp1	forkhead box P1; regulation of tissue- and cell type-specific gene transcription
1420821_at	NM_030750	Sgpp1	sphingosine-1-phosphate phosphatase 1; apoptosis; sphingolipid metabolism
1455953_x_at	BF320427	5730458D16Rik	unknown
1460369_at	BC003267	LOC233987	similar to zinc finger protein 97
1427518_at	AI892455		similar to DNA-binding protein
1427349_x_at	AK012776	2810021G02Rik	RIKEN cDNA 2810021G02 gene; nucleic acid binding
1438181_x_at	BB302809	2410018G23Rik	unknown

Group E: Genes upregulated by greater than two-fold over mock, in wildtype and nt3A mutant VRP infected cells

Affymetrix Probe ID	Genbank ID	Gene Symbol	Description
1422931_at	NM_008037	Fosl2	fos-like antigen 2; transcription regulation
1427005_at	BM234765	Plk2	polo-like kinase 2 (Drosophila)
1424735_at	BC019978	1110030N17Rik	mitochondrial Ca2+-dependent solute carrier
1424942_a_at	BC006728	Myc	myelocytomatosis oncogene; regulation of apoptosis; transcription factor
1425537_at	AF259672	Ppm1a	protein phosphatase 1A, magnesium dependent, alpha isoform
1417516_at	NM_007837	Ddit3	DNA-damage inducible transcript 3; regulation of apoptosis; cell cycle arrest; response to ER-overload
1417158_at	BB238025	BC003332	unknown
1417273_at	NM_013743	Pdk4	pyruvate dehydrogenase kinase, isoenzyme 4
1418280_at	NM_011803	Copeb	core promoter element binding protein; regulation of transcription
1418156_at	NM_021342	Kcne4	potassium voltage-gated channel, Isk-related subfamily, gene 4
1418025_at	NM_011498	Bhlhb2	basic helix-loop-helix domain containing, class B2; negative regulation of transcription
1416101_a_at	NM_015786	Hist1h1c	histone 1, H1c
1415996_at	AF173681	Txnip	thioredoxin interacting protein; response to oxidative
1416505_at	NM_010444	Nr4a1	nuclear receptor subfamily 4, group A, member 1; regulation of transcription
1416630_at	NM_008321	Idb3	inhibitor of DNA binding 3
1421228_at	AF128193	Ccl7; MCP-3	chemokine (C-C motif) ligand 7; chemotaxis; inflammatory immune response
1421322_a_at	NM_008394	Isgf3g; IRF-9; p48	interferon dependent positive acting transcription factor 3 gamma
1418932_at	AY061760	Nfil3	nuclear factor, interleukin 3, regulated; regulation of transcription
1418949_at	NM_011819	Gdf15	growth differentiation factor 15
1419209_at	NM_008176	Cxcl1; GRO1; KC	chemokine (C-X-C motif) ligand 1; inflammatory response
1418835_at	NM_009344	Phlda1	pleckstrin homology-like domain, family A, member 1; FasL biosynthesis
1450971_at	AK010420	Gadd45b	growth arrest and DNA-damage-inducible 45 beta; activation of MAPKK; apoptosis; cell cycle regulation
1450976_at	AI987929	Ndr1	N-myc downstream regulated 1
1451538_at	BC024958	Sox9	SRY-box containing gene 9; cell differentiation; transcription factor
1451338_at	BC003270	Nisch	nischarin; actin cytoskeleton organization and biogenesis
1449519_at	NM_007836	Gadd45a	growth arrest and DNA-damage-inducible 45 alpha; apoptosis; cell cycle regulation; response to DNA damage
1449773_s_at	AI323528		similar to MyD118, a myeloid differentiation primary response
1452324_at	BE956863	H2afy2	H2A histone family, member Y2
1451959_a_at	U50279	Vegfa	vascular endothelial growth factor A; angiogenesis; cell growth
1453851_a_at	AK007410	Gadd45g	growth arrest and DNA-damage-inducible 45 gamma; T-helper cell differentiation; interferon gamma biosynthesis; apoptosis regulation
1452519_a_at	X14678		Mouse TPA-induced mRNA.
1432155_at	AK014104	Wasl	Wiskott-Aldrich syndrome-like (human); actin nucleation; regulation of transcription
1430271_x_at	AA672926	4930553M18Rik	RIKEN cDNA 4930553M18 gene
1434364_at	BG072756	Map3k14	mitogen-activated protein kinase kinase kinase 14
1433508_at	AV025472	Copeb	core promoter element binding protein; regulation of transcription
1428083_at	AK018202	2310043N10Rik	unknown
1448830_at	NM_013642	Dusp1	dual specificity phosphatase 1; cell cycle regulation; protein dephosphorylation
1448325_at	NM_008654	Myd116	myeloid differentiation primary response gene 116; cell differentiation
1448328_at	BC010198	Sh3bp2	SH3-domain binding protein 2; intracellular signaling cascade
1448420_a_at	NM_013911	Fbxl12	F-box and leucine-rich repeat protein 12; ubiquitin-dependent protein catabolism
1435176_a_at	BF019883	Idb2	inhibitor of DNA binding 2

1435866_s_at	AV297651	Hist3h2bb	histone 3, H2bb
1438133_a_at	BM202770	Cyr61	cysteine rich protein 61
1437271_at	BB825816	Bsf3; Clcf1	B-cell stimulating factor 3; cardiotrophin-like cytokine factor 1; IL-6 family of cytokines; astrocyte differentiation
1436994_a_at	BB533903	Hist1h1c	histone 1, H1c

Group F: Genes downregulated by greater than two-fold of mock, in wildtype and nt3A mutant VRP infected cells

Affymetrix Probe ID	Genbank ID	Gene Symbol	Description
1424118_a_at	BC027121	2600017H08Rik	unknown
1415928_a_at	AU080586		strong similarity to microtubule-associated proteins 1A/1B light chain 3
1419662_at	BB542051	Ogn	osteoglycin
1419444_at	NM_009119	Sap18	Sin3-associated polypeptide 18; regulation of transcription
1456380_x_at	BB490338		similar to Sprague-Dawley acidic calponin mRNA
1439461_x_at	AV151371	2410003A14Rik	unknown
1448373_at	NM_026310	Mrpl18	mitochondrial ribosomal protein L18
1438527_at	BG073445		unknown

(**Highlighted genes represent those modulated by greater than four-fold in each group**.)

CHAPTER THREE

EARLY REPLICATION OF VEE REPLICON PARTICLES IN VIVO RAPIDLY INDUCES A SYSTEMIC INNATE RESPONSE AND PROTECTS FROM LETHAL VIRUS CHALLENGE

Jennifer L. Konopka, Joseph M. Thompson, Drue L. Webb, and Robert E. Johnston

ABSTRACT

The host innate immune response, in particular the interferon response, provides a critical first line of defense against invading pathogens, inducing an antiviral state designed to impede the spread of infection in the body. While numerous studies have documented the profound changes imposed by the antiviral response within actively infected tissues, few have described on a molecular level how the infected animal is systemically affected. Here, utilizing Venezuelan equine encephalitis virus replicon particles (VRP) to limit infection to the initially infected cells *in vivo*, a rapid, systemic activation of the antiviral response was demonstrated both in distal tissues as well as within the draining lymph node, where VRP infection is confined following footpad inoculation. In the liver and brain, the expression of a panel of interferon-stimulated genes was detected by 1 to 3 hours (h) following VRP footpad inoculation, and reached peak expression levels of greater than 100-fold over mock. Although these distal tissues had not encountered VRP, they were nevertheless subject to high levels of soluble immune modulators, including serum interferon. Moreover, we found that mice receiving a footpad VRP inoculation 6, 12, or 24h prior to an otherwise lethal Venezuelan equine encephalitis virus (VEE) footpad challenge were completely protected from death. This VRP pretreatment dramatically reduced challenge virus titers in the serum and brain, and also provided protection from intranasal VEE challenge. Interferon signaling was necessary for both the induction of the antiviral response, as well as for protection from VEE challenge. However, interferon itself was likely not the sole responsible immune mediator, as VRP-pretreated mice challenged with a heterologous, interferon-

sensitive virus were not protected. The results presented here document the rapid modulation of the host innate response within hours of pathogen invasion, a response capable of transforming the entire infected animal. Furthermore, this system provides a promising model to investigate the components of innate immunity required for a protective response to VEE infection.

INTRODUCTION

Venezuelan equine encephalitis virus (VEE) is an arthropod-borne, single-stranded, message-sense RNA virus, belonging to the *Alphavirus* genus in the *Togaviridae* family. Associated with periodic epidemics and equine epizootics in the Western Hemisphere, VEE also serves as a leading model for the study of alphavirus pathogenesis *in vivo*. In the murine model, which closely mimics infection of horses in nature, VEE causes a two-phase disease: an initial, acute lymphotropic phase characterized by a high serum viremia, followed by invasion of the central nervous system during a neurotropic phase that leads to fatal encephalitis (1, 2). Utilizing the infectious molecular clone of VEE, as well as an extensive panel of mutants blocked in various stages of infection, the course of pathogenesis in the mouse model has been well described (2-6).

Studies examining the molecular aspects of VEE-induced pathogenesis have underscored the critical role of virus genetics, and the subsequent host response in dictating the course and outcome of infection (2, 7-13). However, many details of the earliest host-pathogen interactions during VEE infection remain largely unknown. A tool paramount to studying the early events in infection are VEE replicon particles

(VRP). VRP are propagation-defective particles that can undergo only one round of infection, as the structural genes which normally drive the assembly of progeny virions are deleted from the replicon genome. VRP are assembled using packaging-defective helper RNAs, supplied *in trans* (14). As such, VRP infection is limited to the first infected cells *in vivo*, allowing examination of the earliest interactions between virus and host.

The utilization of VRP facilitated the identification of the draining lymph node (DLN) as the initial site of viral replication *in vivo,* documenting the migration of infected dendritic cells to this tissue from the site of inoculation in the skin (15). It has been hypothesized that the earliest host-pathogen interactions occurring within the DLN set the stage for the specific course of events that define VEE-induced pathogenesis. In fact, utilizing a VRP-based mRNP-tagging system *in vivo,* we recently reported the robust activation of the host innate antiviral response directly within the infected cells of the DLN, as well as in the surrounding uninfected bystander cells, at early times post infection (J.L.K., submitted manuscript).

It has been well documented that the innate immune response plays a critical role in controlling viral infection and spread, with the interferon (IFN) system at the forefront of this first-line defense to a spreading infection (16-18). It is likely, therefore, that one the effects of an early, robust innate immune response in the tissue(s) where replication first occurs is the contemporaneous induction of an antiviral state in tissues distal to the initial infection.

We postulated that if early replication in the DLN induces the production of soluble immune mediators, such as IFN$\alpha\beta$, the induction of an innate immune

response may be rapidly transmitted downstream from the primary site of replication to distal tissues. Therefore, utilizing VRP to limit viral spread, we examined the host antiviral response within the DLN at early times following infection, as well as in tissues remote from the site of replication. Although such distal tissues had not encountered VRP, they were subject to signaling by the early systemic innate response induced by infection. This included high levels of serum interferon detected by 3 to 6h following VRP footpad inoculation. In the liver and brain, the robust expression of a panel of interferon-stimulated genes, a hallmark of the antiviral state elicited by IFN$\alpha\beta$, was detected by 1 to 3h following VRP footpad inoculation, and peaked at 6 - 12h with a subset of genes reaching levels of over 100-fold of that measured in mock infected animals. These results clearly suggest that the early innate response to VRP infection is capable of inducing a systemically active, antiviral state within the entire infected animal. Moreover, we found that mice pretreated by footpad inoculation with VRP for 6, 12, or 24h prior to an otherwise lethal VEE footpad challenge were completely protected from death. The same VRP pretreatment also provided protection from VEE challenge by intranasal inoculation, and significantly extended the average survival time of mice challenged with VEE intracranially.

While protection from VEE infection has typically been associated with the presence of neutralizing antibody (19-23), nonspecific protection against VEE also has been suggested, including the involvement of the innate immune response (13, 24-28). In one instance, mice “vaccinated” with an attenuated clone of VEE were protected against lethal VEE challenge administered just 24h after vaccination (27).

In another study, the complete attenuation of a VEE mutant differing from wildtype VEE by a single noncoding nucleotide change in the 5' untranslated region was attributed to the heightened sensitivity of the mutant to the host antiviral state (13). Additionally, mice with severe combined immunodeficiency infected with virulent VEE survive longer than immunocompetent mice (9 as opposed to 6 days) (10), whereas mice lacking the type I interferon receptor die within 48h. These findings strongly indicate that the nonspecific response to infection is a critical component of controlling early VEE infection.

While interferon and the interferon-induced antiviral state are undoubtedly key immune mediators of the initial response to VRP infection *in* vivo, they may not however be solely responsible for the rapid protection observed in the model presented here. While therapeutic regimens of IFNα or IFNγ, administered after virulent VEE infection, improve the outcome of infection in mice (29, 30), studies in which interferons or IFN-inducing agents (dsRNA/poly I:C, LPS) were administered for a short interval prior to VEE challenge provided no protection from death (26, 31). This was further supported here, by the failure of VRP pretreatment to protect against a heterologous challenge with another interferon-sensitive virus, vesicular stomatitis virus (VSV).

The data presented here provide new insight into the rapid mobilization of the host innate response which transforms the entire VRP infected animal, and offers a promising model system in which the components of innate protection from VEE-induced disease can be further investigated.

MATERIALS AND METHODS

Virus and replicon particles

The construction of the full-length VEE cDNA clone pV3000, derived from the Trinidad donkey isolate of VEE, has been described previously (2, 3, 5). Virus stocks of wildtype virulent VEE (V3000) were produced by electroporating infectious RNA into BHK-21 cells (2, 10). Virus particles were harvested from the supernatant at 24 h post-infection when significant CPE was evident, and were clarified by centrifugation (10,000 x *g*, 30 min, 4°C). Virus stocks were further concentrated by pelleting through 20% (wt/vol) sucrose in low endotoxin phosphate-buffered saline (PBS) at 72,000 x g for 5 h at 4°C. Virus titers were determined by standard plaque assay on BHK-21 cells, and stocks were stored in single-use aliquots at -70°C.

The construction and packaging of VEE replicon particles (VRP) using a split helper system have been described previously (14). Replicon plasmid constructs that do not encode any functional transgene sequence downstream of the 26S promoter were utilized throughout this study. The resulting particles, termed null VRP, contain the VEE nonstructural genes, 14 nucleotides (nt) of VEE sequence downstream of the 26S mRNA transcription start site and the 43 nt multiple cloning site (32). The null VRP genome also includes the authentic viral 5' and 3' untranslated regions. All replicon particles used in this study were packaged in the wildtype (V3000) VEE envelope, as described previously (14). Briefly, the replicon RNA genome along with two helper RNAs providing the wildtype capsid and glycoprotein genes were co-electroporated into BHK-21 cells. As the helper RNAs lack the cis-acting virus-specific packaging signal, and the replicon genome does not

encode the viral structural genes, infectious but non-propagating VRP undergo only one round of infection. The absence of propagating recombinant virus was confirmed by blind passage in BHK-21 cells. VRP were concentrated from supernatants by centrifugation through a 20% sucrose cushion and resuspended in endotoxin-free PBS. BHK-21 titers were determined by immunocytochemistry using mouse sera containing antibody to the VEE nonstructural proteins.

Vesicular stomatitis virus (VSV) was utilized as a heterologous challenge virus. Stocks of VSV (Indiana-1 serotype, Orsay strain) were the generous gift of Douglas Lyles and John Connor (Wake Forest University, Winston-Salem, NC).

Cells

BHK-21 cells (ATCC CCL-10) and murine L929 fibroblasts (ATCC CCL-1) were maintained in alpha-minimum essential media (Gibco) supplemented with 10% donor calf serum, 10% tryptose phosphate broth, 0.29 mg of L-glutamine/ml, 100 U of penicillin/ml, and 0.05 mg of streptomycin/ml (37°C, 5% CO_2).

Mice

Specific-pathogen-free BALB/c mice were obtained commercially (Charles River Laboratories). Unless otherwise noted, 10-12 week old female BALB/c mice were utilized. Breeding pairs of IFNαβR-/- 129Sv/Ev mice were kindly provided by Barbara Sherry (North Carolina State University, Raleigh, N.C.). Mice were bred under specific-pathogen-free conditions in the Department of Laboratory Animal Medicine breeding colony facilities at the University of North Carolina, Chapel Hill.

Age- and sex-matched wildtype 129Sv/Ev (129S6/SvEvTac) mice were obtained commercially from Taconic (Germantown, N.Y.). Animal housing and care were in accordance with all UNC-CH Institutional Animal Care and Use Committee guidelines. All mouse studies were performed in an environmentally controlled room in a biosafety level 3 facility, allowing mice to acclimate for 3 to 5 days in the facility before experimental manipulation.

Mice pretreated with VRP were inoculated in the right rear footpad (RRFP) with $2x10^6$ IU of null VRP (unless otherwise stated) in 10 ul of endotoxin-free PBS diluent containing 1% donor calf serum. Mock-pretreated animals received diluent alone. When footpad was the route of challenge, mice received 10 PFU of wildtype virulent VEE (V3000) inoculated in the opposing left rear footpad (LRFP) (10 ul total volume). Mice challenged intracranially were anesthetized with isoflurane and inoculated with 10^3 PFU of wildtype virulent VEE (V3000) in 10 ul diluent. Mice challenged intranasally with VEE received a dose of 10^3 PFU of wildtype VEE (V3000) in a 10ul volume, with 5 ul administered into each nare. Mice challenged intranasally with VSV received a dose of 2×10^6 PFU of VSV diluted in 20 ul RPMI media (Gibco), with 10 ul administered into each nare.

For morbidity and mortality studies, mice were monitored for clinical signs of disease and weighed every 24h for 14-18 days. Morbidity was defined as greater than 10% weight loss and/or signs of clinical disease for two or more consecutive days. Clinical signs of disease included ruffled fur, hunching, ataxia, paresis (dragging of hind limb), paralysis (complete loss of hind limb function) and/or a moribund state. In the interest of animal welfare and in accordance with UNC-CH

Institutional Animal Care and Use Committee guidelines, mice experiencing a loss in weight of more than 20% of starting weight while showing clinical signs of disease were euthanized. To determine viral titers in the serum and brain, mice were euthanized by anesthesia overdose, followed by cardiac puncture and exsanguination to collect blood samples. The serum was separated in microtainer tubes, aliquoted and stored at -70°C. Each animal was perfused with 1× PBS, and the brain removed by dissection, weighed, and stored at -80°C in a 20% (wt/vol) suspension of 1x PBS supplemented with 1% donor calf serum, 110 mM Ca^{2+}, and 50 mM Mg^{2+}. After one freeze-thaw cycle, the samples were homogenized and clarified by centrifugation at 10,000 x g, and viral titers were assessed by standard BHK-21 plaque assay.

RNA isolation and cDNA synthesis

At the indicated times post-infection, mice were euthanized and perfused with PBS. The draining popliteal lymph node, liver, and brain were dissected and stored at -80°C in RNA*later* (RNA stabilization reagent, Ambion). According to the manufacturer's protocol, tissue homogenates were prepared using a plastic pestle and handheld motor, as well as passage through an 18 gauge needle. Total cellular RNA was isolated using the RNeasy Protect kit (Qiagen).

A one-tube DNase treatment and reverse transcription protocol was used to generate cDNA, using the SuperScript III Reverse Transcriptase First Strand cDNA kit (Invitrogen). 0.75 - 1.0 ug of total RNA was brought to a final volume of 10 ul with RNase-free water. This was combined with 1 ul 10 mM dNTP mix (Amersham

Biosciences), 4 ul 5X SuperScript III reverse transcriptase buffer, 1 ul 0.1 mM dTT, 1 ul 40 U/ul RNaseOUT (Invitrogen), and 1 ul RQ1 RNase-free DNase (Promega) per sample. The samples were DNase treated at 37°C for 30 min, followed by the addition of 1 ul RQ1 Stop Solution (Promega) and heat inactivation of the samples at 65°C for 10 min. Following the addition of random hexamer primers (150 ng, Invitrogen), reverse transcription of the samples was continued in the same tube, according to the SuperScript III protocol (Invitrogen). cDNA samples were stored at -20°C.

Real-time PCR and analysis

Real-time PCR was performed to determine the relative abundance of specific cellular mRNAs in tissues isolated from mock and VRP-infected animals (3 mice per group). Taqman Gene Expression primer probe sets (Applied Biosystems) for various target host messages were used, with each reaction performed in a 25 ul total volume [5ul cDNA, 12.5 ul TaqMan Universal PCR Master Mix without AmpErase UNG (Applied Biosystems), 1.25 ul probe/primer mix (Applied Biosystems), and 6.25 ul RNase-free water]. For all samples, an equivalent amount of RNA was reverse transcribed and an internal reference control of 18s rRNA was included. The default amplification profile was performed in the ABI Prism 7000 Real-Time PCR System. Using the 7000 Sequence Detection Software (v1.2.3, Applied Biosystems), the results were converted into cycle threshold (C_T) values corresponding to the cycle number at which the fluorescence of the PCR product reached significant levels above the background level. Results are presented as

the fold gene expression in the infected samples over that in the mock samples, analyzed using the well established delta C_T (ΔC_T) method [*User Bulletin*, ABI Prism 7000 Sequence Detection System (Applied Biosystems)]. Briefly, for each cDNA sample, the 18s C_T value was subtracted from the C_T value of the target gene of interest, yielding a ΔC_T value. The ΔC_T value generated for the VRP-infected sample was then subtracted from the ΔC_T value of the corresponding mock sample, yielding a $\Delta\Delta C_T$ value. This widely-used method assumes the target and reference genes were amplified with the same efficiency, thus the increase in host mRNA levels in the infected samples compared to the mock treated samples was calculated as $2^{-(\Delta\Delta CT)}$.

Interferon bioassay

The levels of type I interferon present in the serum of infected mice were measured by a standard biological assay on L929 cells, as described previously (13, 33). Briefly, L929 murine fibroblasts were seeded in 96-well plates. Serum samples were diluted 1:10 in alpha-minimum essential media (Gibco), and acidified to a pH of 2.0 for 24 h. Following neutralization to pH 7.4, the samples were added to the cells by titration of twofold dilutions down the plate. Twenty-four hours after the addition of the serum dilutions, interferon-sensitive encephalomyocarditis virus (EMCV; 2 x 10^5 PFU) was added to each well and incubated at 37°C. At 18 to 24 h post-infection, 3-[4,5-dimethylthylthiazol-2yl]-2,5-diphenyltetrazolium bromide (MTT; Sigma), an indicator of viable cells, was added to each well. The MTT product was then dissolved in isopropanol-0.4% HCl, and absorbance was read on a microplate

reader at 570 nm. Each plate contained twofold dilutions of an IFN standard (Chemicon or R&D Systems), ranging from 500 to 0.49 international units (IU) per ml. The concentration of type I IFN in each serum sample was based on the standard curves generated with the interferon standard. The end-point titers were based on the dilution at which an optical density reading of 0.5 was reached, corresponding to ~50% protection of the cell monolayer from EMCV-induced cell death, and adjusted for the original titration of the serum samples.

RESULTS

VRP infection induces a robust antiviral state *in vivo* at the site of replication, as well as in remote downstream tissues.

Several studies have previously highlighted the importance of the DLN during VEE infection (2, 13, 15, 27, 32, 34)(J.L.K., submitted manuscript). *In vivo*, the DLN serves as the earliest known site for viral replication, with infected dendritic cells migrating there from the site of inoculation in the skin (15). Consequently, the DLN is the site where the early host response to VEE infection is established, demonstrated by a robust induction of the host antiviral gene response (27). In addition, a recent study utilizing VRP to limit infection to the initially infected cells *in vivo,* revealed a robust activation of the host defense response directly within the infected cells of the DLN at early times post infection (J.L.K., submitted manuscript). Accordingly, it has been hypothesized that early events within the DLN, such as those described above, set the stage for a specific pattern of virus replication and host response that define VEE-induced pathogenesis.

Utilizing VRP which do not propagate beyond the initially infected cells, we examined the early impact of infection not only within the DLN, but also at sites downstream from this primary site of replication. To determine whether the strong antiviral state established early in the DLN leads to a systemic response throughout the animal, mice were inoculated in the right rear footpad (RRFP) with 2 x 10^6 IU of null VRP. At 1, 3, 6, 12, and 24h post inoculation, mice were euthanized, serum collected by cardiac puncture, and each animal perfused with PBS. The popliteal DLN, liver (one lobe), and brain (including olfactory bulbs), were dissected from each animal, and total RNA isolated. The expression level of a panel of host antiviral genes (IFNβ, IP-10, p56, and Isgf3γ) was measured from each sample (3 mice per group) by real-time PCR.

The results, shown in Fig. 3.1, demonstrate a robust activation of the innate immune response not only in the DLN (Fig. 3.1A), but also distally in both the liver (Fig. 3.1B) and the brain (Fig. 3.1C), tissues that are remote from the active site of VEE replicon RNA replication. As early as 1h to 3h following footpad inoculation, a high level of antiviral gene induction was detected in the DLN, with IFNβ, IP-10, and p56 gene expression at levels of 100-fold over that in mock infected mice. This response reached a peak in the DLN at 6 - 12h following footpad inoculation, with expression levels of IP-10, p56, and IFNβ at 400- to greater than 5,000-fold over that in mock infected animals. By 24h, the response within the DLN appeared to be waning.

In uninfected tissues distal to the site of active replication in the DLN, a mounting antiviral response was detected in both the liver and brain following

footpad VRP inoculation. Interestingly, the kinetics of this downstream induction were similar to that observed in the DLN, with the antiviral gene response initially detected at 1 to 3hpi in the liver and brain, peaking at 6 to 12h, and waning by 24h. It is important to note that these remote tissues were completely devoid of replicon RNA as indicated by real-time PCR for the VEE nsP1 gene (data not shown). At its peak, this antiviral response in the liver and brain reached levels of 10 to nearly 1,000-fold of that measured in mock animals, suggesting that the entire infected animal responded to the invading pathogen, mounting a systemic antiviral response reaching far beyond the site of active replication. Although these remote organs did not encounter VRP, they nevertheless were subjected to systemic soluble mediators of the innate immune response induced by the active infection in the DLN. In fact, very high levels of biologically active interferon detected in the serum of these same mice correlated with the peak antiviral gene response, reaching nearly 400,000 IU/ml by 6h post infection (Fig. 3.2).

Short duration pretreatment with VRP protects mice from footpad challenge with virulent VEE.

The extent and rapidity of the observed systemic antiviral state induced following VRP inoculation led to questions regarding the protective nature of this response. To address whether VRP inoculation rapidly induced a protective state, adult female BALB/c mice were inoculated with 2 x 10^6 IU of null VRP in the RRFP for 6, 12, or 24h prior to a virulent challenge with 10 PFU of wildtype VEE administered into the opposing LRFP. Mice were weighed and observed every 24h

for signs of clinical disease, with morbidity and mortality compared to mice receiving a mock pretreatment followed by virulent VEE challenge. The results, summarized in Table 3.1 and Fig. 3.3, demonstrate that at a dose of 2 x 10^6 IU, a short duration pretreatment with VRP delivered in the footpad can protect animals from death following virulent VEE challenge in the opposing footpad. The 100% mortality observed following VEE challenge in mock-pretreated animals was reduced to 0% in animals receiving VRP at all pretreatment times tested. The incidence of morbidity observed in VRP treated animals was largely reduced as well, falling from the 100% incidence of morbidity in mock-pretreated mice to a range of 0 to 33% morbidity in mice receiving VRP. Allowing even a short 6h window between VRP inoculation and VEE challenge was sufficient to effectively protect animals from death, a testament to the effectiveness of the early antiviral response induced by VRP.

To further assess the protective quality of this VRP pretreatment, more rigorous routes of VEE challenge were examined. Following footpad inoculation, VEE causes a two-phase disease in mice, much like that which occurs in horses following subcutaneous inoculation. An initial lymphotropic phase is characterized by a high serum viremia which seeds infection of the olfactory neuroepithelium, followed by invasion of the central nervous system and initiation of a neurotropic phase leading to fatal encephalitis (2, 35). Intranasal delivery of VEE bypasses the necessity of a high serum viremia for establishment of the neurotropic phase, by granting direct access to the olfactory neuroepithelium. However, this route still requires neuroinvasion of the CNS to establish lethal encephalitis. When BALB/c mice where pretreated by footpad inoculation of 2 x 10^6 IU of null VRP for 12h or

24h prior to virulent intranasal VEE challenge (10^3 PFU), they were completely protected from death. This is in comparison to the 100% mortality observed in mock-pretreated animals (Table 3.2, Fig. 3.4). Therefore, administering VRP in the footpad 12 to 24h prior to a rigorous, intranasal challenge with VEE, effectively protected animals from death. While a 6h VRP pretreatment was sufficient to completely protect animals from VEE footpad challenge, the percent mortality following intranasal VEE challenge under the same conditions was 50%, indicating that the progression of the challenge virus from footpad to brain is likely to be a critical parameter of protection within this pretreatment model.

Intracranial inoculation of VEE bypasses the need for neuroinvasion into the CNS by granting direct access to the brain, and therefore serves as a means to directly measure viral neurovirulence. Thus, in our model of protection, intracranial VEE inoculation served as the most rigorous challenge route examined. As demonstrated in Fig. 3.5 and summarized in Table 3.3, footpad pretreatment with VRP failed to protect animals from a virulent 10^3 PFU VEE intracranial challenge. However, a statistically significant increase in the average survival time of mice that received the VRP pretreatment was observed, as compared to the average survival time of mice receiving mock-pretreatment. An intracranial challenge with a lower dose of 10 PFU of VEE also resulted in 100% mortality of both mock and VRP pretreated animals (data not shown). Taken together, the VEE challenge experiments suggest that while a short duration pretreatment with VRP can effectively protect animals from peripheral (footpad) or mucosal (intranasal)

challenge with virulent VEE, it cannot protect animals against the extensive neurovirulence evident upon direct intracranial administration of VEE.

VRP pretreatment reduces the viral load in the serum and brain of mice challenged with VEE.

To determine whether VRP pretreatment functionally reduced and/or limited the replication of VEE following challenge, standard BHK-21 plaque assay was used to measure the titer of challenge virus present in the serum and brain. In parallel to the mice monitored for morbidity and mortality following footpad challenge of VEE (referring back to Table 3.1 and Fig. 3.3), an additional four mice per group were utilized for titer determination. At 6, 12, or 24h following the standard pretreatment of 2 x 10^6 IU null VRP in the RRFP, mice were challenged in the LRFP with 10 PFU of VEE. At 24h post challenge, serum was collected from the tail vein, followed by PBS perfusion and dissection of the brain (including the olfactory bulbs) at 88h post challenge. Titers from VRP pretreated animals were compared to those from mock pretreated animals.

The results, shown in Fig. 3.6, demonstrate that short duration VRP pretreatment dramatically reduced the viral load in serum and the brain following virulent VEE footpad challenge. At 24h post challenge, the serum viremia in mock pretreated animals had reached 6.5 x 10^5 PFU/ml, while the viral load in the serum of VRP pretreated animals was reduced over two logs to 2.1 x 10^3 PFU/ml. Furthermore, in the brain of mock pretreated animals, viral titers had reached nearly 7.5 x 10^6 PFU/gram by 88h post challenge, while in VRP pretreated animals the

amount of virus measured in the brain was at or below the limit of detection (≤ 500 PFU/gram). Therefore, it is clear that short duration VRP pretreatment effectively reduces the viral load in both the serum and brain, thereby controlling viral spread following VEE challenge.

Protection from virulent VEE challenge is dependent on the dose of VRP pretreatment.

A VRP pretreatment dose of 2 x 10^6 IU not only induces a strong antiviral response in the DLN and in downstream tissues, but can completely protect animals from virulent footpad challenge with VEE when the pretreatment is given a mere 6h before challenge. This same time interval of pretreatment protected 50% of mice challenged with VEE intranasally; however, complete protection from intranasal challenge ensued if the pretreatment was extended to 12h or 24h. These results, along with the observed extension in the average survival time of intracranially challenged mice, suggest that there do exist limitations to the magnitude of protection that this VRP pretreatment confers. To begin elucidating factors fundamental to establishing this protection, we first addressed the effect of pretreatment dose (Table 3.4, Fig. 3.7).

Adult BALB/c mice were pretreated with decreasing doses of null VRP in the RRFP, and then challenged 6h later in the opposing LRFP with 10 PFU of virulent VEE. Consistent with our previous results, mice that received the standard pretreatment dose of 2 x 10^6 IU of VRP were completely protected from death, while those receiving mock pretreatment all succumbed to VEE infection. However, at

VRP pretreatment doses of 10^5 or 10^4 IU, protection against mortality was lost, suggesting a fairly abrupt dose threshold for the protective effect. However, it is possible that protection may have been observed if pretreatment with a lower dose was extended beyond 6h.

Signaling through the IFNαβ receptor is necessary for induction of the downstream antiviral gene response, and protection from virulent VEE.

We have demonstrated that by 6h post inoculation, large amounts of biologically active interferon are circulating in the serum of VRP pretreated mice. The kinetics of this serum interferon response correlate with the induction of a robust host antiviral gene response in pretreated animals, occurring both at the site of replication in the DLN as well as in downstream tissues such as the brain and liver. We hypothesize that administering a virulent VEE challenge in the context of this rapidly induced host innate antiviral response subsequently leads to protection from death. To begin addressing what role the observed innate response plays in the protection conferred by VRP pretreatment, mice lacking the IFNαβ receptor were employed. Although levels of serum interferon circulating in IFNαβR-/- mice at early times after VRP footpad inoculation are equivalent to those in wildtype 129 mice, IFN declines in the knockout mice by 12h (13). Furthermore, while our group recently demonstrated that the lack of the IFNαβ receptor had little effect on the antiviral paracrine response within uninfected bystander cells of the DLN, the autocrine antiviral gene response in infected cells however was greatly impaired (J.L.K., submitted manuscript). To investigate whether signaling through the IFNαβ

receptor was required for the rapid, VRP-induced antiviral response in downstream tissues, wildtype 129 or IFNαβR-/- mice were inoculated with 2 x 10^6 IU of null VRP (RRFP). At 6h post inoculation, the mice were euthanized and PBS perfused. The liver and brain were dissected, and total RNA extracted. The expression of the same panel of four interferon-stimulated genes (IFNβ, IP-10, p56, and Isgf3γ) was measured by real-time PCR and compared to levels in mock infected mice.

The results, shown in Fig. 3.8, demonstrate a virtually complete elimination of the downstream antiviral gene response at 6h in mice lacking the IFNαβ receptor. This is in stark contrast to the robust responses measured in the same tissues isolated from wildtype IFNαβR+/+ 129 mice. Therefore, although the presence of near wildtype levels of serum interferon have been reported in IFNαβR-/- mice at this 6h post inoculation timepoint, the lack of the IFNαβ receptor greatly impairs the early, systemic antiviral response that is induced in downstream tissues of wildtype animals. However, it also is possible that the induction kinetics of the systemic antiviral response may only be delayed in IFNαβR-/- mice.

Protection against VEE challenge was not observed in IFNαβR-/- mice (Table 3.5 and Fig. 3.9). However, several studies have described the intrinsic sensitivity of VEE to the host interferon response (12, 13, 24, 26, 36-39). As such, the intrinsic interferon sensitivity of VEE makes it difficult to determine whether the lack of protection observed in our IFNαβR-/- experiment is truly due to a dampened or impaired pretreatment response, or merely a function of the general increased susceptibility of these mice to infection with VEE.

VRP pretreatment does not protect mice from challenge with a heterologous, interferon-sensitive virus.

VRP pretreated animals were challenge with Vesicular stomatitis virus (VSV) to determine whether protection extended to a heterologous yet interferon-sensitive virus. VSV is a negative-sense, ssRNA virus that has been utilized extensively to study viral pathogenesis, and the interferon response to infection. In the mouse model, VSV is highly virulent when delivered intracranially; however, it is difficult to induce mortality in animals infected from a subcutaneous route. The reported mortality rate following intranasal inoculation of VSV varies, usually falling between 30-60% mortality in adult mice (40-42). However, similar to infection with VEE, intranasal inoculation of VSV delivers the virus to the neuroepithelium, where replication occurs and spread to the olfactory bulb ensues (43). Due to the well documented interferon sensitivity of VSV, as well as its amenability to the intranasal challenge model in which we demonstrated the ability of VRP to protect from lethal VEE challenge, VSV was selected as our heterologous challenge virus.

To address whether a short duration VRP pretreatment could protect from a heterologous virus challenge, 6 - 7 week old male BALB/c mice were inoculated in the RRFP with 2×10^6 IU of null VRP, and then challenged 24h later with 2×10^6 PFU of VSV, delivered intranasally. The mice were monitored daily, and their weight and clinical scores recorded. As summarized in Table 3.6 and Figure 3.10, a 24h pretreatment with null VRP was not sufficient to induce protection from a lethal intranasal VSV challenge. These results suggest that the mechanism of protection mediated by VRP pretreatment may not be solely attributable to interferon, and/or

may be more specifically effective against VEE. On the other hand, it is possible that either the magnitude, duration, or kinetics of the interferon response were not sufficient or ideal to bestow protection from VSV challenge. However, it is clear under the conditions tested, that a VRP pretreatment regimen that is capable of protecting animals from lethal VEE intranasal challenge cannot protect animals from death upon intranasal VSV challenge.

DISCUSSION

During the course of viral infection *in vivo*, the manifestation of clinical signs in the infected animal serves as a physical indication of the ongoing pathogenesis. Countless studies have documented specific changes induced within infected cells as the invading pathogen is sensed, and the host response is mounted. This response includes the induction of host defense genes, the activation of immune cells, and the presence of soluble immune modulators (e.g., cytokines and chemokines). Alphaviruses are no exception, inducing a strong antiviral response both *in vitro* as well as *in vivo.* However, few studies describe on a molecular level how the entire infected animal is affected systemically, particularly in tissues that are distal to the site(s) of active viral replication.

Here, utilizing VRP to limit infection to the first infected cells *in vivo*, we demonstrate that not only do host cells at the site of replication sense and respond to infection, but systemically there is a rapid activation of the antiviral response, including within remote tissues. Within the liver and brain, distal to the site of VRP replication limited to the DLN, antiviral gene expression of greater than 100-fold over

mock was detected within hours of VRP footpad inoculation, and peaked at 6 to 12 h. This included induction of several interferon-stimulated genes, namely Isgf3γ (IRF-9), IP-10 (Cxcl10), p56 (Ifit1), and IFNβ itself, all having well documented roles in the host antiviral response. Isgf3γ, along with STAT1 and STAT2, form the ISGF3 transcription factor complex which translocates to the nucleus and binds interferon-stimulated response elements (ISRE) to induce the expression of interferon-inducible genes (16-18). The chemokine IP-10, which possesses an ISRE-containing promoter, is a potent chemoattractant for Th1 lymphocytes and monocytes, regulating the *in vivo* migration of these effector immune cells to sites of inflammation. The p56 gene belongs to a class of stress-inducible antiviral genes which are upregulated in response to interferon, dsRNA, and infection by several viruses (18, 44). The specific antiviral action of p56 is mediated through its directed disruption of translation initiation, by inhibiting the action of the initiation factor eIF3 (45, 46).

Our observation of this rapid, intense induction of genes encoding products with a diverse range of antiviral activities, both within the DLN as well as in downstream tissues, suggests that the invading pathogen was sensed almost immediately following VRP infection, and an innate response initiated on an animal-wide scale. Several candidates responsible for this innate detection of VRP infection exist, including the pattern recognition receptors (PRR). PRRs, such as the dsRNA-dependent protein kinase (PKR), retinoic acid inducible gene-1 (RIG-1), and the Toll-like receptors (TLRs), serve as sentinels for the innate detection of viral invasion (17, 47-49). They do so by recognizing conserved molecular motifs, or “pathogen-

associated molecular patterns (PAMPs), and upon sensing these pathogenic molecules, induce the production of soluble immune mediators. With mounting evidence of the critical role of PRRs in the establishment of both innate and adaptive immunity, particularly in dendritic cell populations, future studies within this system certainly will include investigating the potential involvement of these innate sensors in VRP infection.

The innate antiviral state that was subsequently induced following VRP footpad inoculation appeared, moreover to rapidly promote a protective response, as short duration pretreatment with VRP prior to virulent VEE challenge was sufficient to effectively protect animals from death. This included complete protection in mice receiving a footpad inoculation with VRP at 6, 12, or 24h prior to challenge in the opposing footpad with VEE. Similar results were observed when VRP pretreated mice were challenged intranasally with VEE, with only a slight shift to 50% mortality in mice receiving the 6h VRP pretreatment. The duration of this protective VRP pretreatment not only correlated with the timing of peak antiviral gene induction in the DLN, liver, and brain, but also with the presence of massive amounts of biologically active interferon measured in the serum of pretreated animals.

Although the same VRP pretreatment was capable of extending the average survival time of mice challenged intracranially with VEE, it was insufficient to protect these animals from death. The differences in protection observed from intracranial versus footpad or intranasal challenge suggest that the short duration VRP pretreatment may be effective in limiting or preventing neuroinvasion, but appears to be ineffective in protecting against direct VEE neurovirulence. Following footpad

challenge of VRP pretreated animals, viral titers within the brain were reduced to levels at or below the level of assay detection, from the nearly 10^7 PFU/gram titers in mock pretreated animals, suggesting that invasion of the brain may have been blocked. This was coupled with a greater than 2.5 log reduction in serum viremia titers to just over 10^3 PFU/ml measured at 24h. In previous studies, a correlation was established between reaching a critical concentration of at least 10^4 PFU/ml of virus in the serum and the capability of effectively seeding infection of the neuroepithelium to achieve neuroinvasion of the CNS (K.A. Bernard and R.E.J., unpublished data). Therefore, it remains unclear whether the reduction in viral brain titers following footpad challenge of VRP pretreated animals was the result of an antiviral state induced in the neuroepithelium that limited or prevented neuroinvasion, or if it was a function of the overall reduction in serum viremia, or both. However, future studies exploiting differences in mortality, antiviral gene responses, as well as serum and brain titers in animals receiving less than the standard VRP pretreatment dose of 2×10^6 IU of VRP may further elucidate how the brain is protected within this system.

The exact mechanism underlying the protection granted by short duration VRP pretreatment remains to be fully defined. However, direct homologous interference between replicon and challenge virus particles is not likely to play a role, as the footpad pretreatment and subsequent challenge were administered in opposing footpads. Likewise, the protection from intranasal challenge evident in mice pretreated in the footpad with VRP, further argues against homologous interference as the mechanism of protection. Elements of the adaptive immune

response also are unlikely contributors to this rapid protection, as the time necessary for a protective antibody response strongly argues against involvement of VEE-specific antibody. In studies where mice were inoculated with a high dose (10^5 PFU) of a vaccine strain of VEE (TC-83), detectable levels of VEE-specific serum IgG are not evident until five days post inoculation (50). However, a future challenge study may be designed in mice deficient in B- and T-cells (RAG-/-) to address the contribution, if any, of an early adaptive response.

The rapidly induced innate response observed systemically in VRP pretreated animals may be responsible for the protection from VEE challenge. The observed protection is temporally correlated with the induced innate defense response. When animals were challenged with VEE at times during which the host antiviral gene response and the serum interferon levels were suboptimal (e.g., at 1h and 3h post VRP pretreatment), they were not protected from death (100% and 50% mortality rates, respectively; data not shown). The most obvious candidate responsible for inducing the systemic innate and protective responses may be interferon itself, particularly given the well-documented sensitivity of VEE to the interferon response. This was supported by the strong local and remote induction of antiviral genes soon after VRP administration, and nearly complete loss of the early antiviral gene response in the brain of VRP pretreated IFN$\alpha\beta$R-/- mice. However, past studies have found that while interferon is necessary for protection against lethal VEE infection, it is not sufficient (26, 31). If there is a another soluble component(s) responsible for the protection conferred by VRP pretreatment, then future studies designed to transfer serum from pretreated to naïve animals (including IFN$\alpha\beta$R-/-

mice) prior to VEE challenge may help to elucidate the role of such serum factors in protection.

The failure of VRP pretreatment to protect animals from challenge with VSV, a virus that is also sensitive to an interferon-induced antiviral state, suggests that an element of the VRP-induced protective response may be specific to VEE. Although VEE and VSV share certain pathogenetic features (e.g., interferon sensitivity, CNS access through the olfactory neuroepithelium), the antiviral response induced by VRP pretreatment seems to differentially affect each virus. One possibility is that the kinetics of the robust antiviral response following VRP pretreatment are naturally well-suited to protect against VEE, a virus that replicates and disseminates very quickly *in vivo*. Following footpad inoculation of VEE in mice, peak serum viremia is established by 12 to 24h. This is followed by clearance of the virus from the serum and peripheral organs by approximately 72h, when the virus has invaded the brain, resulting in lethal encephalitis by 6 - 8 days post infection (2). Therefore, administering the VRP pretreatment at 6, 12, or 24h prior to VEE challenge in effect confers a head start for the antiviral response to reach peak state at the time of VEE inoculation, and/or during early times post challenge when inhibiting VEE replication is most critical for protection.

In contrast, the course and duration of VSV pathogenesis *in vivo* is generally extended in comparison to VEE, evident in the delayed average survival time of infected mice. As such, the rapidly established, peak VRP antiviral response may have already resolved at times critical to suppressing VSV replication. Alternatively, or in addition, VRP treated animals may have lapsed into an interferon unresponsive

state at a critical point in VSV challenge virus infection (51). Future studies in which the VRP pretreatment is administered at times closer to the VSV challenge may elucidate kinetic components among the differences between VEE and VSV challenge models.

On the other hand, the action of interferon-induced genes can be virus-specific (18, 52, 53). Thus, it is also possible that VEE and VSV are differentially sensitive to the particular antiviral response profile induced by VRP pretreatment. It may be informative to challenge VRP-pretreated animals with another alphavirus, or conversely, to pretreat animals with another alphavirus-based replicon particle, followed by challenge with VEE. Such studies may help to define in a larger context the specific, antiviral gene profile that is most effective against alphavirus infection.

The rapid, robust, but transient activation of a systemic antiviral response throughout animals receiving VRP pretreatment sheds new light on the dynamics of virus replication and host response. Within just a few hours following infection of the first cells in the DLN, the animal begins to respond. The initial response is in the infected cells themselves, where induced mediators of the innate immune response act in an autocrine fashion to modulate replication in those cells. Paracrine mediators rapidly induce a response in uninfected bystander cells of the DLN, and the same or additional soluble mediators act at a distance to alter the gene expression profile in remote uninfected tissues. By only 6 hrs post-infection, and under conditions where the infection is limited only to the first infected cells, the innate response is activated throughout the body. These results suggest a new

paradigm of acute virus disease in which the ultimate pathogenesis of the virus may be largely determined by events in the first few moments after infection.

ACKNOWLEDGMENTS

We thank the entire Carolina Vaccine Institute for stimulating discussions, and Melissa Parsons for excellent technical assistance. This work was supported by the National Institutes of Health (NIH) Public Health Service Grant R01-AI51990 (to R.E.J.), and the NIH Predoctoral Training Grant T32-AI07419.

REFERENCES

1. Gleiser, C. A., W. S. Gochenour, Jr., T. O. Berge, and W. D. Tigertt. 1962. The comparative pathology of experimental Venezuelan equine encephalomyelitis infection in different animal hosts. *J Infect Dis* 110:80-97.

2. Grieder, F. B., N. L. Davis, J. F. Aronson, P. C. Charles, D. C. Sellon, K. Suzuki, and R. E. Johnston. 1995. Specific Restrictions in the Progression of Venezuelan Equine Encephalitis Virus-Induced Disease Resulting from Single Amino Acid Changes in the Glycoproteins. *Virology* 206:994-1006.

3. Davis, N. L., N. Powell, G. F. Greenwald, L. V. Willis, B. J. Johnson, J. F. Smith, and R. E. Johnston. 1991. Attenuating mutations in the E2 glycoprotein gene of Venezuelan equine encephalitis virus: construction of single and multiple mutants in a full-length cDNA clone. *Virology* 183:20-31.

4. Davis, N. L., F. B. Grieder, J. F. Smith, G. F. Greenwald, M. L. Valenski, D. C. Sellon, P. C. Charles, and R. E. Johnston. 1994. A molecular genetic approach to the study of Venezuelan equine encephalitis virus pathogenesis. *Arch Virol Suppl* 9:99-109.

5. Davis, N. L., L. V. Willis, J. F. Smith, and R. E. Johnston. 1989. In vitro synthesis of infectious venezuelan equine encephalitis virus RNA from a cDNA clone: analysis of a viable deletion mutant. *Virology* 171:189-204.

6. Aronson, J. F., F. B. Grieder, N. L. Davis, P. C. Charles, T. Knott, K. Brown, and R. E. Johnston. 2000. A Single-Site Mutant and Revertants Arising in Vivo Define Early Steps in the Pathogenesis of Venezuelan Equine Encephalitis Virus. *Virology* 270:111-123.

7. Greene, I. P., S. Paessler, L. Austgen, M. Anishchenko, A. C. Brault, R. A. Bowen, and S. C. Weaver. 2005. Envelope Glycoprotein Mutations Mediate Equine Amplification and Virulence of Epizootic Venezuelan Equine Encephalitis Virus. *J. Virol.* 79:9128-9133.

8. Bernard, K. A., W. B. Klimstra, and R. E. Johnston. 2000. Mutations in the E2 Glycoprotein of Venezuelan Equine Encephalitis Virus Confer Heparan Sulfate Interaction, Low Morbidity, and Rapid Clearance from Blood of Mice. *Virology* 276:93-103.

9. Johnson, B. J., R. M. Kinney, C. L. Kost, and D. W. Trent. 1986. Molecular determinants of alphavirus neurovirulence: nucleotide and deduced protein sequence changes during attenuation of Venezuelan equine encephalitis virus. *J Gen Virol* 67 (Pt 9):1951-1960.

10. Charles, P. C., J. Trgovcich, N. L. Davis, and R. E. Johnston. 2001. Immunopathogenesis and Immune Modulation of Venezuelan Equine Encephalitis Virus-Induced Disease in the Mouse. *Virology* 284:190-202.

11. Schoneboom, B. A., K. M. K. Catlin, A. M. Marty, and F. B. Grieder. 2000. Inflammation is a component of neurodegeneration in response to Venezuelan equine encephalitis virus infection in mice. *Journal of Neuroimmunology* 109:132-146.

12. Spotts, D. R., R. M. Reich, M. A. Kalkhan, R. M. Kinney, and J. T. Roehrig. 1998. Resistance to Alpha/Beta Interferons Correlates with the Epizootic and Virulence Potential of Venezuelan Equine Encephalitis Viruses and Is Determined by the 5' Noncoding Region and Glycoproteins. *The Journal of Virology* 72:10286-10291.

13. White, L. J., J. g. Wang, N. L. Davis, and R. E. Johnston. 2001. Role of Alpha/Beta Interferon in Venezuelan Equine Encephalitis Virus Pathogenesis: Effect of an Attenuating Mutation in the 5' Untranslated Region. *The Journal of Virology* 75:3706.

14. Pushko, P., M. Parker, G. V. Ludwig, N. L. Davis, R. E. Johnston, and J. F. Smith. 1997. Replicon-Helper Systems from Attenuated Venezuelan Equine Encephalitis Virus: Expression of Heterologous Genes in Vitro and Immunization against Heterologous Pathogens in Vivo. *Virology* 239:389-401.

15. MacDonald, G. H., and R. E. Johnston. 2000. Role of Dendritic Cell Targeting in Venezuelan Equine Encephalitis Virus Pathogenesis. *The Journal of Virology* 74:914-922.

16. Malmgaard, L. 2004. Induction and Regulation of IFNs During Viral Infections. *Journal of Interferon & Cytokine Research* 24:439-454.

17. Perry, A. K., G. Chen, D. Zheng, H. Tang, and G. Cheng. 2005. The host type I interferon response to viral and bacterial infections. *Cell Res* 15:407-422.

18. Sen, G. C. 2001. Viruses and interferons. *Annual Review of Microbiology* 55:255-281.

19. Pittman, P. R., R. S. Makuch, J. A. Mangiafico, T. L. Cannon, P. H. Gibbs, and C. J. Peters. 1996. Long-term duration of detectable neutralizing antibodies after administration of live-attenuated VEE vaccine and following booster vaccination with inactivated VEE vaccine. *Vaccine* 14:337-343.

20. Rivas, F., L. A. Diaz, V. M. Cardenas, E. Daza, L. Bruzon, A. Alcala, O. De la Hoz, F. M. Caceres, G. Aristizabal, J. W. Martinez, D. Revelo, F. De la Hoz, J. Boshell, T. Camacho, L. Calderon, V. A. Olano, L. I. Villarreal, D. Roselli, G.

Alvarez, G. Ludwig, and T. Tsai. 1997. Epidemic Venezuelan equine encephalitis in La Guajira, Colombia, 1995. *J Infect Dis* 175:828-832.

21. Charles, P. C., K. W. Brown, N. L. Davis, M. K. Hart, and R. E. Johnston. 1997. Mucosal immunity induced by parenteral immunization with a live attenuated Venezuelan equine encephalitis virus vaccine candidate. *Virology* 228:153-160.

22. Greenway, T. E., J. H. Eldridge, G. Ludwig, J. K. Staas, J. F. Smith, R. M. Gilley, and S. M. Michalek. 1998. Induction of protective immune responses against Venezuelan equine encephalitis (VEE) virus aerosol challenge with microencapsulated VEE virus vaccine. *Vaccine* 16:1314-1323.

23. Hart, M. K., W. Pratt, F. Panelo, R. Tammariello, and M. Dertzbaugh. 1997. Venezuelan equine encephalitis virus vaccines induce mucosal IgA responses and protection from airborne infection in BALB/c, but not C3H/HeN mice. *Vaccine* 15:363-369.

24. Casals, J., S. M. Buckley, and D. W. Barry. 1973. Resistance to arbovirus challenge in mice immediately after vaccination. *Appl Microbiol* 25:755-762.

25. Huprikar, J., M. C. Dal Canto, and S. G. Rabinowitz. 1990. Protection against lethal Venezuelan equine encephalitis (VEE) virus infection by cell-free supernatant obtained from immune spleen cells. *Journal of the Neurological Sciences* 97:143-153.

26. Grieder, F. B., and S. N. Vogel. 1999. Role of Interferon and Interferon Regulatory Factors in Early Protection against Venezuelan Equine Encephalitis Virus Infection. *Virology* 257:106-118.

27. Grieder, F. B., B. K. Davis, X. D. Zhou, S. J. Chen, F. D. Finkelman, and W. C. Gause. 1997. Kinetics of Cytokine Expression and Regulation of Host Protection Following Infection with Molecularly Cloned Venezuelan Equine Encephalitis Virus. *Virology* 233:302-312.

28. Schoneboom, B. A., J. S. Lee, and F. B. Grieder. 2000. Early Expression of IFN-alpha/beta and iNOS in the Brains of Venezuelan Equine Encephalitis Virus-Infected Mice. *Journal of Interferon & Cytokine Research* 20:205-216.

29. Lukaszewski, R. A., and T. J. G. Brooks. 2000. Pegylated Alpha Interferon Is an Effective Treatment for Virulent Venezuelan Equine Encephalitis Virus and Has Profound Effects on the Host Immune Response to Infection. *J. Virol.* 74:5006-5015.

30. Pinto, A. J., P. S. Morahan, and M. A. Brinton. 1988. Comparative study of various immunomodulators for macrophage and natural killer cell activation

and antiviral efficacy against exotic RNA viruses. *International Journal of Immunopharmacology* 10:197-209.

31. Bradish, C. J., and D. Titmuss. 1981. The effects of interferon and double-stranded RNA upon the virus-host interaction: studies with togavirus strains in mice. *J Gen Virol* 53:21-30.

32. Thompson, J. M., A. C. Whitmore, J. L. Konopka, M. L. Collier, E. M. B. Richmond, N. L. Davis, H. F. Staats, and R. E. Johnston. 2006. Mucosal and systemic adjuvant activity of alphavirus replicon particles. *PNAS* 103:3722-3727.

33. Shabman, R. S., T. E. Morrison, C. Moore, L. White, M. S. Suthar, L. Hueston, N. Rulli, B. Lidbury, J. P. Y. Ting, S. Mahalingam, and M. T. Heise. 2007. Differential Induction of Type I Interferon Responses in Myeloid Dendritic Cells by Mosquito and Mammalian-Cell-Derived Alphaviruses. *J. Virol.* 81:237-247.

34. Johnston, L. J., G. M. Halliday, and N. J. C. King. 2000. Langerhans Cells Migrate to Local Lymph Nodes Following Cutaneous Infection with an Arbovirus. 114:560-568.

35. Charles, P. C., E. Walters, F. Margolis, and R. E. Johnston. 1995. Mechanism of Neuroinvasion of Venezuelan Equine Encephalitis Virus in the Mouse. *Virology* 208:662-671.

36. Anishchenko, M., S. Paessler, I. P. Greene, P. V. Aguilar, A.-S. Carrara, and S. C. Weaver. 2004. Generation and Characterization of Closely Related Epizootic and Enzootic Infectious cDNA Clones for Studying Interferon Sensitivity and Emergence Mechanisms of Venezuelan Equine Encephalitis Virus. *J. Virol.* 78:1-8.

37. Gresser, I. 1984. Role of interferon in resistance to viral infection in vivo. In *Interferon: Vol 2: Interferons and the immne system*. J. Vilcek, De Maeyer E., ed. Elsevier Science, Amsterdam. 221-247.

38. Jahrling, P. B., E. Navarro, and W. F. Scherer. 1976. Interferon induction and sensitivity as correlates to virulence of Venezuelan encephalitis viruses for hamsters. *Arch Virol* 51:23-35.

39. Jordan, G. W. 1973. Interferon sensitivity of Venezuelan equine encephalomyelitis virus. *Infect Immun* 7:911-917.

40. Letchworth, G. J., L. L. Rodriguez, and J. Del cbarrera. 1999. Vesicular stomatitis. *Vet J* 157:239-260.

41. Forger, J. M., 3rd, R. T. Bronson, A. S. Huang, and C. S. Reiss. 1991. Murine infection by vesicular stomatitis virus: initial characterization of the H-2d system. *J Virol* 65:4950-4958.

42. Durbin, R. K., S. E. Mertz, A. E. Koromilas, and J. E. Durbin. 2002. PKR protection against intranasal vesicular stomatitis virus infection is mouse strain dependent. *Viral Immunol* 15:41-51.

43. Reiss, C. S., I. V. Plakhov, and T. Komatsu. 1998. Viral Replication in Olfactory Receptor Neurons and Entry into the Olfactory Bulb and Brain. *Ann NY Acad Sci* 855:751-761.

44. Wacher, C., M. Muller, M. J. Hofer, D. R. Getts, R. Zabaras, S. S. Ousman, F. Terenzi, G. C. Sen, N. J. C. King, and I. L. Campbell. 2007. Coordinated Regulation and Widespread Cellular Expression of Interferon-Stimulated Genes (ISG) ISG-49, ISG-54, and ISG-56 in the Central Nervous System after Infection with Distinct Viruses. *J. Virol.* 81:860-871.

45. Terenzi, F., S. Pal, and G. C. Sen. 2005. Induction and mode of action of the viral stress-inducible murine proteins, P56 and P54. *Virology* 340:116-124.

46. Hui, D. J., F. Terenzi, W. C. Merrick, and G. C. Sen. 2005. Mouse p56 Blocks a Distinct Function of Eukaryotic Initiation Factor 3 in Translation Initiation. *J. Biol. Chem.* 280:3433-3440.

47. Iwasaki, A., and R. Medzhitov. 2004. Toll-like receptor control of the adaptive immune responses. *Nat Immunol* 5:987-995.

48. Kawai, T., and S. Akira. 2006. Innate immune recognition of viral infection. *Nat Immunol* 7:131-137.

49. Janeway, C. A., and R. Medzhitov. 2002. Innate Immune Recognition. *Annual Review of Immunology* 20:197-216.

50. Bennett, A. M., S. J. Elvin, A. J. Wright, S. M. Jones, and R. J. Phillpotts. 2000. An immunological profile of Balb/c mice protected from airborne challenge following vaccination with a live attenuated Venezuelan equine encephalitis virus vaccine. *Vaccine* 19:337-347.

51. Alsharifi, M., M. Regner, R. Blanden, M. Lobigs, E. Lee, A. Koskinen, and A. Mullbacher. 2006. Exhaustion of Type I Interferon Response following an Acute Viral Infection. *J Immunol* 177:3235-3241.

52. Katze, M. G., Y. He, and M. Gale, Jr. 2002. Viruses and interferon: a fight for supremacy. *Nat Rev Immunol* 2:675-687.

53. Samuel, C. E. 1991. Antiviral actions of interferon interferon-regulated cellular proteins and their surprisingly selective antiviral activities. *Virology* 183:1-11.

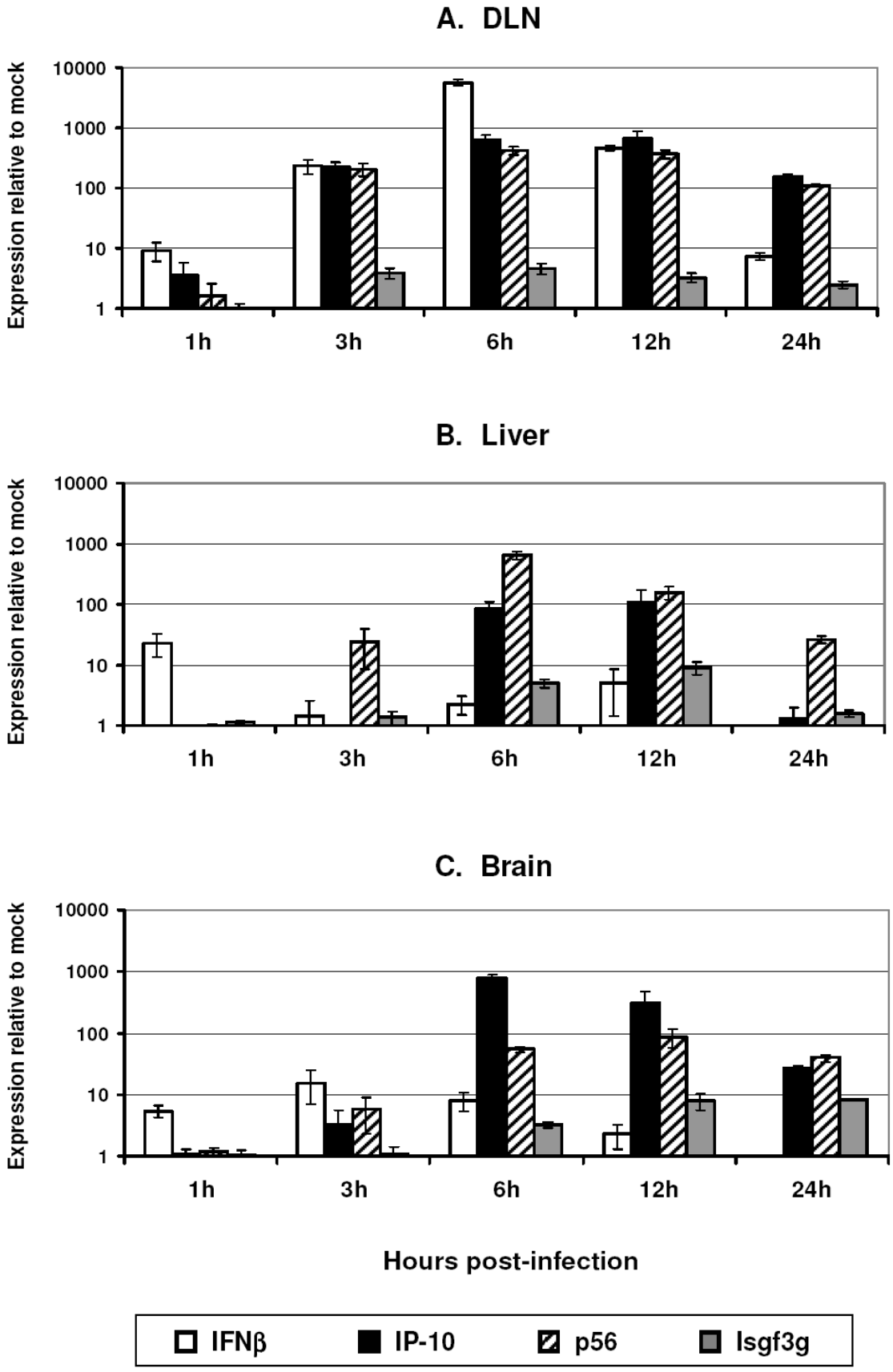
A. DLN
B. Liver
C. Brain
Expression relative to mock
10000
1000
100
10
1
1h
3h
6h
12h
24h
Hours post-infection
IFNβ
IP-10
p56
Isgf3g

Figure 3.1. Rapid, systemic activation of the host antiviral response following footpad VRP inoculation. Adult BALB/c mice were inoculated in the right rear footpad with 2 x 10^6 IU of null VRP, or were mock infected with diluent. At 1, 3, 6, 12, and 24h following inoculation, the mice were euthanized, perfused with PBS, and tissues removed by dissection. Total cellular RNA was isolated, cDNA synthesized, and the expression of a panel of interferon-stimulated genes (IFNβ, IP-10, p56, Isgf3g) was assessed by Taqman real-time PCR in the (A) draining lymph node, (B), liver, and (C) brain. The fold induction of each gene is represented by the expression in VRP infected animals relative to the expression in mock infected animals. Each bar represents groups of three animals each, plus or minus the standard error of the mean (SEM).

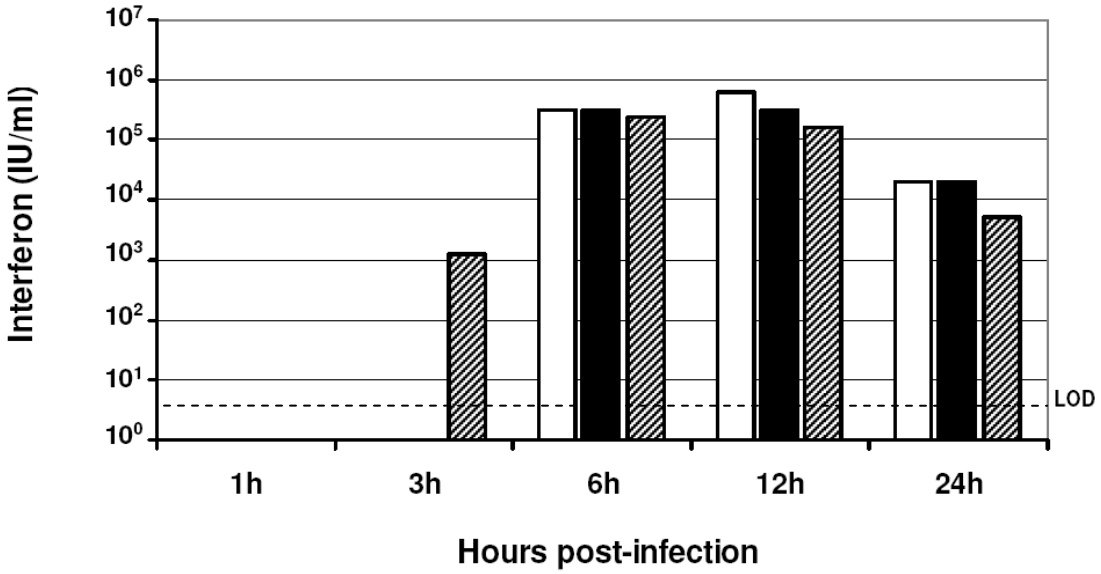

Figure 3.2. High levels of biologically active interferon are present in the serum of mice inoculated with VRP. Adult BALB/c mice were inoculated in the right rear footpad with 2 x 10^6 IU of null VRP. At 1, 3, 6, 12, and 24h following inoculation, the mice were euthanized, followed by cardiac puncture and exsanguination to collect blood samples. The levels of type I interferon present in the serum of infected mice were measured by a standard biological assay on L929 cells, and presented as international units (IU) per milliliter. Each bar represents an individual animal, with the limit of detection (LOD) for the assay indicated by the dotted line. The data in this figure and the previous figure correspond to the same group of mice.

Table 3.1. Morbidity and mortality of VRP-pretreated (RRFP) adult BALB/c mice following challenge with virulent VEE (LRFP)

Pretreatment (Footpad)			Challenge (Footpad)				
VRP	Duration	Dose (IU)	Virus	Dose (PFU)	% Morbidity (sick/total)	% Mortality (dead/total)	AST (days) (+/- SEM)*
mock	6h	-	VEE	10	100.0 (6/6)	100.0 (6/6)	6.0 (+/- 0.0)
null VRP	6h	2×10^6	VEE	10	33.3 (2/6)	0 (0/6)	-
null VRP	12h	2×10^6	VEE	10	16.7 (1/6)	0 (0/6)	-
null VRP	24h	2×10^6	VEE	10	0 (0/6)	0 (0/6)	-

*Average survival time (AST), plus or minus the standard error of the mean (SEM)

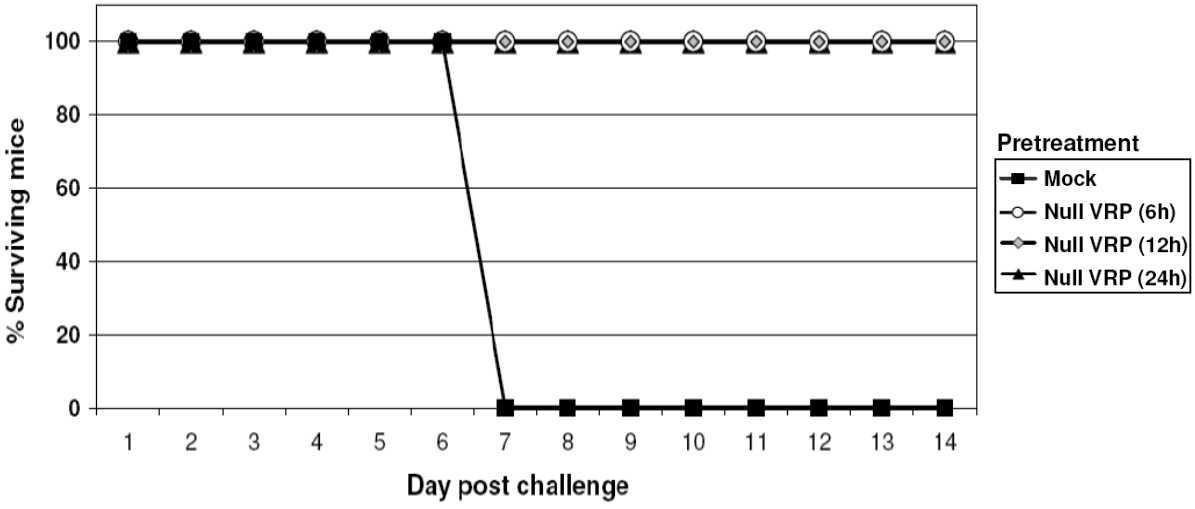

Figure 3.3. Survival of VRP-pretreated (RRFP) BALB/c mice following virulent VEE challenge (LRFP). Adult BALB/c mice, 6 mice per group, were pretreated by inoculation in the right rear footpad (RRFP) with 2×10^6 null VRP for 6, 12, or 24h prior to challenge with 10 PFU of virulent VEE in the opposing left rear footpad (LRFP). Mock pretreated mice received diluent alone, in the RRFP, 6h prior to challenge.

Table 3.2. Morbidity and mortality of VRP-pretreated (RRFP) adult BALB/c mice following intranasal challenge with virulent VEE.

Pretreatment (Footpad)			Challenge (Intranasal)				
VRP	Duration	Dose (IU)	Virus	Dose (PFU)	% Morbidity (sick/total)	% Mortality (dead/total)	AST (days) (+/- SEM)*
mock	6h	-	VEE	10^3	100.0 (5/5)	80.0 (4/5)	6.3 (+/- 0.2)
null VRP	6h	2 x 10^6	VEE	10^3	50.0 (3/6)	50.0 (3/6)	6.7 (+/- 0.9)
null VRP	12h	2 x 10^6	VEE	10^3	0 (0/5)	0 (0/5)	-
null VRP	24h	2 x 10^6	VEE	10^3	0 (0/5)	0 (0/5)	-

*Average survival time (AST), plus or minus the standard error of the mean (SEM)

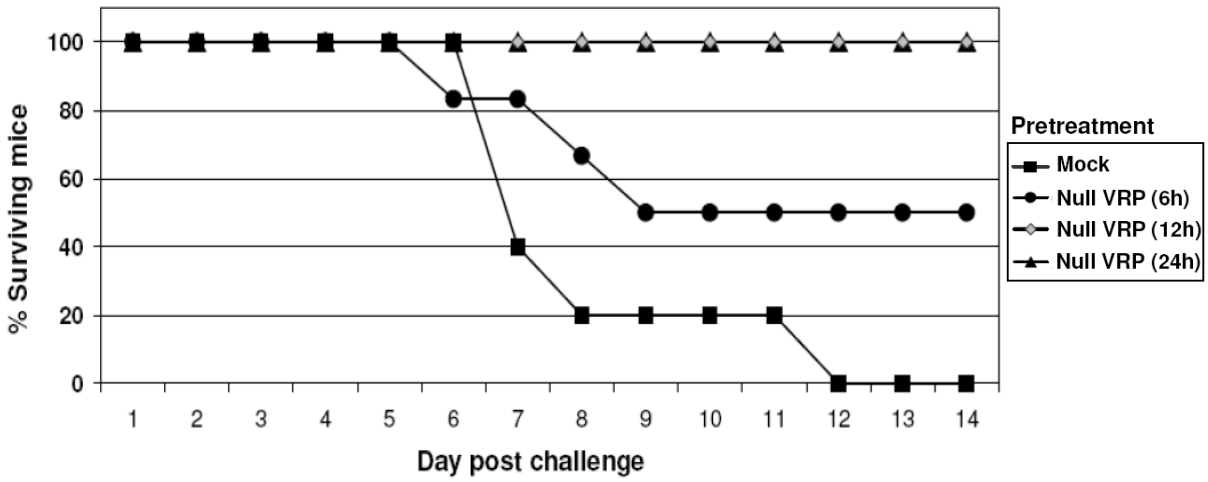

Figure 3.4. Survival of VRP-pretreated (RRFP) BALB/c mice following intranasal challenge with virulent VEE. Adult BALB/c mice, 5-6 mice per group, were pretreated by inoculation in the right rear footpad (RRFP) with 2 x 10^6 null VRP for 6, 12, or 24h prior to intranasal challenge with 10^3 PFU of virulent VEE. Mock pretreated mice received diluent alone, in the RRFP, 6h prior to challenge. A higher challenge dose of 10^3 PFU was necessary to achieve a 100% mortality rate in mock pretreated animals, due to the inefficiency of intranasal delivery.

Table 3.3. Morbidity and mortality of VRP-pretreated (RRFP) adult BALB/c mice following intracranial challenge with virulent VEE.

Pretreatment (Footpad)			Challenge (Intracranial)				
VRP	Duration	Dose (IU)	Virus	Dose (PFU)	% Morbidity (sick/total)	% Mortality (dead/total)	AST (days) (+/- SEM)*
mock	6h	-	VEE	10^3	100.0 (6/6)	100.0 (6/6)	2.7 (+/- 0.0)
null VRP	6h	2×10^6	VEE	10^3	100.0 (6/6)	100.0 (6/6)	5.0 (+/- 0.0)†
null VRP	12h	2×10^6	VEE	10^3	100.0 (6/6)	100.0 (6/6)	5.0 (+/- 0.3)†
null VRP	24h	2×10^6	VEE	10^3	100.0 (6/6)	100.0 (6/6)	4.0 (+/- 0.4)††

*Average survival time (AST), plus or minus the standard error of the mean (SEM); † p-value of <0.001, by one way ANOVA analysis; †† p-value of <0.05, by one way ANOVA analysis.

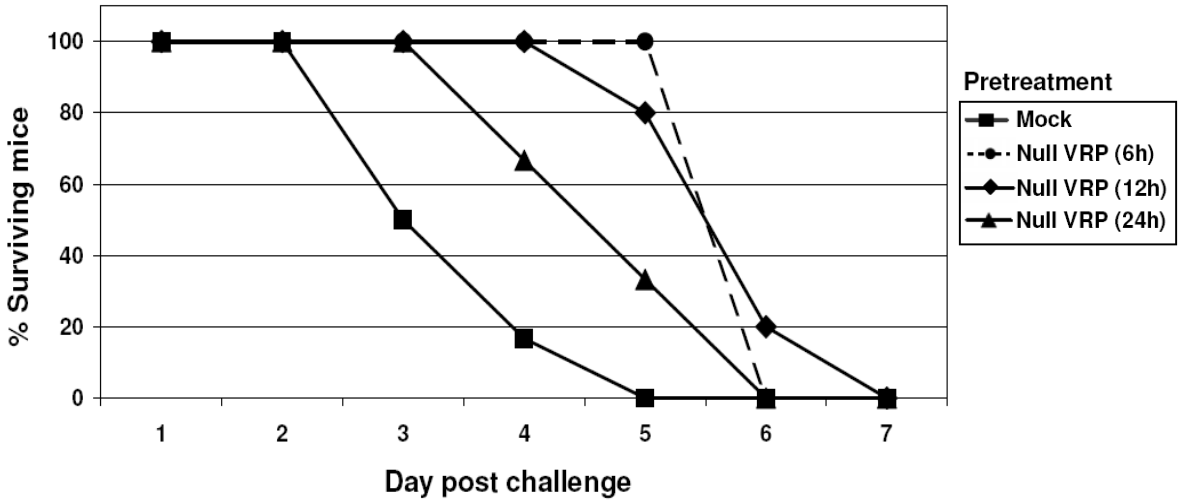

Figure 3.5. VRP-pretreatment of BALB/c mice extends the average survival time upon intracranial challenge with virulent VEE. Adult BALB/c mice, 6 mice per group, were pretreated by inoculation in the right rear footpad (RRFP) with 2 x 10^6 null VRP for 6, 12, or 24h prior to intracranial challenge with 10^3 PFU of virulent VEE. Mock pretreated mice received diluent alone, in the RRFP, 6h prior to challenge.

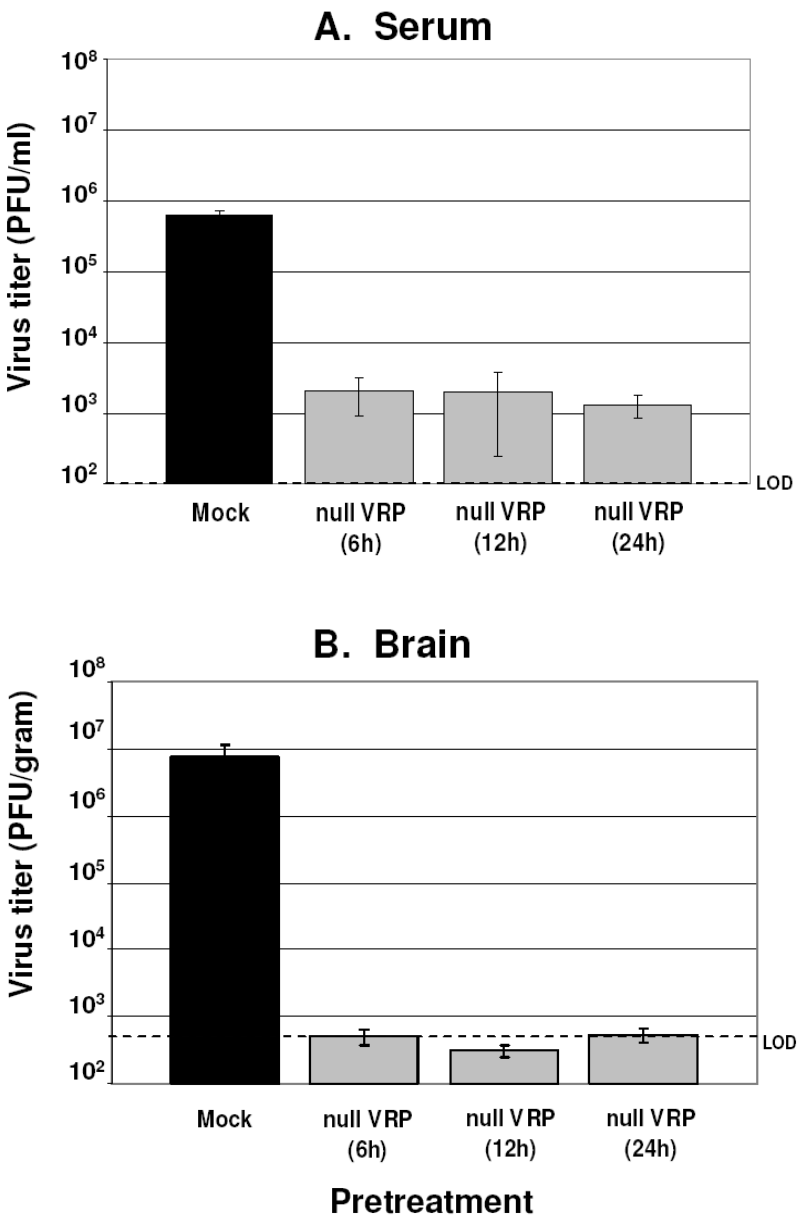

Figure 3.6. VRP pretreatment dramatically reduces the viral load in the serum and brain of animals challenged with VEE. Adult BALB/c mice, 3 mice per group, were pretreated by inoculation in the right rear footpad (RRFP) with 2 x 10^6 null VRP for 6, 12, or 24h prior to challenge with 10 PFU of virulent VEE in the opposing left rear footpad (LRFP). Mock pretreated mice received diluent alone, in the RRFP, 6h prior to challenge. (A) At 24h post challenge, serum was collected by tail vein bleed. (B) At 88h post challenge, the mice were euthanized, perfused with PBS, and the brain (including the olfactory bulbs) removed by dissection. Viral titers were determined by standard BHK cell plaque assay. The limit of detection (LOD) in each assay is indicated by the dotted line.

Table 3.4. The effect of VRP pretreatment dose on morbidity and mortality following virulent VEE footpad challenge.

Pretreatment (Footpad)			Challenge (Footpad)				
VRP	Duration	Dose (IU)	Virus	Dose (PFU)	% Morbidity (sick/total)	% Mortality (dead/total)	AST (days) (+/- SEM)*
mock	6h	-	VEE	10	100.0 (5/5)	100.0 (5/5)	5.8 (+/- 0.2)
null VRP	6h	10^4	VEE	10	100.0 (5/5)	100.0 (5/5)	6.0 (+/- 0.0)
null VRP	6h	10^5	VEE	10	100.0 (5/5)	100.0 (5/5)	7.0 (+/- 0.0)
null VRP	6h	2×10^6	VEE	10	40.0 (2/5)	0 (0/5)	-

*Average survival time (AST), plus or minus the standard error of the mean (SEM)

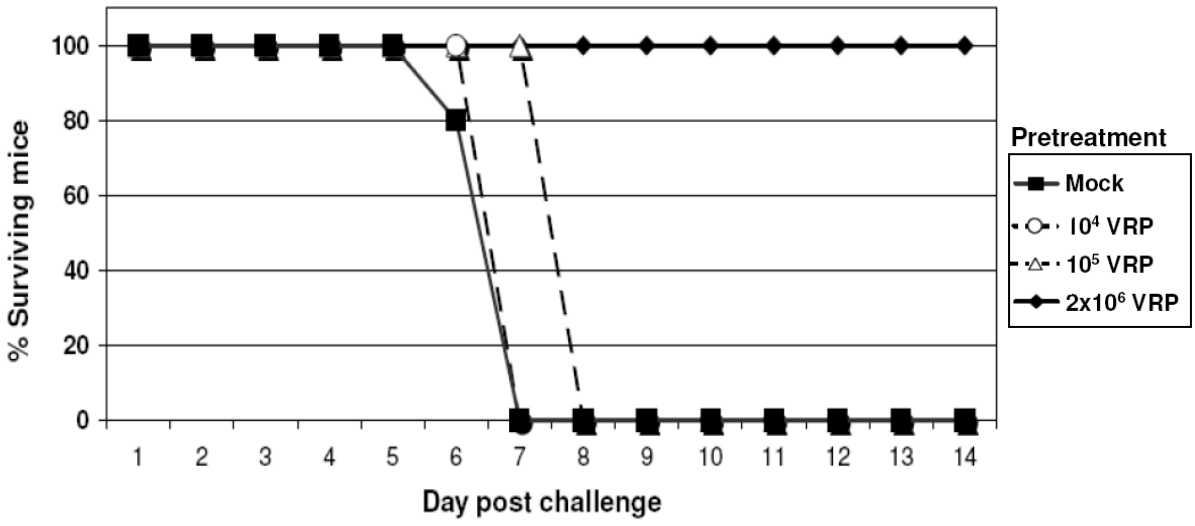

Figure 3.7. The dose of the VRP pretreatment is a critical parameter of protecting mice from subsequent VEE challenge. Adult BALB/c mice, 5 mice per group, were pretreated with decreasing doses of null VRP (2×10^6 IU, 10^5 IU, or 10^4 IU) inoculated in the RRFP for 6h prior to challenge with 10 PFU of virulent VEE (LRFP). Mock pretreated mice received diluent alone, in the RRFP, 6h prior to challenge.

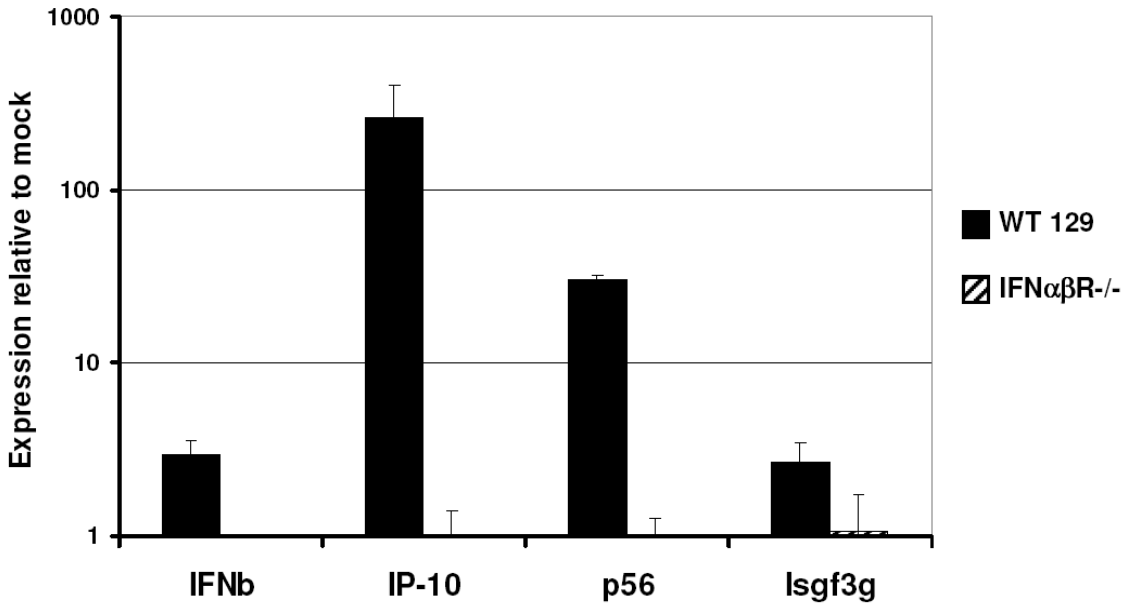

Figure 3.8. Antiviral gene induction in the brain of VRP pretreated animals is diminished in IFNαβ receptor knockout mice. Adult, wildtype 129 or IFNαβ receptor knockout (IFNαβR-/-) mice were inoculated in the right rear footpad with 2 x 10^6 IU of null VRP, or were mock infected with diluent. At 6h following inoculation, the mice were euthanized, perfused with PBS, and tissues removed by dissection. Total cellular RNA was isolated, cDNA synthesized, and the expression of a panel of interferon-stimulated genes (IFNβ, IP-10, p56, Isgf3g) was assessed by Taqman real-time PCR. The black bars represent gene expression in wildtype 129 mice, and the striped bars represent gene expression in IFNαβR-/- mice. The fold induction of each gene is represented by the expression in VRP infected animals relative to the expression in mock infected animals. Each bar represents groups of three animals each, plus or minus the standard error of the mean (SEM).

Table 3.5. Morbidity and mortality of VRP-pretreated (RRFP) adult 129 and IFNαβ receptor knockout mice following challenge with virulent VEE (LRFP)

	Pretreatment (Footpad)			Challenge (Footpad)				
Mouse Strain	VRP	Duration	Dose (IU)	Virus	Dose (PFU)	% Morbidity (sick/total)	% Mortality (dead/total)	AST (days) (+/- SEM)
129	mock	6h	-	VEE	10	100.0 (5/5)	100.0 (5/5)	6.6 (+/- 0.2)
129	null VRP	6h	2×10^6	VEE	10	40.0 (2/5)	20.0 (1/5)	7.0 (+/- 0.0)
129	null VRP	12h	2×10^6	VEE	10	0 (0/5)	0 (0/5)	-
129	null VRP	24h	2×10^6	VEE	10	0 (0/5)	0 (0/5)	-
IFNαβR-/-	mock	6h	-	VEE	10	100.0 (8/8)	100.0 (8/8)	2.4 (+/- 0.2)
IFNαβR-/-	null VRP	6h	2×10^6	VEE	10	0 (0/8)	100.0 (8/8)	2.0 (+/- 0.0)
IFNαβR-/-	null VRP	12h	2×10^6	VEE	10	0 (0/8)	100.0 (8/8)	2.0 (+/- 0.0)
IFNαβR-/-	null VRP	24h	2×10^6	VEE	10	0 (0/8)	100.0 (8/8)	2.0 (+/- 0.0)

*Average survival time (AST), plus or minus the standard error of the mean (SEM)

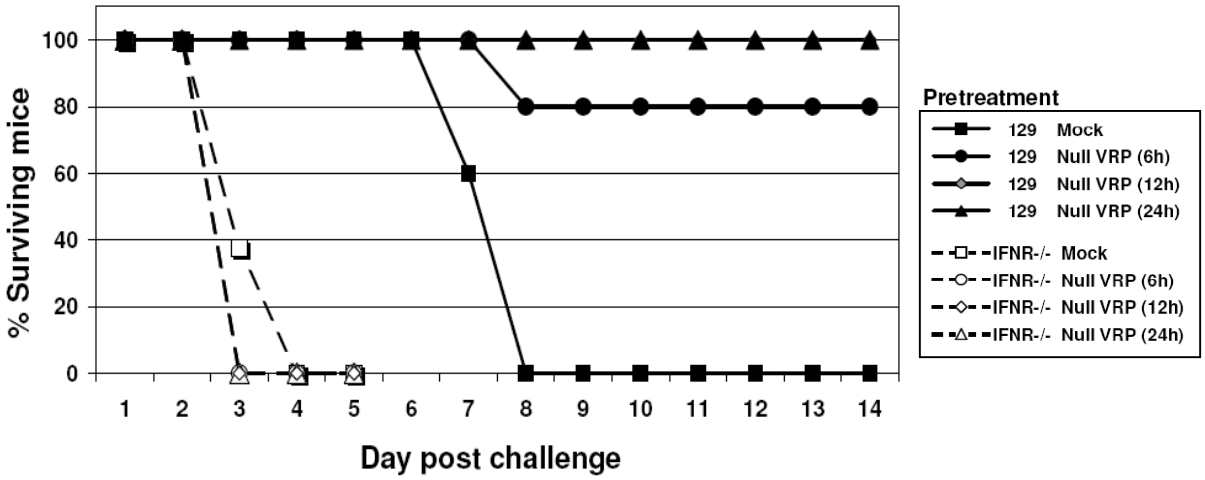

Figure 3.9. VRP-pretreated, IFNαβ receptor knockout mice are not protected against virulent VEE challenge. Adult, wildtype 129 (5 mice per group) or IFNαβ receptor knockout mice (8 mice per group) were pretreated by inoculation in the right rear footpad (RRFP) with 2×10^6 null VRP for 6, 12, or 24h prior to challenge with 10 PFU of virulent VEE in the LRFP. Mock pretreated mice received diluent alone, in the RRFP, 6h prior to challenge.

Table 3.6. Morbidity and mortality of VRP-pretreated (RRFP) adult BALB/c mice following heterologous, intranasal challenge with VSV.

Pretreatment (Footpad)			Challenge (Intranasal)				
VRP	Duration	Dose (IU)	Virus	Dose (PFU)	% Morbidity (sick/total)	% Mortality (dead/total)	AST (days) (+/- SEM)*
mock	24h	-	VSV	2×10^6	100.0 (7/7)	42.9 (3/7)	9.0 (+/- 0.0)
null VRP	24h	2×10^6	VSV	2×10^6	100.0 (8/8)	50.0 (4/8)	7.5 (+/- 0.5)

*Average survival time (AST), plus or minus the standard error of the mean (SEM)

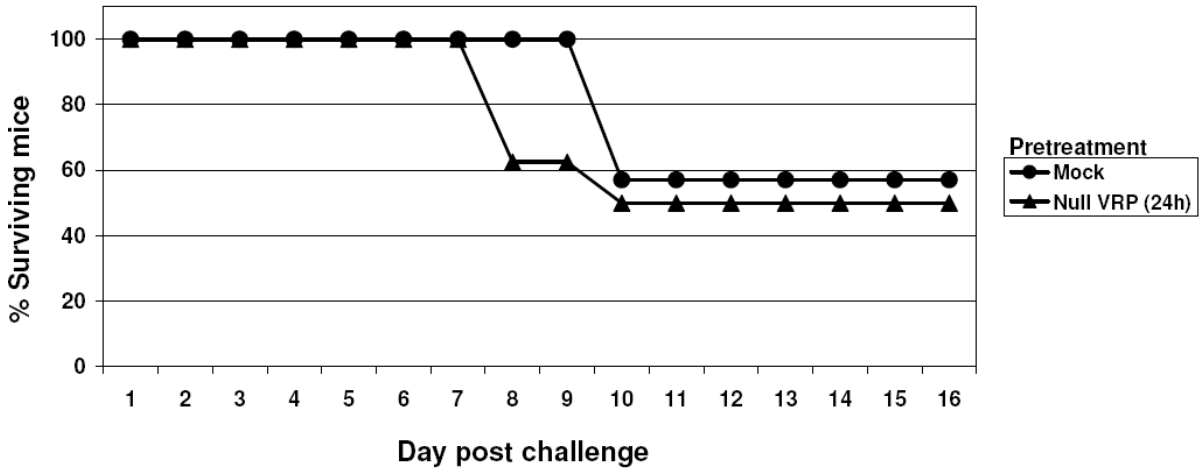

Figure 3.10. VRP-pretreated BALB/c mice are not protected against a heterologous challenge with VSV. Adult BALB/c mice, 7-8 mice per group, were pretreated by inoculation in the right rear footpad (RRFP) with 2×10^6 null VRP for 24h prior to challenge with 2×10^6 PFU of vesicular stomatitis virus (VSV) in the LRFP. Mock pretreated mice received diluent alone, in the RRFP, 24h prior to challenge.

CHAPTER FOUR

DISCUSSION AND FUTURE DIRECTIONS

The interface of viral infection and host response embodies a complex series of interactions and regulatory pathways. As the host senses the virus, and seeks to eradicate infection and reestablish homeostasis, the virus seeks to continue its own survival and spread. Thus, the pathogenesis of any given virus and the associated injury it causes induces numerous changes in the host. The consequences are dependent on several viral and host factors, which together dictate the outcome of infection. Accordingly, this has been a constant area of active investigation, and our understanding of this process advances as innovative tools and sophisticated systems fall into place. However, much remains to be learned.

In this body of work, we utilized two such systems in an effort to characterize the molecular markers of the early virus-host interactions central to Venezuelan equine encephalitis virus (VEE) pathogenesis. First, VEE replicon particles (VRP) were utilized to limit infection to the first infected cells. Second, an mRNP-tagging system was developed to overcome an inherent limitation in the application of traditional gene profiling methods post viral infection; namely, the inability to discriminate the expression profile in infected versus surrounding uninfected bystander cells. Such discrimination is particularly crucial following infection *in vivo*, as the infected cells in a given tissue most often represent a minority population set against a background of mostly uninfected cells. The development and application of the VRP mRNP-tagging system bestowed the capability to directly profile the infected cell response to VEE, doing so in a sensitive manner. In fact, had the mRNA-tagging system not been utilized, the induction of several genes would have gone undetected. Combined with simultaneous total RNA analysis of the collective

response, this system not only revealed the infected cell response, but also granted insight into the contribution of the uninfected bystander cell population in the early host response to VEE infection.

We found the response of these two different populations, within the same *in vitro* cell culture or the same tissue *in vivo,* to be dramatically different, varying in quantitative, qualitative, and temporal terms, indicating that the transcriptional programs of infected and uninfected cells within the same culture or tissue are uniquely affected. This included, for example, the discovery that infected cells are the primary source of the early IL-6 and GM-CSF response to VRP infection in BMDC and the DLN. Furthermore, the induction kinetics of the infected and uninfected cell response differed. Analysis revealed a two-phase innate host response to VEE in the DLN. The first phase consisted of a rapid response within the infected cells of the DLN, including the robust activation of several host defense genes (IFNβ, IP-10, and GM-CSF) by 6h. As the infected cell response was waning, a second phase of innate response was underway in the surrounding uninfected DLN cells, reminiscent of an antiviral autocrine-paracrine signaling loop. However, signaling through the IFNαβ receptor did not appear to be the primary paracrine mediator of the defense response in the uninfected DLN cells, while conversely autocrine signaling through this receptor was critical to the high levels of antiviral gene induction in the infected cell population. Direct analysis of the infected versus uninfected cell responses, including the details of autocrine and paracrine signaling, have previously been difficult, if not impossible, to achieve *in vivo*.

The activation of autocrine and paracrine signaling pathways is critical to the establishment of the antiviral state. This is particularly evident from consequences inflicted on the host when these pathways are antagonized by the virus (1-4). However, much remains unknown concerning the underlying regulatory elements of these responses (5-9), In this regard, the mRNP-tagging system offers a novel means to tease apart the relative contributions of the infected and bystander cell populations, granting unique perspective into the autocrine and paracrine responses induced following infection.

A common phenomenon during viral infection is the interaction of vastly different cell types. In the brains of mice infected with VEE, this includes the interaction of infected neurons with bystander glial cells, such as astrocytes. Astrocytes have been implicated in several events that occur in the brains of VEE-infected animals, including mediating a strong iNOS and TNFα proinflammatory response which seems at least partially responsible for the neurodegeneration associated with VEE infection (10-13). Future application of the VRP mRNP-tagging system may include direct intracranial inoculation of FLAG-PABP VRP into the brain. This analysis would be valuable in deciphering the direct response of infected neurons, as well as that of the surrounding uninfected cells which also contribute to VEE-induced CNS pathogenesis. In studies where CNS tissue sections were labeled for VEE antigen, and adjacent sections double-labeled for an astrocyte marker and apoptosis, it was revealed that apoptosis of neurons not only occurs in areas of the brain positive for VEE-antigen, but also in areas of astrogliosis (12). These findings suggest that the inflammatory response contributes to VEE-induced

pathology in the brain, both within the infected and uninfected cell populations (12-14). Application of the VRP mRNP-tagging system in the brain may facilitate the identification of the early molecular markers of VEE neurovirulence, including the kinetics of the proinflammatory response, as well as the induction of apoptosis within these different cell populations.

In addition, the mRNP-tagging system will be applicable to other viral systems. For example, a directly applicable pathogenesis model is Ross River virus (RRV), a related alphavirus. RRV is an Old World alphavirus endemic to Australia, which causes severe, and often persistent arthritis/arthralgia in humans (15). A mouse model of RRV disease has been developed, with infected mice exhibiting severe disease characterized by inflammation of muscle tissue and muscle damage (16, 17). Disease is thought to be initiated by viral replication as well as inflammatory cell infiltrates in the affected joints (18, 19), with the primary targets of RRV infection recently identified as bone, joint, and skeletal muscle tissues of the hind limbs (17). Characterization of the inflammatory infiltrate within skeletal tissue has identified macrophages, NK cells, and T lymphocytes (17).

At least two recent studies have implicated the innate immune response in the induction of RRV-associated disease. For instance, depletion of macrophages prior to infection completely prevents RRV-induced muscle inflammation (16). The complement system also has been suggested to play a role, perhaps by mediating proinflammatory functions of the infiltrates in infected tissues (20). Certainly the development of an RRV mRNP-tagging system would address several aspects of RRV pathogenesis in the mouse model. By discriminating between the infected

cells within the joint-associated tissue and the recruited, uninfected inflammatory infiltrates, the relative induction of the innate mediators associated with disease could be established. Additionally, comparison of such studies to that in mice lacking components of the complement pathway may help identify the specific innate effector functions in the proinflammatory infiltrates targeted during RRV infection. Such studies would also present an opportunity to compare and contrast the modulation of the host response by the New World (encephalitic, e.g., VEE) and Old World (arthritic, e.g., RRV) alphaviruses.

Comparing the host response to wildtype VEE and the nt3A interferon-sensitivity mutant did not elucidate a novel antiviral effector gene(s) involved in the documented attenuation of the mutant. However, new data suggests that this sensitivity may be driven by an alternative pathway, one independent of Mx, PKR, and RNaseL. Infection of mice triply deficient (TD) for these factors were still protected upon infection with the nt3A mutant, while wildtype VEE remained virulent (L.J. White and R.E. Johnston, unpublished data). This suggests that an alternative innate pathway may exist that is capable of mediating protection from VEE infection. It may therefore be pertinent to examine the host response to nt3A mutant in the context of this alternative pathway, in other words, within the TD system. Applying the biological pressure induced by the absence of these pathways may be necessary to facilitate the activation of key antiviral mediators involved in the nt3A attenuation. In fact, a similar investigation using a strain of Sindbis virus with a comparable attenuating phenotype successfully utilized infection in the TD model to identify a set of 44 candidate effectors of the alternative pathway (21, 22). An

examination of these 44 candidate genes in the context of VEE infection, as well as contrasting host gene induction in TD mice infected with the nt3A mutant, is an important next step.

In the second set of studies presented here, we utilized a VRP-based system to ask whether the earliest events following viral infection could establish an antiviral response that was sufficient to transform the entire infected animal. Within just a few hours following VRP footpad inoculation, there was a rapid, systemic activation of the host antiviral response, both within the DLN and beyond. Within the liver and brain, distal to the site of replication in the DLN, antiviral gene expression of greater than 100-fold over mock was detected within hours of VRP footpad inoculation, peaking by 6 to 12 h. The antiviral effects of the VRP pretreatment were evident by the dramatic reduction in challenge virus titers in the serum and brain. In fact, pretreatment of mice by footpad VRP inoculation for 6, 12, or 24h prior to virulent VEE footpad challenge conferred complete protection from death. This set of experiments successfully documented a rapid modulation of the host innate response, occurring within just moments of pathogen invasion, capable of transforming the entire infected animal and potentially affecting the outcome of infection.

Although intact interferon signaling was found to be necessary for the induction of this systemic antiviral response, interferon itself may not have been the sole mediator of protection. This was demonstrated by the lack of protection in VRP-pretreated mice challenged with a heterologous, interferon-sensitive virus (VSV). Future studies involving modified pretreatment regimens and serum transfer

will likely facilitate a greater understanding of the underlying mechanism in this protection system. There may, however, be another explanation for the lack of protection in the VSV challenge experiments. A recent study described a phenomenon in which the host interferon response experienced a period of exhaustion following infection with Semliki Forest virus (SFV) (23). A rapid, interferon-dependent activation of B and T lymphocytes was described following SFV infection, which reverted back to a resting phenotype within 5 days. However, when a secondary infection with an unrelated virus was administered during a period of 5 to 9 days after SFV exposure, there was an inability of these lymphocytes to reactivate due to an apparent exhaustion of the interferon system. This refractory period, during which the animals could not mount a type I interferon response, was likened to a transient immunosuppression, and rendered the mice more susceptible to acute viral infections (23).

In light of the extended replication kinetics of VSV versus VEE infection (discussed in Chapter three), it may be pertinent to investigate whether a refractory period is induced following VRP pretreatment. This could be done by administering the VRP pretreatment over an extended timecourse, mimicking the 5 to 9 day kinetics that were observed in the SFV system, and then challenging with VEE or VSV. Perhaps it makes sense that a period of unresponsiveness should occur for some period following acute infection, as the transient nature of the innate immune response to infection is an important aspect protecting against the deleterious effects of an exaggerated immune response. In fact, we have documented this transient nature in our kinetic examination of host gene responses in the VRP-

infected animal. However, the presence of a refractory period and the consequences of this phenomenon remain to be defined in our system.

VEE, being an arthropod-borne virus, is transmitted by mosquitoes in nature and targets host dendritic cells at the site of inoculation in the skin (24-26). In light of this natural transmission cycle, another recently published study has interesting future implications for the direction of the experimental systems presented here. Shabman *et al.* recently reported that alphaviruses grown in mosquito cells, including RRV and VEE, differed in their ability to induce type I interferon responses in comparison to mammalian-cell derived alphaviruses (27). While mosquito-cell derived VEE (mos-VEE) was able to infect dendritic cells as effectively as mammalian-cell derived VEE (mam-VEE), mos-VEE was a poor inducer of type I interferon. These results led to a proposed model in which alphaviruses delivered by the bite of an infected mosquito can efficiently infect dendritic cells while having the ability to avoid the host type I interferon response. It is likely that this effect would only occur during the first round of infection, within the initially infected dendritic cells, as virus amplified within the now mammalian host would give rise to mam-VEE. However, this one time advantage is speculated to be critical in establishing alphavirus infection in the mammalian host (27).

An entirely new line of investigation could be developed in which mosquito-cell derived VRP (mos-VRP) are used throughout the studies presented here. This would include applying a mos-VRP mRNP-tagging system, and contrasting the effect on host antiviral gene induction *in vivo* with that of mam-VRP. The utilization of VRP within this context would allow us to model the initial interaction of mos-VEE

with host dendritic cells at the site of inoculation, eliminating the amplification of mam-VEE progeny. In addition, the mRNP-tagging system would provide the sensitivity required to specifically profile that minority cell population following infection *in vivo*. It would be equally interesting to use mos-VRP in our VRP pretreatment regimen, and ask if antiviral gene responses are still rapidly induced in tissues downstream of the DLN. If mos-VRP could effectively evade activation of a systemic antiviral state, perhaps the observed protection from lethal virus challenge would be diminished. This set of future studies has exciting implications as it returns our focus to the natural virus-host interactions occurring during the transition of alphavirus infection in the arthropod vector to the vertebrate host. The body of work presented here, as well as the studies proposed for the future, promise to further define the impact of early virus-host interactions on the progression of pathogenesis and the outcome of alphavirus infection.

REFERENCES

1. Long, M., and A. J. Adler. 2006. Cutting Edge: Paracrine, but Not Autocrine, IL-2 Signaling Is Sustained during Early Antiviral CD4 T Cell Response. *J Immunol* 177:4257-4261.

2. Barro, M., and J. T. Patton. 2007. Rotavirus NSP1 Inhibits Expression of Type I Interferon by Antagonizing the Function of Interferon Regulatory Factors IRF3, IRF5, and IRF7. *J. Virol.*:JVI.02498-02406.

3. Vincent, I. E., C. Balmelli, B. Meehan, G. Allan, A. Summerfield, and K. C. McCullough. 2007. Silencing of natural interferon producing cell activation by porcine circovirus type 2 DNA. *Immunology* 120:47-56.

4. Klouche, M., G. Carruba, L. Castagnetta, and S. Rose-John. 2004. Virokines in the Pathogenesis of Cancer: Focus on Human Herpesvirus 8. *Ann NY Acad Sci* 1028:329-339.

5. Malmgaard, L. 2004. Induction and Regulation of IFNs During Viral Infections. *Journal of Interferon & Cytokine Research* 24:439-454.

6. Levy, D. E., I. Marie, E. Smith, and A. Prakash. 2002. Enhancement and diversification of IFN induction by IRF-7-mediated positive feedback. *J Interferon Cytokine Res* 22:87-93.

7. Marie, I., J. E. Durbin, and D. E. Levy. 1998. Differential viral induction of distinct interferon-alpha genes by positive feedback through interferon regulatory factor-7. *Embo J* 17:6660-6669.

8. Prakash, A., E. Smith, C.-k. Lee, and D. E. Levy. 2005. Tissue-specific Positive Feedback Requirements for Production of Type I Interferon following Virus Infection. *J. Biol. Chem.* 280:18651-18657.

9. Seeds, R. E., S. Gordon, and J. L. Miller. 2006. Receptors and ligands involved in viral induction of type I interferon production by plasmacytoid dendritic cells. *Immunobiology* 211:525-535.

10. Charles, P. C., J. Trgovcich, N. L. Davis, and R. E. Johnston. 2001. Immunopathogenesis and Immune Modulation of Venezuelan Equine Encephalitis Virus-Induced Disease in the Mouse. *Virology* 284:190-202.

11. Charles, P. C., E. Walters, F. Margolis, and R. E. Johnston. 1995. Mechanism of Neuroinvasion of Venezuelan Equine Encephalitis Virus in the Mouse. *Virology* 208:662-671.

12. Schoneboom, B. A., K. M. K. Catlin, A. M. Marty, and F. B. Grieder. 2000. Inflammation is a component of neurodegeneration in response to Venezuelan equine encephalitis virus infection in mice. *Journal of Neuroimmunology* 109:132-146.

13. Schoneboom, B. A., J. S. Lee, and F. B. Grieder. 2000. Early Expression of IFN-alpha/beta and iNOS in the Brains of Venezuelan Equine Encephalitis Virus-Infected Mice. *Journal of Interferon & Cytokine Research* 20:205-216.

14. Jackson, A. C., and P. R. John. 1997. Apoptotic cell death is an important cause of neuronal injury in experimental Venezuelan equine encephalitis virus infection of mice. *Acta Neuropathologica* V93:349-353.

15. Griffin, D. E. 2001. Alphaviruses. In *Fields virology, 4th ed.* D. M. Knipe, B. N. Fields, and P. M. Howley, eds. Lippincott Williams & Wilkins, Philadelphia, Pa. . 917-962.

16. Lidbury, B. A., C. Simeonovic, G. E. Maxwell, I. D. Marshall, and A. J. Hapel. 2000. Macrophage-induced muscle pathology results in morbidity and mortality for Ross River virus-infected mice. *J Infect Dis* 181:27-34.

17. Morrison, T. E., A. C. Whitmore, R. S. Shabman, B. A. Lidbury, S. Mahalingam, and M. T. Heise. 2006. Characterization of Ross River Virus Tropism and Virus-Induced Inflammation in a Mouse Model of Viral Arthritis and Myositis. *J. Virol.* 80:737-749.

18. Fraser, J. R., V. M. Ratnamohan, J. P. Dowling, G. J. Becker, and G. A. Varigos. 1983. The exanthem of Ross River virus infection: histology, location of virus antigen and nature of inflammatory infiltrate. *J Clin Pathol* 36:1256-1263.

19. Soden, M., H. Vasudevan, B. Roberts, R. Coelen, G. Hamlin, S. Vasudevan, and J. La Brooy. 2000. Detection of viral ribonucleic acid and histologic analysis of inflamed synovium in Ross River virus infection. *Arthritis Rheum* 43:365-369.

20. Morrison, T. E., R. J. Fraser, P. N. Smith, S. Mahalingam, and M. T. Heise. 2007. Complement contributes to inflammatory tissue destruction in a mouse model of Ross River virus-induced disease. *J. Virol.*:JVI.02799-02706.

21. Ryman, K. D., L. J. White, R. E. Johnston, and W. B. Klimstra. 2002. Effects of PKR/RNase L-Dependent and Alternative Antiviral Pathways on Alphavirus Replication and Pathogenesis. *Viral Immunology* 15:53-76.

22. Ryman, K. D., K. C. Meier, E. M. Nangle, S. L. Ragsdale, N. L. Korneeva, R. E. Rhoads, M. R. MacDonald, and W. B. Klimstra. 2005. Sindbis Virus

Translation Is Inhibited by a PKR/RNase L-Independent Effector Induced by Alpha/Beta Interferon Priming of Dendritic Cells. *The Journal of Virology* 79:1487-1499.

23. Alsharifi, M., M. Regner, R. Blanden, M. Lobigs, E. Lee, A. Koskinen, and A. Mullbacher. 2006. Exhaustion of Type I Interferon Response following an Acute Viral Infection. *J Immunol* 177:3235-3241.

24. Weaver, S. C., C. Ferro, R. Barrera, J. Boshell, and J.-C. Navarro. 2004. Venezuelan equine encephalitis. *Annual Review of Entomology* 49:141-174.

25. Weaver, S. C., and A. D. T. Barrett. 2004. Transmission cycles, host range, evolution and emergence of arboviral disease. *Nature Reviews Microbiology* 2:789-801.

26. MacDonald, G. H., and R. E. Johnston. 2000. Role of Dendritic Cell Targeting in Venezuelan Equine Encephalitis Virus Pathogenesis. *The Journal of Virology* 74:914-922.

27. Shabman, R. S., T. E. Morrison, C. Moore, L. White, M. S. Suthar, L. Hueston, N. Rulli, B. Lidbury, J. P. Y. Ting, S. Mahalingam, and M. T. Heise. 2007. Differential Induction of Type I Interferon Responses in Myeloid Dendritic Cells by Mosquito and Mammalian-Cell-Derived Alphaviruses. *J. Virol.* 81:237-247.

APPENDIX A

ADDITIONAL DATA CHARACTERIZING THE NT3A MUTANT OF VENEZUELAN EQUINE ENCEPHALITIS VIRUS

A.

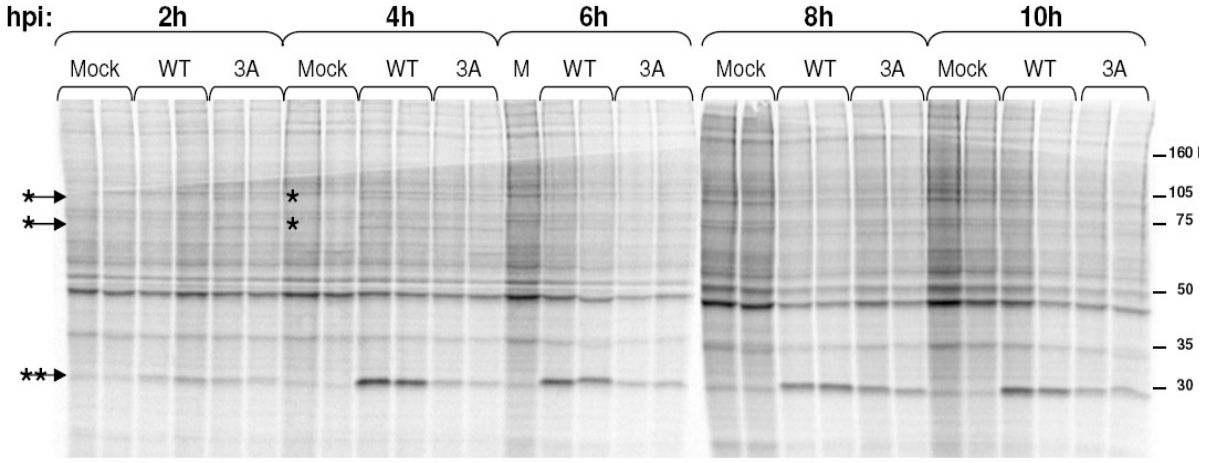

B.

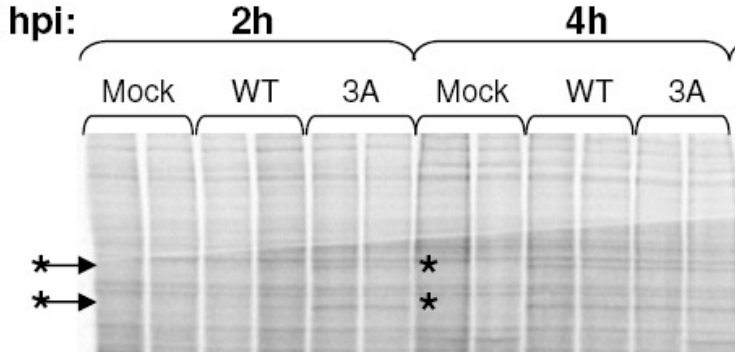

Figure A.1. Infection with both wildtype and nt3A mutant VRP induces the shutoff of host translation, but results in different levels of nonstructural and 26S protein expression. (A) Pulse-chase radiolabeling was utilized to assess the level of host protein synthesis at various times following VRP infection, in order to determine the extent of VRP-induced host translation shutoff. 10^5 L929 cells were either mock treated or infected with wildtype GFP-VRP or nt3A mutant GFP-VRP at an MOI of 10. Two hours before the indicated time post-infection, the media was removed and replaced with media lacking methionine and cysteine, and incubated for 1 hr at 37°C. This starvation medium was then supplemented with 33 μCi of [^{35}S]methionine-[^{35}S]cysteine/ml. Immediately after incubation for 1 h at 37°C, monolayers were harvested in NP-40 lysis buffer. Equal volumes of lysate from each time point were then separated by sodium dodecylsulfate-polyacrylamide gel electrophoresis on an 8% gel. Similar levels of host protein shutoff were observed when comparing wildtype and nt3A GFP-VRP infected cells. However, interestingly the nt3A mutation resulted in a decreased production of GFP (≈30 kilodaltons) from

the 26S subgenomic promoter throughout infection, as compared to level of GFP expression during wildtype GFP-VRP infection (shown by double astericks). In contrast, the same nt3A mutation resulted in the increased production of viral nonstructural genes at the earliest times post-infection (nsP2 ≈90 kilodaltons; nsP4 ≈70 kilodaltons), as indicated by the single astericks and expanded in panel (B). These differences in expression levels have been verified by immunoprecipitation against the nonstructural proteins, as well as through FACS analysis of the mean fluorescence intensity of GFP as expressed from wildtype and nt3A mutant GFP-VRP (data not shown).

A. Caspase 3/7 Activity – BMDC 6hpi

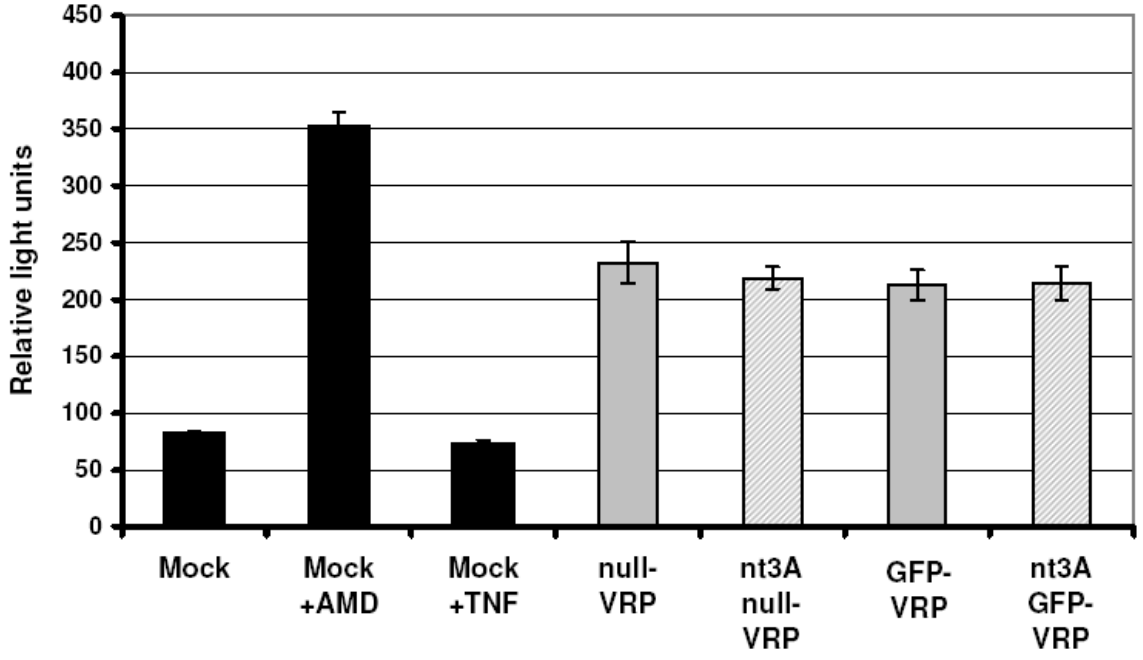

B. Caspase 3/7 Activity – BMDC 24hpi

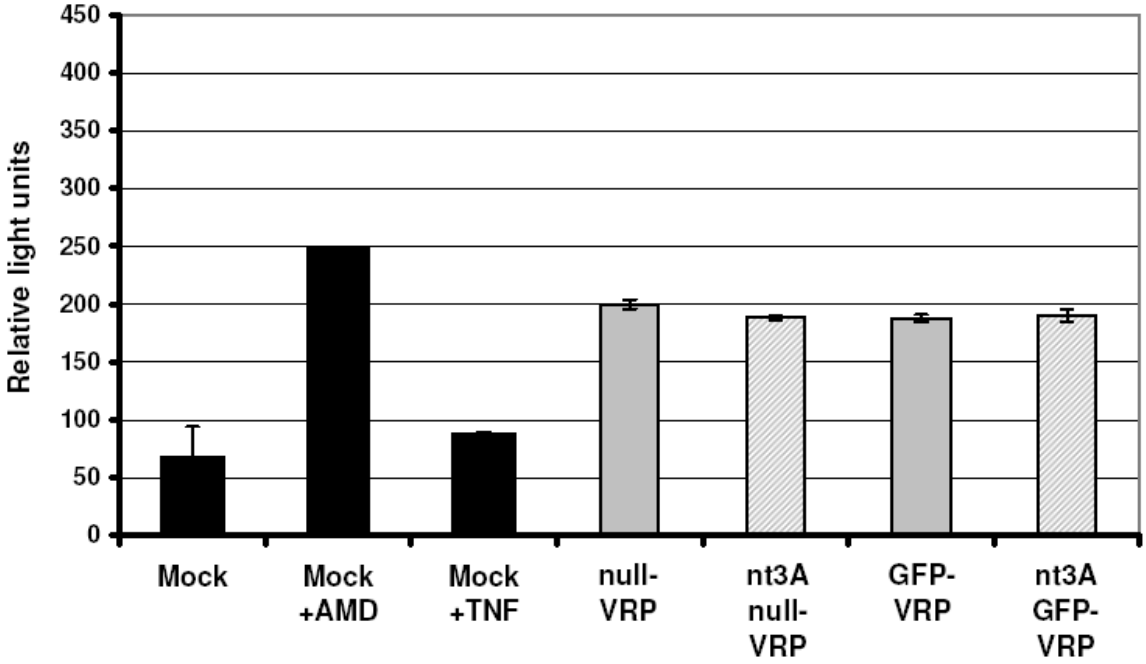

Figure A.2. Infection with wildtype and nt3A mutant VRP induces similar levels of caspase 3/7 activity in primary BMDC. The activation of caspase 3 and 7 is induced by multiple cell death stimuli, ultimately leading to apoptosis. Therefore, caspase 3/7 activity serves as an effective indicator of apoptosis. Here, the Promega Caspase-Glo™ 3/7 One Step Luminescent Assay was utilized to compare caspase 3/7 activity during wildtype versus nt3A mutant VRP infection, as a measure of the relative level of apoptosis induced during each infection. Triplicate samples of primary BMDC (3×10^4 cells), derived from wildtype 129sv/ev mice, were infected at an MOI of 10 with either null-VRP, nt3A mutant null-VRP, GFP-VRP, or nt3A mutant GFP-VRP. Mock treated cells served as the baseline readout for apoptosis occurring naturally in the BMDC cultures, while BMDC treated with apoptosis inducing agents (1 ug actinomycin D (AMD) or 20 ng TNFα) served as positive controls. (A) At 6 and (B) 24 h, the cultures were analyzed for caspase activity by direct lysis in culture, followed by the addition of a proluminescent caspase 3/7 substrate for cleavage by caspase 3/7 present in the cell culture, with measurement of the relative light units by luminometer analysis (see manufacturer's protocol). A high level of caspase 3/7 activity was measured from all VRP-infected samples, regardless of whether a transgene was expressed from the 26S promoter. In addition, a similar level of caspase 3/7 activity was present in BMDC infected with wildtype or nt3A mutant VRP, suggesting that a similar level of apoptosis occurs during each VRP infection.